Universidade do Porto
FEUP Faculdade de Engenharia

MIB Mestrado Integrado em Bioengenharia
Engenharia Biomédica

Experimental Study of the Human Anterolateral Abdominal Wall

Biomechanical Properties of Fascia and Muscles

Maria Helena Sequeira Cardoso
bio06009@fe.up.pt

Porto, July 2012

Universidade do Porto
FEUP Faculdade de Engenharia

MIB Mestrado Integrado em Bioengenharia
Engenharia Biomédica

Experimental Study of the Human Anterolateral Abdominal Wall

Biomechanical Properties of Fascia and Muscles

Student: Maria Helena Sequeira Cardoso
bio06009@fe.up.pt

Supervisor: Pedro Martins, PhD
palsm@fe.up.pt

Co-supervisor: Renato Natal Jorge, PhD
rnatal@fe.up.pt

Porto, July 2012

Abstract

Soft tissues have very different and misunderstood mechanical properties, when comparing to materials engineers are used to work with. Therefore, mechanical tests, namely tensile tests are essential, in order to understand the stress-stretch relationship, which describes the mechanical behavior of a specific material.

The present work is focused on uniaxial and biaxial tensile tests of biological tissues, namely the abdominal fascia, rectus abdominis muscle, internal oblique, external oblique and transverse abdominal muscles. This work also comprises mechanical tensile tests done using isotropic hyperelastic materials. Experimental factors can be determinant for the accurate measurement of a material's stress and stretch values; the present work comprises tensile tests done inside a 37ºC saline bath, in an effort to mimic the physiological environment.

KeyWords: biomechanics, uniaxial, biaxial, tensile tests, abdominal fascia, muscles, rectus abdominis, internal oblique, external oblique, transverse abdominal.

Resumo

Os tecidos moles têm propriedades mecânicas diferentes e pouco estudadas, quando comparados com os materiais com que os engenheiros habitualmente lidam. Por essa razão, é essencial realizar testes mecânicos, nomeadamente ensaios de tração, de modo a compreender a relação tensão-deformação, que descreve o comportamento mecânico de um material específico.

O presente trabalho foca ensaios de tração uniaxiais e biaxiais de tecidos biológicos, nomeadamente da fáscia abdominal e músculos recto abdominal, oblíquo interno, oblíquo externo e transverso abdominal. Este trabalho inclui também testes mecânicos feitos, utilizando materiais isotrópicos hiperelásticos. Vários factores podem ser determinantes durante os ensaios experimentais, influenciando os resultados de tensão e deformação do material em questão; neste trabalho, são apresentados resultados de ensaios de tração que decorreram dentro de um banho salino, a 37ºC, numa tentativa de mimetizar o ambiente fisiológico humano.

Palavras-Chave: *biomecânica, uniaxial, biaxial, ensaios de tração, fáscia abdominal, músculo recto abdominal, oblíquo interno, oblíquo externo, transverso abdominal.*

Agradecimentos

Ao finalizar a dissertação e rematando os últimos seis anos, quero deixar palavras de gratidão a todas as pessoas que participaram na minha vida, enquanto estudante universitária.

Em primeiro lugar, estou muito agradecida ao meu orientador, Pedro Martins. Depois de todas as preocupações e dificuldades em encontrar um orientador e um tema a meu gosto, não poderia ter tido mais sorte. Obrigada pelos conselhos e, em geral, por todo o esforço, boa vontade, disponibilidade e orientação.

Uma palavra de apreço aos médicos e técnicos da delegação Norte do Instituto Nacional de Medicina Legal, I. P., especialmente à Dra. Maria Moura e ao Dr. Bessa, por tudo o que aprendi na sala de autópsias e por me chamarem a atenção para algumas das contribuições da bioengenharia à medicina.

Agradeço a todos os professores e funcionários da Universidade do Porto que contribuíram para meu crescimento pessoal e académico.

Obrigada, família. Estou feliz por ter nascido, sim, apesar de não conhecer a alternativa!

Estou muito grata ao Catota, pela cumplicidade, paciência, companheirismo, estupidez e por todo o apoio em momentos de insanidade e angústia.

Obrigada a todos os estudantes que partilharam estes anos comigo. Aquele abraço a Metal&Bio, a todo o grupo que me proporcionou tão bons (e alguns, felizmente poucos, menos bons) momentos e que, ao fim de seis anos, ainda me consegue surpreender positivamente. Para todos, Jogo. Palavra de apreço particularmente dedicada às afilhadas, aos companheiros de tese e aos catraios do Douro! Agradeço sobretudo aos que me receberam da melhor forma na faculdade e a quem eu devo tanto, Jabarus, Dragão, Catota, Vera, Luísa e também um muito obrigada à Mangas! A todo o meu ano 2006, obrigada! Por todas as atividades que conseguimos desenvolver por nossa conta! Pelas noites passadas a trabalhar nos departamentos e também pelas idas ao Mar de Minas! A tirar e a pôr árvores! Especial agradecimento à Ori, Bibi, Ju, Sofia, Ivan, Villa, Célinha, Deco, Caracóis, Sheila, Martinha, Adriano! A todos, muito obrigada, excepto ao Gordalina (tu é que tens que me agradecer)! Às noites passadas em ótima companhia, a comer pimentos padrón ou a beber vinho do Porto ao som de um fado. Devo mil agradecimentos à Sara! Por tudo! Mas não vão faltar ocasiões para chá acompanhado de nostalgia da faculdade.

Obrigada à Daniela e ao Válter, que não me deixaram ser tão anti-social! Bom bom.

"A vida de trabalho é longa o suficiente, acredita que um ano de vida académica a mais não é desperdício, é investimento pessoal!" Obrigada, Mé!

Por fim, quero saudar todos os que lerem este trabalho!

Saúdo-os e desejo-lhes sol,
E chuva, quando a chuva é precisa,
E que as suas casas tenham
Ao pé duma janela aberta
Uma cadeira predilecta
Onde se sentem, lendo os meus versos.
E ao lerem os meus versos pensem
Que sou qualquer coisa natural
(Alberto Caeiro)

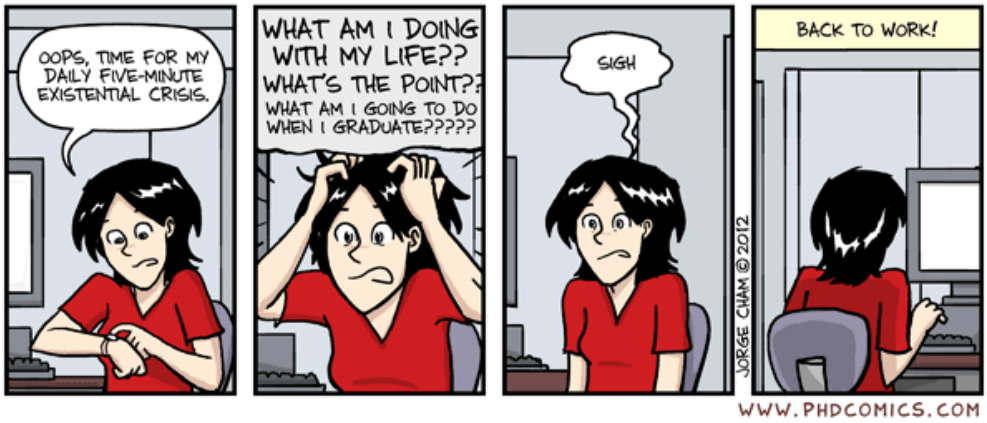

FERRUCCIO: “Schopenhauer dice che con la volontà si può fare tutto”

… funziona!

Contents

List of Figures

List of Tables

List of Abbreviations

ECM	Extracellular matrix
ATP	Adenosine Triphosphate
GAGs	Glycosaminoglycans
F	Load
Δl	Elongation
σ	Stress
ε	Strain
λ	stretch
E	Elasticity Modulus
Ψ	Strain energy function
P	Piola-Kirchhoff stress tensor
F	Deformation gradient
J	Jacobian determinant
C	Right Cauchy-Green tensor
b	Left Cauchy-Green tensor
λ_U	Ultimate Stretch
U_S	Strain Energy Density
E_t	Tangent Modulus
E_s	Secant Modulus
σ_Y	Yield Strength
σ_{max}	Tensile Strength
BMI	Body Mass Index
R^2	Coefficient of determination
FEM	Finite Element Method

Chapter 1

1. Introduction

"Biomechanics is mechanics applied to biology" [4]. It consists on the study of physical properties of living systems, permitting the understanding of their normal function, the prediction of changes due to alterations and the creation of models for surgery simulations, diagnosis, surgery and prosthesis.

To understand a biomechanical problem, a researcher usually studies the morphology of the organism, anatomy of the organ, histology of the tissue and the structure of the materials, so that its geometric configuration can be known. Then, it is necessary to determine the mechanical properties of the materials or tissues involved in the problem, which may be a difficult step to overcome, since some tissues cannot be isolated, because of the size of the specimen available or because it is difficult to keep the tissue in an environment similar to the living condition. From the data collected in these previous steps, a researcher can build a mathematical model representing the constitutive equation of the material, with certain numerical parameters left to be determined by experiments (mechanical, electrical, etc.). Afterwards, it is important to understand the environment in which an organ/tissue works in order to obtain meaningful boundary conditions and do experiments in physiological conditions to make sure that the theory and experiment correspond to each other. From that point on, it is possible to compare the experimental results with the corresponding theoretical models, and from this comparison, one can determine whether the hypothesis made in theory is justified and if it is, find the numerical values of the undetermined coefficients in the constitutive equations. Only then, when a researcher achieves a deep understanding of the problem, it is possible to predict with some confidence any changes in the behavior of the material under study, as some boundary conditions or material properties are changed [4].

There is a great need to have extended information concerning the biomechanical properties of human tissues. Biomaterial research is gaining ground, as more versatile materials are being studied and produced every day; this, however is happening before there is a solid base of knowledge of the physical properties that engineers are attempting to mimic, i.e. artificial substitutes of biological tissues are being developed based on the mechanical (and chemical) properties of materials similar to the biological tissues, instead of studying the properties of human tissues themselves. It is not simple to experiment on human tissues, because it of course involves many ethical questions, besides the difficulties of getting samples without risking the health of the donor. A common approach in health sciences is the use of animal models as a basis of

comparison, and many valuable studies are being developed, though the human morphology and physiology have significant differences when comparing to most animal models, which are quadruped (mice, rabbits, sheep, etc) [5, 6].

Here, human cadaveric tissues are used, in an effort to obtain data from human subjects, though living and cadaveric tissues may behave differently. After death, the corpse's tissues, mainly muscles, get stiff and chemical changes take place, as enzymes act to decompose the body. It is important to mention that biochemical and temperature changes happening to the body, *post mortem*, can have a significant effect on the biomechanical properties of the different tissues. The most obvious changes occurring after death are the stiffening of the corpse's muscular tissues – *rigor mortis* – and the underlying chemical changes [7]. *Rigor mortis* is an important early *post mortem* change that helps determine the *post mortem* interval. After death, cellular respiration stops and the corpse becomes depleted of oxygen, used to produce adenosine triphosphate (ATP). Consequently, when the ATP level falls to a set level, actin and myosin filaments combine irreversibly, causing a continued contraction that only stops when tissue is broken down and liquefied by enzymes during decomposition [8]. Many researchers have determined that the onset and progress of *rigor mortis* can be influenced by several factors such as temperature, pH in the muscles, exercise preceding death and cause of death [8]. In the present work, for all the samples, the date of death presented refers to the death certification by a medical doctor, meaning that it is not necessarily the actual time of death of the individual. It is also important to mention that for some cadavers, the time between death and autopsy extends for days, which involves refrigerating the body to prevent further tissue damage; though this procedure delays deterioration, biochemical reactions can still take place, potentially influencing the biomechanical tests results. In order to prevent the aggravation of these effects, all the experiments took place within the 24h after autopsy/tissue collection. For this reason, it is reasonable to consider the samples fresh, meaning there is an endeavor towards a limited but rather reliable comparison between the obtained results and the actual behavior of living human tissue.

Soft tissues have very different and misunderstood properties, when comparing to materials engineers are used to work with. Therefore, mechanical tests, namely tensile tests are essential, in order to understand the stress-stretch or stress-strain relationships, which describe the mechanical behavior of a specific material.

The present work falls under the scope of several previous studies on biological tissues [6, 9], and artificial meshes properties [10, 11], mainly focused on characterizing the mechanical behavior of the female pelvic cavity [5, 12-18].

Through the multidisciplinary cooperative work of engineers and medical doctors, and the approval of the ethics committee, a collaboration between Instituto Nacional de Medicina Legal do Porto, Portugal (INML) and Institute of Mechanical Engineering

(IDMEC), in Faculdade de Engenharia da Universidade do Porto (FEUP)was established. Thanks to this group work, it was possible for engineers to mechanically test samples dissected by medical doctors, during autopsy.

1.1 Motivation

The abdominal wall is a composite of different layers, whose mechanical properties play a significant role in developing a hernia [19]. From a biomechanical point of view the abdominal hernia is an opening in the abdominal wall layer, which leads to impossibility of the wall to withstand intra-abdominal pressure. The individual layers contribute to different extent to the biomechanical behavior of the abdominal wall and, therefore, it is necessary to examine their mechanical properties [20].

Operations on the abdominal wall are frequently performed in surgical practice, given that it is an important way for opening the peritoneal cavity and because it is involved in hernial sac formation [21]. Studies directed to the human abdominal fascia and anteroabdominal wall muscles mechanical properties have been increasing, since there is a great potential impact in fields such as plastic surgery, herniation process and hernia repair [6, 20, 22-25].Acquired umbilical hernias (central abdomen) occur most commonly in women and obese people, under the form of fat protuberances in the hernia sac. The lines along which the fibers of the abdominal aponeuroses interlace are also potential sites of herniation. Epigastric (upper abdomen) hernias tend to occur in people over forty years, and are usually associated with obesity [26]. Inguinal hernias (lower lateral abdomen), are the most common type, accounting for approximately 1,00,000 operations per year in the United Kingdom [20].

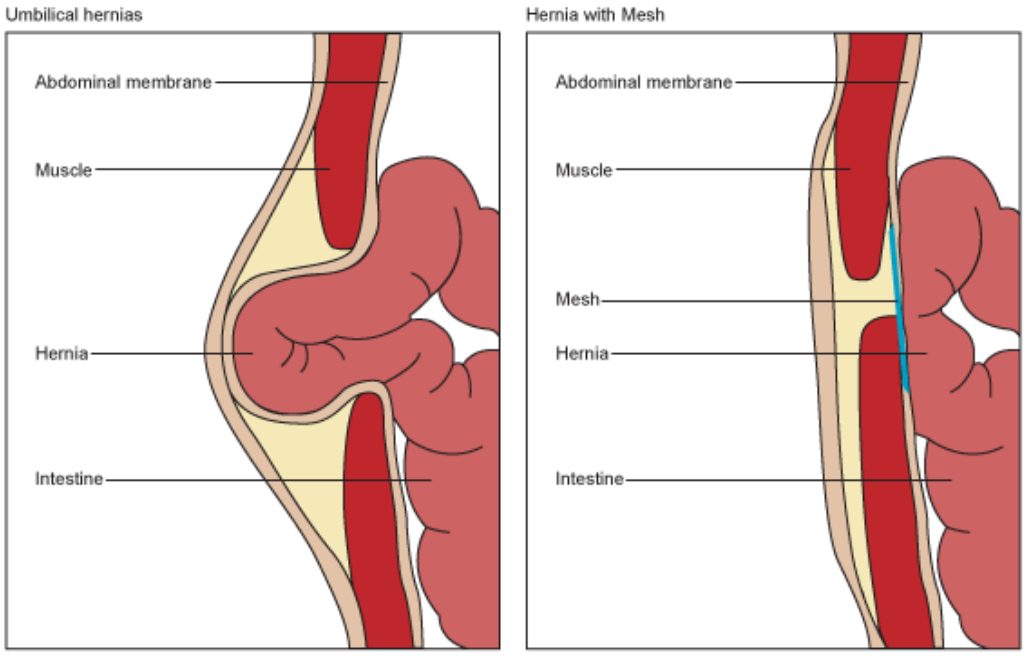

Figure 1.1 Schematic representation of an umbilical hernia repair, using a mesh (represented in blue) [27]

Hernia repair by implantation of synthetic meshes, represented in Figure 1.1, is the most widely used surgery for the treatment of this type of abdominal pathology. In technical terms, the repair of a hernial defect in the abdominal wall using a biomaterial has become routine clinical practice. Surgical repairs of inguinal hernia and umbilical hernia are the most common procedures among adult population. Hernia recurrences and inflammatory reactions are fairly frequent [22]; incisional hernia, which is a protrusion through a surgical incision, occurs at a rate of 11–15% in the first postoperative year and it is a poorly controlled complication of primary abdominal wall closure. Studies have shown that nearly every third abdominal wall closure is unable to resist loads and culminates in tissue rupture [28]. From a mechanical point of view, a harder material in contact with a softer one can induce erosion, which is why the contact interface is so important. When repairing a hernia, mesh stiffness may not conform to the surrounding tissue, interfering with its integration. A more flexible mesh means easier adhesion and conformation to the underlying tissue [10].

Researchers have been actively seeking the desired properties for the ideal prosthesis, in terms of structure, porosity, and adaptability to the biological and mechanical demands of the body. The most popular material is currently polypropylene, being available in a wide range of configurations, both to support the mechanical efforts required and to reduce the foreign body reaction and fibrosis provoked at the implant site [22]. However, there is a general ignorance, when it comes to the mechanical characterization of abdominal wall constituents and, since the implantation of synthetic meshes is the most widely used treatment for hernia repair, it is on our best interest to learn about the mechanical properties of the tissue being repaired, in order to achieve knowledge about the ideal mesh properties.

Correlation between Mechanical Properties and Pathologies

Mechanical properties of normal and diseased human tissue as well as prosthetics meshes' can be studied and compared. For example, uniaxial tensile test results of herniated and non-herniated tissue samples cut in transverse and longitudinal anatomical planes have been analyzed, suggesting that herniated and non-herniated *fascia transversalis* displays anisotropy and samples from herniated donors cut in the longitudinal anatomical plane are weaker than transversally cut samples, while the tendency for non-herniated samples is reversed [19].

Some studies have suggested herniation is not a local disease, but a manifestation of a systemic disorder of collagen metabolism. In fact, it has been shown that patients with inguinal hernia have some anomalies in collagen metabolism and changed ratio of collagen types [25], though it is still unclear if this predisposes the alteration of fascial function or is simply a consequence of micro repair (localized repair around microscopic tears). The mechanism by which the cells, of a formerly stable, load

bearing collagen matrix, extend that matrix in response to mechanical demand is of wide interest in the biomedical engineering field [20].

These results may be used to improve the quality of the meshes to prevent further surgical interventions, according to the patient pathology profile.

Surgical Simulations

Health professionals are becoming more aware of the computer simulation tools available in the study of physiology and pathophysiology of tissues, organs and systems. In this context, it is very useful to develop finite element simulations which link the theoretical modeling to the biological material specificity which is provided by experimental measurement and the subsequent determination of the material model parameters [6, 18, 21].

By getting more information about the tissues biomechanical properties, when operating, the surgeon can have a more detailed plan of action, since the tissue reactions can be predicted and simulation models can be produced [24].

In order to produce a realistic model of a human tissue/organ, it is important to do experimental tests and to understand the anatomy and physiology of the nonlinear soft tissues. An accurate model, using for instance finite elements methods, depends on the available information about the material physical properties, as well as the geometry and boundary conditions, specific for each organ part. Under the nonlinear theory of elasticity, soft tissues can be treated as hyperelastic materials and their properties studied accordingly. Furthermore, initial strains are needed to take into account the actual initial configuration and associated strain and stress distributions [29].

1.2 Objectives

Biomechanical testing on biological tissues provides quantitative information regarding the material mechanics, when generating or responding to physiological forces. These measurements can provide insight into the tissues inherit biochemical composition and spatial organization, as well as information about pathology and efficacy of treatment. From the test results, some mechanical properties of the materials under study can be directly obtained, using simple mathematic relationships.

It is the main goal of this work to produce biaxial tensile tests of cadaveric human abdominal fascia tissue and uniaxial tensile tests of cadaveric human abdominal fascia and muscle tissue. This thesis also presents results from uniaxial and biaxial tests performed using isotropic hyperelastic materials (vulcanized rubber and silicone), both inside and out the 37ºC saline bath. All biological tissues' tensile tests take place in a controlled environment consisting of a 37ºC saline bath. The tensile testing equipment

used allows control over testing conditions (load and displacement), in order to assure reproducibility.

After the tests, this work will provide the mechanical properties analysis of all samples, through the classic approach, which allows the direct comparison between results from different subjects, as well as different tissues from the same individual. A primary study on hyperelastic behavior of biological tissue will also be attempted.

1.3 Outline

Chapter 2 – Anatomical and Physiological Context – In this section, the human abdominal fascia and muscle tissue is seen in an anatomical and physiological perspective, building the background needed to be able to contextualize the tissues which will be analyzed.

Chapter 3 – Biomechanical Studies –This section presents the biomechanical concepts and definitions, as well as some concerns that have to be taken into account when dealing with soft biological tissue samples. It overviews some tension tests specificities and limitations. There is also information about the biomechanical tests and the material models that can be used to treat the data acquired during the tension tests.

Chapter 4 – Experimental Setup – This section explains the basics about sample collection and preparation. There is also a description of the experimental equipment used and a brief discussion about the results method of analysis.

Chapter 5 – Results and Discussion – This chapter presents a primary analysis of the specimen's characteristics, as well as the results obtained through the assessment of the mechanical properties by the classic approach and through the study of hyperelastic behavior models. Isotropic hyperelastic materials are studied, as well as the biological anisotropic hyperelastic materials, and the influence of some donor's characteristics is considered, in order to perform a critical analysis of the results.

Chapter 6 – Conclusion – Here, the main conclusions for this thesis are proposed.

Chapter 7 – Future Directions– This section provides suggestions for some improvements for the developed work, as well as points the way to future work directions.

Chapter 2

2. Anatomical and Physiological Context

The abdomen is a flexible and dynamic container which houses most of the organs of the digestive system and part of the urogenital system. It is able to enclose and protect the internal organs, while allowing flexibility between the thorax and pelvis, required by respiration, posture and locomotion [1].

This chapter overviews general notions about the anatomical structure of the abdominal tissues considered in this study. Special focus on the fascia tissues' and abdominal muscles' characteristics is given. Therefore, morphologic and functional descriptions are presented, so that both the tissues and their insertion/role/physiology in the human body can be understood.

2.1 The Abdominal Wall

For descriptive purposes, the abdominal wall can be subdivided into the anterior wall, right and left lateral walls (flanks), and posterior wall. The term anterolateral abdominal wall is often used, because the boundary between the anterior and lateral walls is indefinite [26].The anterolateral abdominal wall extends from the thoracic cage to the pelvis, and the present study is focused on its components, namely fascia tissue, vertical anterior abdominal muscles and flat anterolateral abdominal muscles, which can be seen in figure 2.1.

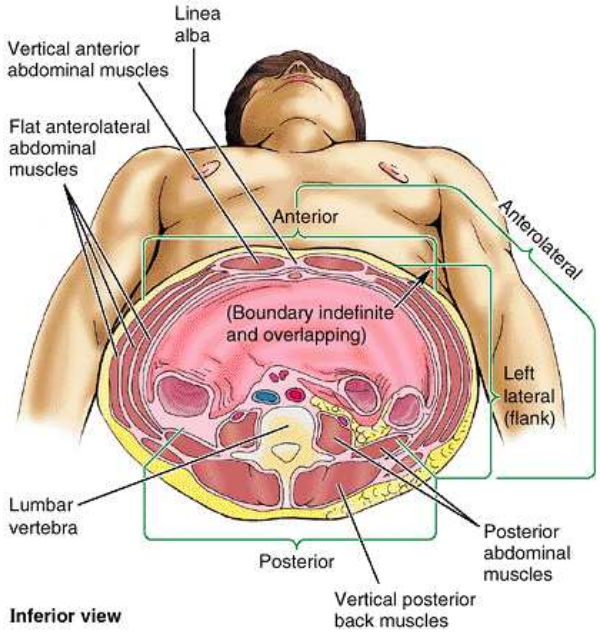

Figure 2.1 Representation of the subdivisions of the abdominal wall, discriminating the vertical anterior abdominal muscles and flat anterolateral abdominal muscles [26].

The abdominal wall is composed of several, interacting tissue types. Every tissue type has a different organization, inherent to its component cellular type(s).

2.2 Biological Tissues' Constituents

Histology is the study of the tissues of the body and of how they are arranged to constitute organs. It is performed by examining cells and tissues commonly by sectioning and staining, followed by examination under a light microscope or electron microscope. The ideal section preparation should be preserved, so that the tissue on the slide has the same structure and molecular composition as it had in the body. In order to obtain a permanent section, tissues must be fixed, to avoid digestion by enzymes or bacteria. Fixation is usually done by chemical methods, by immersing the tissue in stabilizing or cross-linking agents. Afterwards, tissues are usually embedded in a solid medium, such as paraffin or plastic resins, to facilitate sectioning. Since most tissues are colorless, most sections must be stained, in order to better distinguish their components. Dyes can stain tissues components more or less selectively, based on the acidic or basic compounds; tissues can also be impregnated with metals, such as silver and gold. These techniques usually provide insight into the chemical nature of the tissue being studied, allowing the observation of the different structures constituting the tissue [3].

The term histochemistry is used to indicate more specific methods for localizing substances in tissue sections, based on chemical reactions and on high-affinity interactions between macromolecules. A molecule present in a tissue section may be identified by using a compound that will interact with it; this compound must be tagged with a label that can be detected under light or electron microscope. Immunohistochemistry is based on a highly specific interaction between molecules, for example detecting antigens (e.g., proteins) in cells of a tissue section by exploiting the principle of antibodies binding specifically to antigens in biological tissues [30].

It is possible to obtain much information about an individual's health, based on tissue observation. By doing immunohistochemical and histological studies on several tissue samples, it is possible to identify specific patterns and, for example, correlate the presence of collagen and elastin with the biomechanical properties of a tissue [25].The mechanical properties of a material result from its internal constitution, including the distributions, orientations and interconnections of constituents. By examining the microstructure of a tissue, it is possible to better understand its functions and interpret what is happening inside the tissue, when it is subjected to applied forces. The microstructure of a tissue is largely dependent on its extracellular matrix (ECM), which provides the tissue with strength and resilience and maintains its shape, orientation, movement and metabolic activity, functioning as a biologically active scaffold, on which the cells can migrate and adhere, in an aqueous environment. ECM is different from one tissue to the other, depending on the cells that populate,

fashion and maintain it, and serves as an anchor for many proteins, such as growth factors and enzymes. The ECM consists primarily of proteins, namely collagen, elastin, fibronectin, laminin and glycosaminoglycans (GAGs) [31]. Some of these proteins can polymerize into elongated structures, forming collagen, reticular and elastic fibers. These elongated fibers are joined together in certain points, by cross-linking, in order to form a three-dimensional network. The molecules are convoluted and thermal energy keeps them in constant thermal motion. Molecular configurations, hence entropy, change with strain and, consequently, elastic stress appears [4]. Collagen and reticular fibers are formed by the protein collagen, and elastic fibers are composed mainly by elastin. These fibers are distributed among the tissue types, conferring specific properties to the tissue, depending on the predominant fiber type.

Collagen is a basic structural element for soft and hard tissues in humans; it gives the body its mechanical integrity and strength, being the main load carrying element in blood vessels, skin, tendons, bone, fascia, etc. It is the most abundant protein in the body (25-30% of all protein, representing 30% of the body's dry weight) and 15 distinct forms have been identified [3, 31].

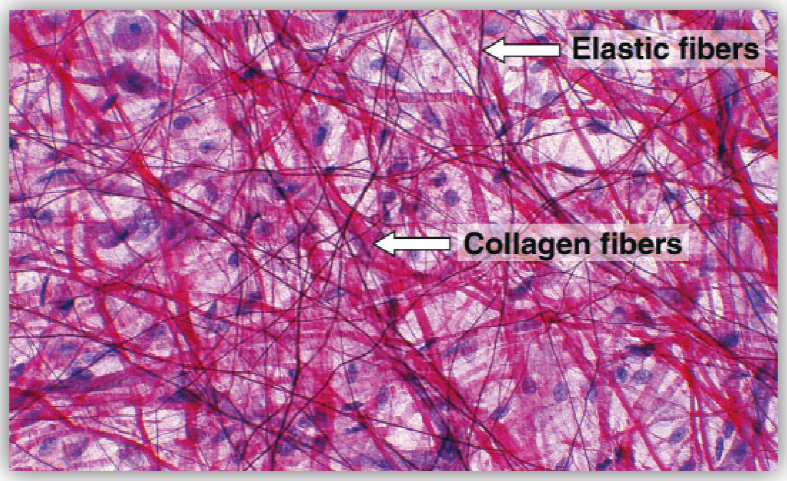

Figure 2.2 Collagen and elastic fibers [3].

Elastin has an amino acid composition similar to that of collagen (both are rich in glycine and proline), but contains two unusual amino acids (desmosine and isodesmosine) whose covalent reactions are thought to account for the rubberlike properties of this protein, which forms fibers at least five times more extensible than rubber [3].

2.3 Tissue types

There are four fundamental tissue types, formed by several sorts of cells and typically by specific associations of cells and extracellular matrix. Most organs are formed by an orderly combination of these tissues, which allows the functioning of complex structures and of the organism as a whole.

Nervous tissue, represented in figure 2.3, is a specialized tissue, which spreads throughout the whole body, allowing the transmission and process of information by the nervous system. It is composed by nerve cells (neurons) and fiber bundles (nerves and ganglia) connected in several interacting networks. Nerves transmit information between brain and spinal cord centers and the sense organs, muscles, etc. Ganglia are responsible for the impulses between different neurological systems. The nervous system has two main components: the central nervous system – which is responsible for stimulus emission and information process – is composed by the cerebrum, cerebellum and spinal cord, with a small amount of connective tissue; and the peripheral nervous system – which connects the body's organs and muscles to the central nervous system – is made of nerve fiber bundles held together by connective tissue sheaths [1, 32].

Figure 2.3 Nervous tissue: microglial cell[1].

Epithelial tissue, represented in figure 2.4, covers the whole body, internal and externally, protecting it and producing secretions. Epithelial layers, which can be formed by a single layer (simple epithelium) or by multiple layers of cells (stratified epithelium), also have absorption, sensation and contractility abilities. Epithelial cells lay on a sheath of connective tissue which provides support and nutrition [1].

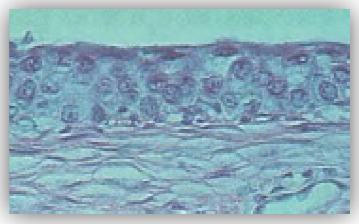

Figure 2.4 Bladder epithelial tissue [1].

Muscle tissue is composed by differentiated elongated cells containing contractile proteins, myofibrils, which can be stimulated electrically or chemically, generating the necessary force for the muscle to contract, using ATP molecules as an energy source. The forces generated by contracting muscle cells are transmitted by the connective tissue that involves the muscle. There are three types of muscle tissue, represented in figure 2.5, that can be distinguished on the basis of morphological and functional characteristics: smooth, cardiac and skeletal, each type with a structure adapted to its physiological role [3].

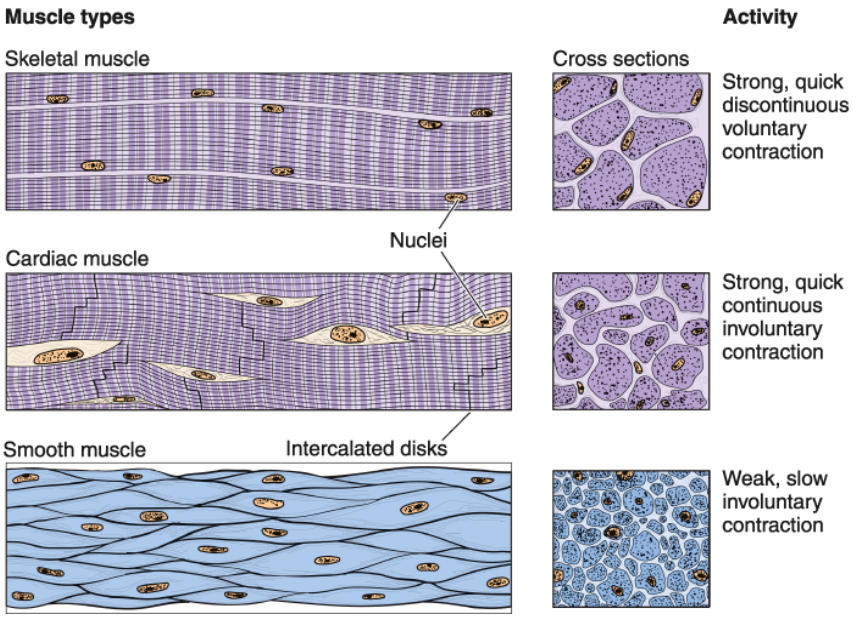

Figure 2.5 Schematic representation of the three muscle types [3].

Smooth muscle consists on sets of fusiform cells, without cross-striations, that form large sheets and produce slow and involuntary contractions being able to remain contracted for long periods of time. Cardiac muscle is very organized, in order to contract and relax in a wave pattern, which produces the heart beatings. It has cross-striations and is composed of elongated and branched individual cells that lie parallel to each other [1].Skeletal muscle is composed of cylindrical multinucleated cells, with a diameter of 10 to 100meanm, forming very long (up to 30cm) bundles – muscle fibers – with cross-striations. The muscle fibers diameter can vary, depending on factors such as the specific muscle, age, sex, nutrition and physical training of the individual. Skeletal muscles are responsible for quick, forceful and voluntary contractions, resulting from the interaction of thin actin filaments and thick myosin filaments whose molecular configuration allows them to slide upon one another; weak interactions in the bridges that bind actin to myosin generate the necessary sliding force. These muscles are connected to bones and tendons, displaying a merge between muscle fibers and connective tissue and having an important role in body movement [3].

Connective tissue, represented in figure 2.6, gives support and protection to the body, being also responsible for the shape taken by the tissue in the body. It is mainly composed of extracellular matrix, combining protein fibers, such as collagen, with viscous and hydrophilic ground substance. It is, therefore, a composite material, having strength and rigidity, provided by the ground substance, as well as flexibility and elasticity, provided by connective tissues' cells (fibroblasts, condroblasts and osteoblasts) and fibers (mainly collagen). There are several types of connective tissue: supportive(bone and cartilage), loose (which holds nerves and vessels in place), dense (similar to loose connective tissue, but containing more collagen) and elastic (abundant in elastic fibers) [3, 5]. Loose connective tissue forms the stroma, which connects tissues of organs, forming sheaths that coat and penetrate the body structures. It can have a support function, for epithelial cells and is able to protect biological structures subjected to low friction and pressure, since it stores water and allows other tissues to move, when subjected to those forces. Dense connective tissue is similar to loose connective tissue, but is stiffer and more resistant to stress, due to the presence of additional collagen fibers. Dense white connective tissue has only a few cells, with fibers as the dominant element. It can be arranged as dense irregular, with collagen fibers arranged in weave bundles, or dense regular connective tissue, having parallel bundles of fibers, molded by directional forces, to offer great resistance to traction [3, 5].

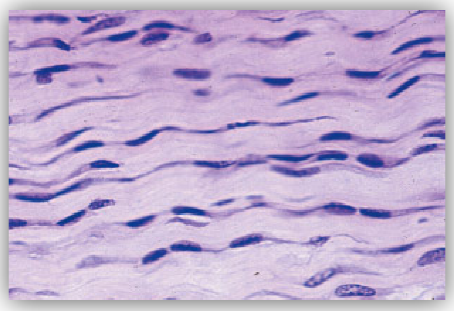

Figure 2.6 Thick bundles of parallel collagen fibers between fibroblasts cells[3].

2.4 Fascia of the Anterior Abdominal Wall

Fascia tissue is the common denomination for all dense, irregular connective tissue sheets in the human body, such as aponeuroses, joint capsules and muscular envelopes. Ligaments and tendons can be considered anatomically as local thickenings of the fascial sheets, adapted to endure increased local tension forces with a denser and more parallel fiber arrangement [33].

Fascia forms a sheath that encloses organs, and muscles, supporting and reducing friction between them. Connective tissue components are continuum with muscles and tendons, connecting these structures to bones. Some authors believe that human fascia may not only act as passive contributor for biomechanical behavior, but also be able to contribute more actively to musculoskeletal dynamics, by spontaneously adjusting its stiffness. This information could help understanding and treating several muscular disorders, associated with increased or decreased myofascial tension or with diminished neuromuscular coordination [33].In fact, some authors have shown that fibroblasts, condroblasts and osteoblasts have contractile properties in the muscle, related to the expression of the gene for α-smooth muscle actin. The expression of this

gene, which can be triggered by environmental factors, happens naturally in fascia tissue, during wound healing or in pathological situations. Furthermore, there are several diseases related to abnormal fascia contractures, such as palmar fibromatosis(Shcleip2005). Fascial sheets also have mechanoreceptors, which provide sensory feedback for muscular coordination. Recently, it was found that patients with chronic back pain have fewer mechanoreceptors in their lumbar fascia, as well as reduced motor coordination [33].

The fascia of the anterolateral abdominal wall consists of subcutaneous (superficial), investing (deep) and intra-abdominal (endoabdominal) portions. The subcutaneous layer is modified in the lower abdomen to include a superficial fatty layer and a deep membranous layer, reinforced by elastic and collagen fibers. This superficial fatty layer is specialized, particularly in males, for lipid storage, whereas the deep membranous layer is complete enough to sustain and accumulate fluids escaping from a ruptured vessel or urethra, as well as allow placement of sutures during surgery. The investing layer is composed by deep fascias, ensheathing voluntary muscles, giving place to the trilaminar arrangement of the flat abdominal muscles and their aponeuroses. The endoabdominal fascia is of particular importance in surgery, enabling the establishment of an extraperitoneal space that allows anterior access to retroperitoneal structures without entering the peritoneal cavity [26].

Superficial, intermediate and deep layers of thin fascia cover the external aspects of the three muscle layers of the anterolateral abdominal wall and their aponeuroses (flat expanded tendons) and cannot easily be separated from them. The internal abdominal wall is lined with a membranous sheet of varying thickness, called endoabdominal fascia. Different parts of this fascia are named according to the muscle it is lining, for example, the portion lining the deep surface of the transverse abdominal muscle and its aponeuroses is called tranversalis fascia [26, 34, 35].

2.4.1Rectus Sheath

The rectus sheath, represented in figure 2.7, is a strong, incomplete and fibrous compartment, composed primarily by collagen fibers, which contains the *rectus abdominis* and pyramidalis muscles, along with nerves, arteries, veins and lymphatic vessels. The rectus sheath allows the muscle to slide through the neighbouring structures, with low friction, protecting them. The sheath is

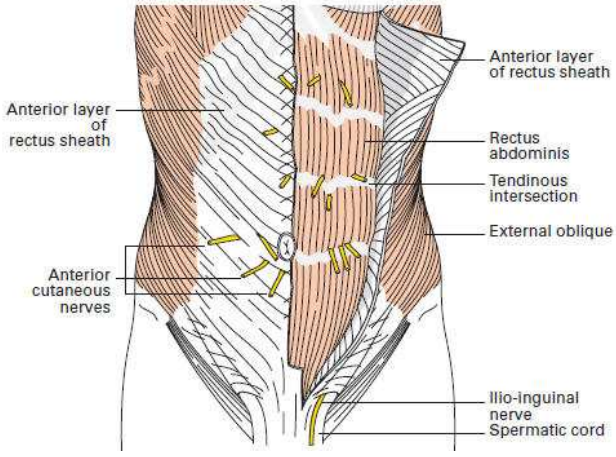

Figure 2.7 Schematic representation of the anterior layer of rectus sheath[2].

formed by the decussation and interweaving of aponeuroses of the flat abdominal muscles. The anterior wall of the sheath is composed by the external oblique's aponeurosis. The superior two thirds of the internal oblique aponeurosis split into two layers, at the lateral border of the *rectus abdominis*; one layer passes anterior to the muscle, joining the aponeurosis of the external oblique, and the other passes posterior to it, joining the aponeurosis of the transverse abdominal. The aponeuroses of the three flat muscles pass anterior to the *rectus abdominis* to form the anterior layer of the rectus sheath, leaving the transversalis fascia to cover the *rectus abdominis* posteriorly. The anterior and posterior layers of fibers interlace in the anterior median line to form the line aalba [26].

2.5 Muscles of the Anterolateral Abdominal Wall

Abdominal wall muscles are constituted by skeletal muscle tissue. The masses of fibers, represented in figure 2.8, are regularly arranged in bundles surrounded by epimysium, which is an external sheath of dense connective tissue that surrounds the entire muscle and extends inward to surround the bundles of fibers within the muscle – the connective tissue around each bundle of muscle fibers is called perimysium, and the connective tissue surrounding each fiber is called endomysium.

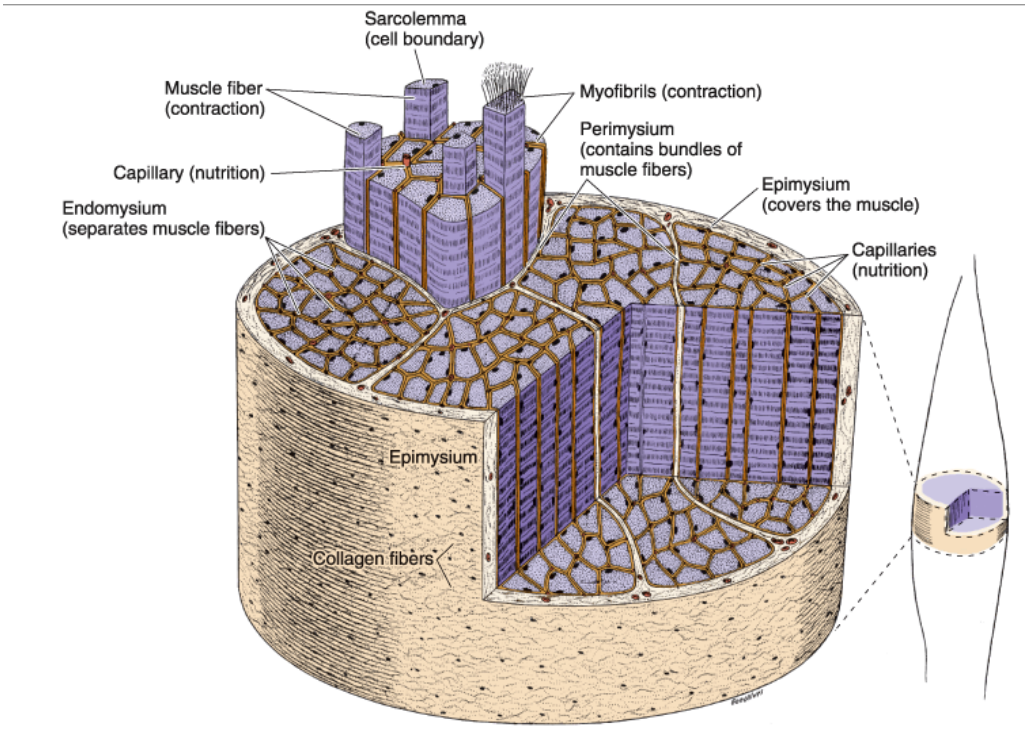

Figure 2.8 Schematic representation of the skeletal muscle internal structure [3].

There are five (bilaterally paired) muscles in the anterolateral abdominal wall: three flat muscles – external oblique, internal oblique and transverse abdominal – and two vertical muscles – *rectus abdominis* and pyramidalis. The muscle fibers of the three concentric layers crisscross each other, with the two outer layers' fibers running diagonally and perpendicular to each other for the main part, and the deep layer's

fibers running transversely. All three flat muscles are continued as strong aponeurotic sheets, which form the rectus sheath, enclosing the *rectus abdominis* muscle. The aponeuroses from both sides interwave, in the abdominal midline, forming the linea alba, so named because it consists of white connective tissue, rather than muscle, extending from the xiphoid process to the public symphysis, as can be seen in figure 2.9 [1]. In this region, the intersection and interweaving of the fibers is not only between right and left sides, but also between superficial and intermediate and intermediate and deep layers.

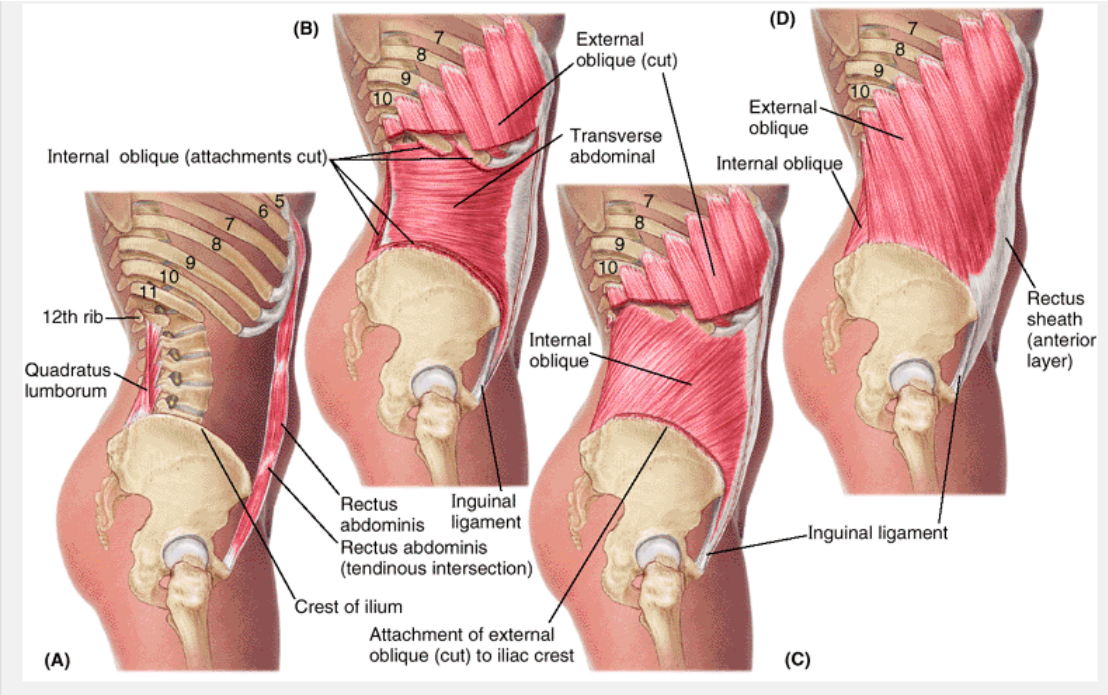

Figure 2.9 Schematic representation of the abdominal muscles: A: Rectus abdominis, B: Transverse Oblique, C: Internal Oblique, D: External Oblique (and Rectus Sheath) [26].

The anterolateral abdominal muscles support the abdominal wall, protect the abdominal viscera from injury, compress the abdominal contents to maintain the intra-abdominal pressure, and also contribute to the trunk movement and posture, against the action of gravity. Compressing the abdominal viscera and increasing intra-abdominal pressure elevates the relaxed diaphragm to expel air during respiration, coughing, sneezing, screaming, etc. When the diaphragm contracts during inspiration, the anterolateral abdominal wall expands and its muscles relax, making room for the organs that are pushed inferiorly. The combined actions of the anterolateral muscles also produce the force required for defecation, micturition, vomiting and parturition [1, 26, 35].

2.5.1 External Oblique Muscle

The external oblique muscle is the largest and most superficial of the three flat anterolateral abdominal muscles. The fleshy part of the muscle contributes primarily to the lateral part of the abdominal wall, and its aponeuroses contribute to the

anterior part of the wall. The more anterior fibers become increasingly horizontally oriented in the medial direction, where the tendinous sheets decussate, at the lineaalba, becoming continuous with the contralateral internal oblique's fibers. The contralateral external and internal oblique muscles together form a working unit, sharing a common central tendon [26].

2.5.2 Internal Oblique Muscle

The internal oblique is a thin muscular sheet and the intermediate of the three flat abdominal muscles. Most of its fleshy fibers run perpendicular to those of the external oblique, becoming aponeurotic in roughly the same line as the external oblique and participating in the formation of the rectus sheath. This muscle is responsible for compressing and supporting abdominal viscera, flexing and rotating the trunk [26].

2.5.3 Transverse Abdominal Muscle

The transverse abdominal muscle is the innermost of the three flat muscles, and its fibers run somewhat transversally, except for the inferior ones, which run parallel to those of the internal oblique. This transverse orientation is suitable for compressing the abdominal viscera and increasing intra-abdominal pressure. Te fibers of the transverse abdominal muscle also end in an aponeurosis, which contributes to the formation of the rectus sheath [26].

2.5.4 Rectus abdominis Muscle

The *rectus abdominis* is the main vertical muscle, consisting on a long, board-like structure, composed by paired rectus muscles, separated by the linea alba. It is a powerful flexor muscle, responsible for the flexion of the trunk and compression of abdominal content. This muscle is three times as wide superiorly as inferiorly, and it is broad and thin superiorly, while narrow and thick inferiorly. Along its course, it is intersected by three or four transverse fibrous bands or tendinous intersections, causing the abdominal wall of a well-muscled person to appear segmented. Most of the *rectus abdominis* muscle is enclosed in the rectus sheath, an aponeurotic tendinous sheath formed by a unique layering of the aponeuroses of the external and internal oblique and transverses abdominis muscles. Approximately 80% of people have a small triangular muscle, the pyramidalis, which is located in the rectus sheath anterior to the most inferior part of the *rectus abdominis* and is responsible for some of the tension applied to the linea alba [26, 35].

Chapter 3

3. Biomechanical Studies

When studying the mechanical properties of a material, it is important to consider the thermodynamics of elastic deformation and the two sources of elasticity, one associated with the internal energy changes and the other with the materials entropy change. Then, the constitutive equations for soft tissues can be obtained [36].

This chapter intends to explain some fundamental concepts which are the foundation for all the biomechanical studies here presented. From the results of these experiments, the mechanical properties of the materials under study can be directly obtained, by using simple mathematic relationships. Since the material in use is composed of organic soft tissue, there are also some handling concerns that have to be taken into account. In order to get the data for analysis, several tension tests have to take place so that the stress-stretch (or stress-strain) mechanical behavior of the material can be understood and modeled.

As a fundamental mean to gather tangible information regarding these tissues' properties, mechanical testing is here presented, in the form of uniaxial and biaxial tensile tests. Such data allows the construction of mathematical models of tissues' behavior and can also be used to enhance the existent synthetic substitutes of the tissues, so as to make the long-term results of implantation acceptable.

3.1 Concepts and Definitions

The most common mechanical tensile test, used to determine structural properties of a tissue is the uniaxial load-elongation test to failure. During the uniaxial assay, the sample is deformed, by applying a gradually increasing tensile load, along the long axis of the specimen and thus producing a deformation which is roughly volume preserving, in the case of highly hydrated soft biological tissues. Uniaxial tensile experiments lead to the concept of quasi linear viscoelasticity, but are limited and do not reflect completely the real situation happening in the organism. In fact, studies have shown that one dimensional loading results cannot be directly compared to results wherein the loads are at least two dimensional in nature [37, 38]. Usually uniaxial experiments are followed by biaxial experiments, which reproduce the three dimensional stresses and strains caused by their complex extracellular matrix components, arranged according to the physiologic demands of that specific tissue's deformation and loading conditions [38].When using a biaxial tension test system, samples are pulled in two perpendicular directions, longitudinal and transversal,

stretching the whole specimen; the specimen's central region suffers the biaxial stress-induced deformation.

Some authors refer to biaxial tensile tests as multiaxial, though multiaxial tests also can be considered as consisting on techniques that imply tension in more than two directions, such as inflation systems, which allows the stress to be spread over a large area, thereby minimizing local concentration and rupture [39, 40].

Tough stiffness is a mechanical property inherent to the material, its measurement is affected by the fact that the specimen is solicited in two directions, simultaneously, causing the obtained stiffness values to increase from uniaxial to biaxial and multiaxial stress states [41].

All tensile tests provide information relating the load (*F*) to which the material is subjected, and the elongation (Δl) that the material consequently suffers. From these quantities, and considering the samples geometry, it is possible to obtain the values for stress (σ) and strain (ε). Stress is the ratio between the load and the samples cross section area, σ=*F*/A, and strain is given by: $\varepsilon = \frac{l_1 - l_0}{l_0} = \frac{\Delta l}{l_0}$, where l_0 represents the initial length and l_1 is the length after deformation.

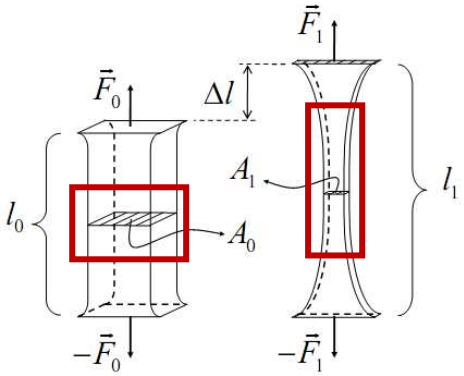

Figure 3.1 Volume preserving transformations during an uniaxial tensile test. Red rectangles represent the volume preserving deformation region of the specimen (adapted from [5]).

Materials which typically display nonlinear behavior, as do the biological soft tissues, are usually studied in view of the nonlinear theory of elasticity [42]. It is usual to use stretch (λ), instead of strain (ε), in the stress-stretch mathematical function σ=f(λ). In this case, stretch is obtained using the expression: $\lambda = \frac{l_0 + \Delta l}{l_0} = \varepsilon + 1$. σ=f(λ) is calculated considering the incompressibility of the material, meaning there is no (significant) volume loss,$V = A_0 l_0 = A_1 l_1$; taking this premise, we consequently get: $\sigma(\lambda_1) = \frac{f}{A_1} = \lambda_1 \frac{f}{A_0}$.

This approximation is more accurate in case the samples deformation is measured on the homogeneous deformation region (Figure 3.1), where the cross section is uniform along the samples length.

To minimize the error induced by this effect, called necking, the samples size should be in a proportion 1:3 or 1:4. When using a biaxial tension test system, samples are pulled in two perpendicular directions (Figure 3.2), longitudinal and transversal, stretching the whole tissue; the necking effect is, therefore, minimized, happening only as a result of the tissues different resistances, due to the different fibers disposition.

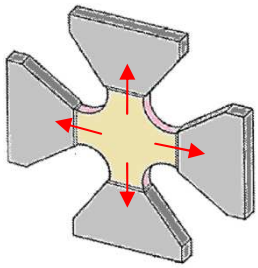

Figure 3.2 Representation of the force direction (red arrows) in the biaxial system(adapted from [43]).

Many tissues are anisotropic, meaning their stress-response varies, depending on the direction the tissue is stretched. Axial coupling is also common, i.e., mechanical properties of the tissue along one axis are dependent on the amount of stress or stretch applied to the other axes. In order to avoid errors, it is important to know tissue orientation prior to testing, and consider all the tissues components.

Thus, to truly characterize tissue behavior, a test should attempt to simulate in vivo loading conditions as closely as possible. Several research groups have developed protocols for biaxial testing of tissue: typically strain is measured optically in both directions, using tissue markers and forces along two orthogonal axes are normalized by the cross-sectional area, to determine the stress. When there is an extended knowledge about the mechanical behavior of the tissue under equibiaxial strain, it is also possible to vary the ratio of stretch between the two axes, and study also the degree and effects of axial coupling [44]. The present work, though, only comprises equibiaxial assays.

3.2 Measurement concerns

It is important to obtain reliable cross-sectional area measurements in order to accurately determine the mechanical properties of a material. When working with soft biological tissues, in particular, there are two methods of obtaining this measurement: contact methods and non-contact methods [44]. Contact methods entail errors due to the need to apply external pressure to the sample, which changes its shape, as well as inaccuracies related to the assumption that the area of a tissue can be described by a geometrical shape, when in fact soft tissues have irregular shapes. Non-contact methods, such as shadow amplitude method, profile method and laser technology, have thus been developed, in order to reduce these errors [44]. Some authors use a micrometer system, which accurately and reliably determine the cross-section area and geometry of soft biological tissues in a non-contact manner [44], while others use

laser reflectance systems, which can measure the cross-sectional area and shape of concave surfaces [44] or, for example, conductance methods to determine the specimen's thickness [38].

It is also necessary to ensure the tensile tests parameters are accurately measured, during the experimental protocols. For this to be accomplished, it is necessary to isolate the tissue and clamp it, securing the tissue, without damaging it. By only measuring the distance between the clamps, in order to determine the length of the specimen for the stretch or strain calculations, some errors are introduced in the measurement. This is due to the artificial boundary condition imposed by the clamp, which can cause local damage as well as unwanted strains near the clamp that can alter the results [44]. To overcome these difficulties, optical techniques can be used, by placing markers (such as reflective tape, ink or contrast beads) on the tissue surface in a region sufficiently far from the clamp, and capturing the position of the markers and their movement, using video registry [38, 40, 44-47]. In the presented work, however, it was not possible to use non contact methods, and for this reason some errors have to be taken into account. In order to reduce the impact of the local damage caused by the clamp, Velcro hooks were used, as explained in the experimental section. All measurements were obtained using a digital caliper even though it may not be the most precise method.

3.3 Mechanical Testing of Soft Biological Tissues

When a classical engineering material is under study, there are two main regions to consider: elastic (A) and plastic (B).

Elastic region represents the linear relation between stress (σ) and strain (ε), given by the Hooke's Law: $\sigma = E\varepsilon$. In this case, the constant of proportionality (E) represents the elasticity modulus, or Young's modulus, which is the slope of the stress-strain curve in the linear section – corresponding to the elastic region – and constitutes the mechanical parameter which indicates the stiffness of a material [4].

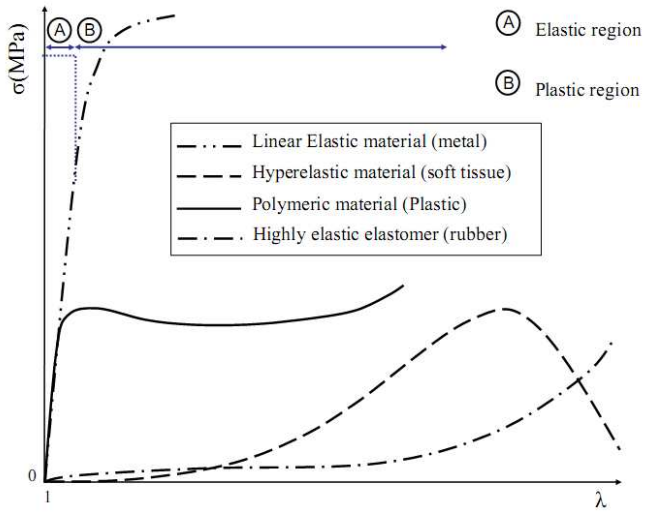

Figure 3.3 Mechanical behavior of linear elastic and hyperelastic materials (adapted from [5]).

Hyperelastic materials don't usually have a linear mechanical behavior, and for this reason, as an alternative to using the Hooke's law of elasticity, a nonlinear mechanical behavior model has to be considered, to represent the permanent, non recoverable deformation that occurs when strain (or stretch) exceeds the elastic limit of the material – the plastic deformation. The plastic deformation region starts at the point, called Yield strength (σ_Y), where the stress-stretch curve becomes nonlinear.

As previously stated, the nonlinear behavior of the biological soft tissue is described by the mathematical function σ=f(λ). In Figure 3.4, the stress-stretch diagram for nonlinear materials, which includes biological soft tissue, is represented.

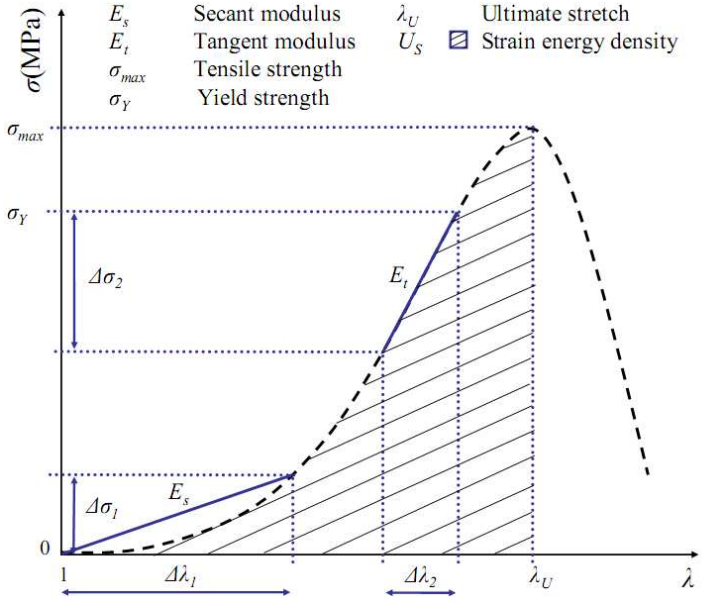

Figure 3.4 Typical mechanical behavior of biological soft tissues(adapted from [5]).

The parameters which describe the mechanical properties obtained from this curve can include the tensile strength (maximal stress), ultimate stretch (stretch

corresponding to the tensile strength), tangent modulus (slope of the stress–stretch curve in the linear region), Yield strength σ_y (which defines the tangent modulus upper limit and represents the point at which the yielding region begins, meaning the stress-stretch curve regains its nonlinear configuration), secant modulus (slope of the stress-stretch curve from the origin to the point where the stress starts having an approximately linear behavior). These parameters can be directly obtained from the graphic representation.

Afterwards, by using mathematical tools, the strain-energy density (area underneath the stress–stretch curve), which is defined as the energy absorbed by the material while being deformed, can be calculated, and further analysis concerning the physical phenomena happening to the tissue can be proposed.

Mechanical properties of a tissue are also dependent on time and strain history (how the tissue is strained up until and during the experiment). For this reason, stress-strain curves during loading and unloading do not follow the same path, and loading-unloading cycles are always different from one to the next, usually displaying an hysteresis effect. This can be related to the viscoelastic phenomenon taking place when the load-deformation (stress-strain/stretch) diagram curve suffers a path deviation [4]. This behavior results from complex interactions of collagen fibers, elastin, proteoglycans and water within the tissue, and can provide us with additional insight into the composition of tissues as well as allow us to build sophisticated models of tissues.

There can be an adaptation of the experimental protocol, in order to include consecutive repetition of identical loading-unloading cycles, with a recovery period between cycles, during which the material is completely unloaded [38, 48]. This procedure is called preconditioning and it (eventually) eliminates the hysteresis effect [4]. However, since the samples are very fragile, and tend to suffer softening effects, and also because some testing equipment is not as flexible as needed, sometimes excessive tissue manipulation is avoided and, for that reason, preconditioning is not always possible to achieve.

3.3.1 Experimental and environmental conditions:

Experimental factors can be determinant for the accurate measurement of rubber-like materials, but most importantly of biological tissues mechanical properties. Several researchers have examined the effects of orientation, strain rate, storage as well as experimental conditions, and their influence on biological tissues properties assessment [44].

Biothermomechanics studies the effects that different thermal treatments can have on materials' biomechanical properties. Though there continues to be a lack of understanding of the temperature level and duration of heating and applied

mechanical loads, many new thermal treatments for diseases and injuries are currently being studied.Data from several scientific studies have revealed that heating-induced changes occur in the material's stiffness, anisotropy, viscoelasticity and extensibility [37]. Many studies have been done, using hyperelastic materials [49], as well as biological tissues, under different temperature states [50].

When examining the properties of a biological tissue, the ideal experimental setting requires to keep the tissue in conditions similar to the physiological ones [51]. Therefore, environmental factors are often considered to ensure a repeatable and reliable protocol, including storage, hydration, and temperature. Rubod et al. have concluded that the effects are minimal, when temperature is kept within levels ranging from 18 to 37ºC, and storage is done using saline solution up to 24h [44].

The presented experiments, similarly to previous studies using biological materials [38], took place inside a 37ºC saline bath, in an effort to mimic the physiological environment.

It is important to notice that, though experimental factors can have significant effects on the measured mechanical properties of a tissue, the effects can vary from tissue type to tissue type, thus when preparing an experiment, it is important not to extrapolate the results of one tissue model to another, without considering the variations dependent on the tissues constituents [38, 45].

Biological tissues' mechanical properties can also vary, depending on age, sex, body mass index, etc, of the individual [3, 38]. Because these parameters can influence the experimental conditions, they have to be considered and were collected, depending on the available information.

3.4 Constitutive Models

The tensile test reflects the resistance of the tissue to applied forces. These tests enable the determination of parameters which are useful for comparisons of the properties of different abdominal layers, but for the purposes of studying the mechanical behavior, appropriate constitutive equations of investigated tissues are necessary [38, 48]. The presented work is based on previous studies [5, 14].

In order to quantify the load and deformation of a certain material, these quantities can be described through constitutive laws. A material's reaction to a certain demand is dependent and characteristic of that material or class of materials, and the main goal of constitutive theories is to develop mathematical models which accurately describe the behavior of the materials, in order to, in the future, be able to predict the mechanical behavior of similar materials [42]. Here, the study is only focused on stress and strain components within a nonlinear regime, and variables such as temperature and entropy are not considered.

Constitutive models can be grouped to include a specific kind of mechanical behavior, such as elasticity, plasticity, viscoelasticity or viscoplasticity. To describe solids behavior, usually Hooke's elastic model for solids is used. However, in the case of soft biological tissues, that model is not adequate.

Elastic behavior is sometimes referred to as non linear, and is associated to the recovery of the initial form, after tension discharge. Because there is a state of deformation different from the initial state, dependent on time, this time effect is taken into account through plastic, viscoplastic, elastoplastic and hyperelastic constitutive laws [42]. When a material presents such behavior, usually a non linear behavior, it does not completely recover its initial form. Hyperelasticity is a constitutive formulation which is particularly convenient, due to its simplicity and is the fundamental basis to more complex models, such as elastoplastic and viscoplastic [42, 52, 53].

3.4.1 Hyperelasticity

The nonlinear theory of elasticity, which constitutes the theoretical basis for the study of hyperelastic materials, such as elastomers and soft biological tissues, uses the Helmholtz free energy function (Ψ) [42], also referred to as strain-energy function or stored-energy function, to describe in energetic terms the mechanical behavior of this class of materials [14]. The strain-energy function $\Psi = \Psi(\mathrm{F})$ is a typical example of a scalar-valued function of one tensor variable F, which is assumed to be continuous. It is obtained from symmetry, thermodynamics and energetic considerations.

On homogeneous materials, the distributions of the internal constituents are assumed to be uniform on the continuous medium, which can be subjected to internal or external forces. For this kind of ideal material, the strain energy function (Ψ) depends solely on the deformation gradient F. On the contrary, for heterogeneous materials, it will depend additionally upon the position of a point in the medium [42].

A hyperelastic material is defined as a subclass of an elastic material, whose response functions have physical expressions of the form:

$$P = \frac{\partial \Psi(\mathrm{F})}{\partial F} \text{ or } P_{aA} = \frac{\partial \Psi}{\partial F_{aA}}. \tag{4.7}$$

Using the following relation for the symmetric Cauchy stress tensor, as the inverse of the expression $\sigma = \mathrm{JPF}^{-\mathrm{T}}$:

$$\sigma = J^{-1} P F^T = \sigma^T \tag{4.8}$$

And keeping in mind the Jacobian determinant, $\mathrm{J} = \det \mathrm{F}$, it is possible to obtain:

$$\sigma = J^{-1} \frac{\partial \Psi(\mathrm{F})}{\partial F} F^T = J^{-1} F \left(\frac{\partial \Psi(\mathrm{F})}{\partial F} \right)^T \tag{4.9}$$

Or,

$$\sigma_{ab} = J^{-1}F_{Ab}\frac{\partial \Psi}{\partial F_{Ab}} = J^{-1}F_{aA}\frac{\partial \Psi}{\partial F_{bA}} \tag{4.10}$$

These types of expression are known as constitutive equations or equations of state. They allow the establishment of an axiomatic or empirical model as the basis for approximating the behavior of a real material [42].

Equations 4.7 and 4.8 present the derivative of the scalar valued function Ψ for a given scalar tensor F determines the energy gradient of Ψ, which is a second order tensor, known as the first Piola-Kirchhoff stress tensor P. The derivation requires that the component function $\Psi(\mathrm{F_{aA}})$ is differentiable with respect to all components $\mathrm{F_{aA}}$.

To simplify, it is assumed that the strain energy function tends to zero, meaning that F=I, and this assumption is expressed by the normalization condition:

$$\Psi = \Psi(\mathrm{I})=0 \tag{4.11}$$

From physical observation, it is known that strain energy function increases with deformation, which allows the deduction:

$$\Psi = \Psi(\mathrm{F}) \geq 0 \tag{4.12}$$

This restricts the ranges of admissible functions occurring in expressions for the strain energy.

These last expressions (4.11 and 4.12) assure that the reference configuration, which is called residual stress, is zero. In this case, the reference configuration is stress-free. Additionally, for the behavior at finite strains, it is necessary to satisfy the following conditions:

$$\Psi(\mathrm{F}) \to +\infty \mathrm{if} \det \mathrm{F} \to +\infty$$

$$\Psi(\mathrm{F}) \to +\infty \mathrm{if} \det \mathrm{F} \to 0^{+}$$

Physically, this means that an infinite amount of strain energy is necessary in order to expand a continuum body to the infinite range or to compress it to a point with vanishing volume [42].

3.4.2 Hyperelastic Incompressible Materials

Hyperelastic incompressible materials are materials that deform, without volume variations, i.e.:

$$J = 1 \tag{4.13}$$

To derive constitutive equations for hyperelastic incompressible materials, it is possible to define the following strain energy function:

$$\Psi = \Psi(\mathrm{F}) - \mathrm{p}(\mathrm{J} - 1) \tag{4.14}$$

Where the strain energy function Ψ is conditioned by $J = detF = 1$. p is a scalar value defined as the undetermined *Lagrange* multiplier, which can be identified as a hydrostatic pressure. This scalar p can only be determined using the equilibrium equations and the boundary conditions.

By differentiating equation 4.14, with respect to the deformation gradient F and using $\frac{\partial J}{\partial F} = JF^{-T}$, it is possible to arrive at a general constitutive expression for the first Piola-Kirchhoff stress tensor P. Hence:

$$P = -pF^{-T} + \frac{\partial \Psi(\mathrm{F})}{\partial F} \tag{4.15}$$

And multiplying this expression by F^{-1}, from the left-hand side, it is possible to conclude that the second Piola-Kirchhoff stress tensor S takes the form:

$$S = -pF^{-1}F^{-T} + F^{-1}\frac{\partial \Psi(\mathrm{F})}{\partial F} = -pC^{-1} + 2\frac{\partial \Psi(\mathrm{C})}{\partial C} \tag{4.16}$$

Where $C^{-1} = F^{-1}F^{-T}$ is the inverse relation of the Right Cauchy-Green tensor $C = F^T F$.

However, if equation 4.16 is multiplied by F^T from the right-hand side, it is possible to conclude, from the expression $\sigma = J^{-1}PF^T = \sigma^T$, that the symmetric Cauchy stress tensor σ can be expressed as:

$$\sigma = -pI + \frac{\partial \Psi(\mathrm{F})}{\partial F}F^T = -pI + F\left(\frac{\partial \Psi(\mathrm{F})}{\partial F}\right)^T \tag{4.17}$$

Fundamental constitutive equations 4.15, 4.16 and 4.17 are the most general forms used to define incompressible hyperelastic materials at finite strains. For the case of isotropy, a suitable strain energy function for isotropic materials, considering a set of independent strain invariants of the symmetric Cauchy-Green tensors C and b, is: $\Psi = \Psi[\mathrm{I}_1(\mathrm{C}), \mathrm{I}_2(\mathrm{C}), \mathrm{I}_3(\mathrm{C})] = \Psi[\mathrm{I}_1(\mathrm{b}), \mathrm{I}_2(\mathrm{b}), \mathrm{I}_3(\mathrm{b})$, where the Left Cauchy-Green tensor $b=FF^T$. However, when considering incompressibility, one should consider the following kinematic restriction:

$$I_3 = detC = detb = 1 \tag{4.18}$$

The two main invariants, I_1 and I_2, are defined as:

$$I_1 = \lambda^2 + \frac{2}{\lambda} \tag{4.19}$$

$$I_2 = 2\lambda + \frac{1}{\lambda^2} \tag{4.20}$$

The strain energy function for isotropic incompressible hyperelastic materials, where p/2 represents an undetermined *Lagrange* multiplier is given by:

$$\Psi = \Psi[I_1(C), I_2(C)] - \frac{1}{2}p(I_3 - 1) = \Psi[I_1(b), I_2(b)] - \frac{1}{2}p(I_3 - 1) \quad (4.21)$$

In order to examine the associated constitutive equation, in terms of the two principal strain invariants I_1 and I_2, it is possible to derive the expression 4.21, with respect to tensor C, obtaining:

$$S = 2\frac{\partial\Psi(I_1,I_2)}{\partial C} - \frac{\partial[p(I_3-1)]}{\partial C} = -pC^{-1} + 2\left(\frac{\partial\Psi}{\partial I_1} + I_1\frac{\partial\Psi}{\partial I_2}\right)I - 2\frac{\partial\Psi}{\partial I_2}C \quad (4.22)$$

Which is basically the constitutive equation:

$$S = 2\frac{\partial\Psi(C)}{\partial C} = 2\left[\left(\frac{\partial\Psi}{\partial I_1} + I_1\frac{\partial\Psi}{\partial I_2}\right)\right]I - \frac{\partial\Psi}{\partial I_1}C + I_3\frac{\partial\Psi}{\partial I_3}C^{-1} \quad (4.23)$$

Where the term $I_3\left(\frac{\partial\Psi}{\partial I_3}\right)$ is replaced by $-\frac{p}{2}$.

In order to find a constitutive equation for incompressible materials, which expresses Ψ as a function of the three principal stretches λ_a, it is possible to write $\Psi(\lambda_1, \lambda_2, \lambda_3) - p(J - 1)$, in the place of equation 4.14, with the indeterminate *Lagrange* multiplier p.

Several materials, including fascia and muscle tissue, are composed of a matrix or ground substance, and one or more families of fibers. Since these materials, called composites or fiber-reinforced composites, have fibers continuously arranged in the matrix material, they have strong directional properties and their mechanical responses are regarded as anisotropic. A material which is reinforced by only one type of fibers has a single preferred direction. Its stiffness in the fibers direction is typically much greater than in the directions orthogonal to the fibers. This material is called transversely isotropic with respect to this preferred direction. When responding to an effort orthogonal to the fibers, the behavior is isotropic [42]. Here, the fibers are assumed to be continuously distributed throughout the material, which is why the following models are based on constitutive equations which model transversely isotropic incompressible materials.

3.4.3 Models for Incompressible Materials

Some strain energy functions, related to the constitutive theory of finite elasticity, particularly for isotropic hyperelastic materials, are known as rubber-like elasticity.

There are several models that can simulate different materials hyperelastic behavior, such as Yeoh, Ogden, Mooney-Rivlin, neo-Hookean models.

Depending on the use of an uniaxial system, an equi-biaxial or a biaxial system, appropriate stress relations must be derived, with respect to the systems specific conditions and restrictions. In the presented work, uniaxial and equi-biaxial systems are focused.

3.4.3.1 Yeoh Constitutive Model

Some authors have pointed out that for rubber-like materials, $\partial\Psi/\partial I_2$ is numerically close to zero. Yeoh simplifies this expression, considering it zero, and proposes a strain energy function of three terms, where the second invariant does not appear:

$$\Psi = C_1(I_1 - 3) + C_2(I_1 - 3)^2 + C_3(I_1 - 3)^3 \quad (4.24)$$

Where, C_1, C_2, and C_3 are material constants which satisfy certain restrictions.

From the expression given in 4.12, the strain energy function can be described as:

$$\Psi \begin{cases} =0, \text{ if } \Psi \text{ has a single real root, corresponding to } I_1=3 \\ >0, \text{ if } I_1>3 \end{cases}$$

Note that for an incompressible material, $I_1>3$, being $I_1=3$ only on the reference configuration. For this reason, the strain energy function increases with $I_1$and $\partial\Psi/\partial I_1 = 0$ without any real root. From the discriminants of the respective cubic and quadratic equations in $(I_1 - 3)$ the appropriate restrictions on values for C_1, C_2 and C_3 may be determined.

Transverse elasticity modulus, G, involves first and second order terms in $(I_1 - 3)$ and approximates a non linear physical behavior with a satisfactory exactitude, if $C_2 < 0$ e $C_1 > 0, C_3 > 0$ [42]:

$$G = 2C_1 + 4C_2(I_1 - 3) + 6C_3(I_1 - 3)^2 > 0 \quad (4.25)$$

In order to obtain the stress relations to the boundary and loading conditions in which the experiments occur, the following is considered:

Biaxial System:

$\lambda_1 \neq \lambda_2$ From which we can obtain:

$$\begin{cases} \sigma_1 = 2\left(\lambda_1^2 - \dfrac{1}{\lambda_1^2\lambda_2^2}\right).(C_1 + 2C_2(I_1 - 3) + 3C_3(I_1 - 3)^2) & (4.26) \\ \sigma_2 = 2\left(\lambda_2^2 - \dfrac{1}{\lambda_1^2\lambda_2^2}\right).(C_1 + 2C_2(I_1 - 3) + 3C_3(I_1 - 3)^2) & (4.27) \end{cases}$$

Equi-biaxial System:

$\lambda_1 = \lambda_2 = \lambda$ From which we can obtain:

$$\sigma = 2\left(\lambda^2 - \frac{1}{\lambda^4}\right).(C_1 + 2C_2(I_1 - 3) + 3C_3(I_1 - 3)^2) \quad (4.28)$$

3.4.3.2 Ogden Constitutive Model

Ogden model presents a good correlation, when dealing with high deformations. Here, the free energy function is based on the principal stretches (λ_1, λ_2, λ_3):

$$\Psi{=}\Psi\ (\lambda_1, \lambda_2, \lambda_3){=}\sum_{p=1}^{N}\frac{\mu_p}{\propto_p}(\lambda_1^{\propto p} + \lambda_2^{\propto p} + \lambda_3^{\propto p} - 3) \quad (4.29)$$

Where N is a positive integer which determines the number of terms in the strain-energy function, μ_p are constant shear moduli and $\propto_p$ are dimensioneless constants.

Again, in order to evidence the stress relations, depending on the conditions in which the experiments occur, it is possible to obtain the following specifications:

Biaxial System:

$\lambda_1 \neq \lambda_2$ From which we can obtain:

$$\begin{cases} \sigma_1 = \sum_{i=1}^{N}\mu_i\left[\lambda_1^{\propto i} - (\lambda_1\lambda_2)^{-\propto i}\right] & (4.30) \\ \sigma_2 = \sum_{i=1}^{N}\mu_i\left[\lambda_2^{\propto i} - (\lambda_1\lambda_2)^{-\propto i}\right] & (4.31) \end{cases}$$

Equi-biaxial System:

$\lambda_1 = \lambda_2 = \lambda$ From which we can obtain:

$$\sigma = \sum_{i=1}^{N}\mu_i\left[\lambda^{\propto i} - (\lambda)^{-2\propto i}\right] \quad (4.32)$$

3.4.3.3 Mooney-Rivlin Constitutive Model

Mooney-Rivlin model can be understood as a particular case of Ogden (4.29), if N=2, $\propto_1 = 2, \propto_2 = -2$.

By using deformation invariants I_1 and I_2, it is possible to obtain the expression:

$I_1 = \lambda_1^2 + \lambda_2^2 + \lambda_3^2$ and $I_2 = \lambda_1^2\lambda_2^2\lambda_3^2 + \lambda_2^2\lambda_3^2$, with the restriction: $I_3 = \lambda_1^2\lambda_2^2\lambda_3^2 = 1$. This way, the strain energy function for this constitutive model is:

$$\Psi = C_1\left(\lambda_1^2 + \lambda_2^2 + \lambda_3^2 - 3\right) + C_2\left(\lambda_1^{-2} + \lambda_2^{-2} + \lambda_3^{-2} - 3\right) = C_1(I_1 - 3) + C_2(I_2 - 3) \quad (4.33)$$

Where C_1 and C_2 are material constants, which verify the restrictions:

$C_1 = \frac{\mu_1}{2}$ and $C_2 = \frac{\mu_2}{2}$

According to [42], this model offers more precision on the representation of non linear isotropic material behavior, such as rubber-like materials.

Deducing the stress relations, taking into account the conditions in which the experiments occur, it is possible to obtain the following specifications:

Biaxial System:

$\lambda_1 \neq \lambda_2$ From which we can obtain:

$$\begin{cases} \sigma_1 = 2\left(\lambda_1^2 - \frac{1}{\lambda_1^2\lambda_2^2}\right)\left\{\frac{\mu_1}{2} - \lambda_2^2\frac{\mu_2}{2}\right\} & (4.34) \\ \sigma_2 = 2\left(\lambda_2^2 - \frac{1}{\lambda_1^2\lambda_2^2}\right)\left\{\frac{\mu_1}{2} - \lambda_1^2\frac{\mu_2}{2}\right\} & (4.35) \end{cases}$$

Equi-biaxial System:

$\lambda_1 = \lambda_2 = \lambda$ From which we can obtain:

$$\sigma = 2\left(\lambda^2 - \frac{1}{\lambda^4}\right)\left(\frac{\mu_1}{2} - \lambda^2\frac{\mu_2}{2}\right) \quad (4.36)$$

3.4.3.4 Neo-Hookean Constitutive Model

Neo-Hookean model is also a particular case of Ogden model, with N=1 and $\propto_1 = 2$. The free energy function, based only upon the first deformation invariant, is:

$$\Psi = C_1\left(\lambda_1^2 + \lambda_2^2 + \lambda_3^2 - 3\right) = C_1(I_1 - 3) \quad (4.37)$$

Once again, adapting these expressions to the conditions in which the experiments occur, it is possible to obtain the following specifications:

Biaxial System:

$\lambda_1 \neq \lambda_2$ From which we can obtain:

$$\begin{cases} \sigma_1 = 2\left(\lambda_1^2 - \frac{1}{\lambda_1^2\lambda_2^2}\right)\frac{\mu_1}{2} & (4.38) \\ \sigma_2 = 2\left(\lambda_2^2 - \frac{1}{\lambda_1^2\lambda_2^2}\right)\frac{\mu_1}{2} & (4.39) \end{cases}$$

Equi-biaxial System:

$\lambda_1 = \lambda_2 = \lambda$ From which we can obtain:

$$\sigma = 2\left(\lambda^2 - \frac{1}{\lambda^4}\right)\frac{\mu_1}{2} \quad (4.40)$$

3.4.4 Final Remarks

Hyperelastic material models can capture more accurately the nonlinear mechanical behavior of materials such as polymers, rubbers and many biological tissues. In Chapter 5 some classical hyperelastic constitutive laws are applied to the constituents of the abdominal wall in an effort to fit a theorized curve to the experimental results obtained during the development of this work.

Chapter 4

4. Experimental Setup

In order to obtain information about the mechanical properties of fascia and muscle tissue, it is necessary to collect, prepare and test the samples. Here an explanation of these steps is given, providing a general overview of these procedures, as well as a description of the biaxial tension tests equipment that will be used and technical requirements for working with highly hydrated biological tissue. Finally, there is a description of the result analysis methods, providing a general idea of the software that is used to process and interpret data.

The experimental component of this work relies mostly on Human soft tissue testing. Tensile testes were done on samples from several tissues: *rectus abdominis* fascia tissue and *rectus abdominis*, internal oblique, external oblique and transverse abdominal muscles.

The tensile testing equipment used for the tests is a prototype developed in the Biomechanics Laboratory (LBM-IDMEC), University of Porto (Portugal). And because the equipment is a prototype, before performing tests on human tissue, which must not be squandered, mechanical testing of hyperelastic materials (vulcanized rubber and silicone) took place. The mechanical properties of both vulcanized rubber and silicone are already well known, but it is still important to do trial tests and obtain a basis for comparison for the biomechanical tests, for which the tensile testing equipment was originally designed.

It is much simpler to prepare samples from rubber and silicone materials, as they are not as soft or slippery. When handling biological tissues, additional precautions have to be considered, not only to prevent injury, but also to assure the accuracy and reproducibility of the tests. Though this chapter comprises tests done on both hyperelastic materials and biological tissues, the experimental procedure is mostly focused on biological tissue preparations, which is the core subject of this work.

4.1 Sample collection

As previously discussed, biomechanical testing was performed using samples from fascia tissue and several muscle groups from the anterolateral abdominal wall. All the samples were excised from human corpses during autopsies carried out at the North branch of Instituto Nacional de Medicina Legal, I.P.l, by medical doctor Maria Moura, by means of dissecting the abdominal wall, layer by layer from the exterior, inwards. In all the autopsies the necessary precautions were taken not to leave noticeable exterior tissue damage on the body and it was given preference to the left side of the

individual, except for Cd02, in which case samples were collected from the right side because, due to an operation of the abdomen, there was scar tissue on the left.

Fascia tissue was separated from the exterior fatty layer and (interiorly) from *rectus abdominis* muscle and delivered as a single sheet, approximately 25 per 25 mm size. Since only uniaxial tests were performed on muscle tissue, muscle samples were provided giving preference to the fibers direction, i.e. all pieces were approximately 25-30mm wide in the transversal direction per 50mm in the fibers direction (longitudinal). Both fascia and muscle samples retrieved were as thick as the tissue itself, meaning that the originally collected fascia and muscle samples depth is the actual thickness of the fascia and muscle of the individual. The samples were then placed in individual analysis containers, with a refrigerated 0,9% saline (B. Braun Medical solution [54]); the containers were kept inside a thermos, in order to be preserved during transportation from INML to IDMEC. All the mechanical tests were done within the 24h after collecting the tissues.

Before mechanically testing the tissues, individual specimens were prepared from the original samples, since the samples were large and had different morphologies. Several laboratorial hygiene and health precautions were taken, such as the use of gloves and disinfectants; after the tests, the remaining tissues were put back in the original containers, frozen and taken to INML to properly be disposed of.

4.2 Specimen Preparation

To mechanically characterize tissues, it is necessary to guarantee a homogeneous geometry of the specimens, a planar surface, and an appropriate sample size. The collected samples have to be cut, so that these requirements can be met. When cutting a specimen, it is essential to mind the fibers direction, the overall structure and adequate size for the test, as well as the tissues inherent defects.

When performing uniaxial tensile tests, it is usual to have a geometrically controlled specimen, in order to facilitate calculations and be able to reproduce the tests. When working with rubber or plastic materials, this is simple to obtain, however, it is not easy to achieve a standard shape, once working with soft tissues, and for this reason there is a source of error here, which has to be considered when analyzing results.

Isotropic hyperelastic engineered materials have a uniform configuration, thus cutting homogeneous (uniaxial and biaxial) specimens is easier. Biological tissues on the other hand present complex element organization, and adjustments have to be thought-out. Given the fibers uniaxially oriented nature of muscle tissue, only uniaxial testing took place in the case of the muscles. As to fascia tissue, depending on the available and usable (not damaged) sample amount, just biaxial or both uniaxial and biaxial tensile tests were performed. As can be seen in figure 4.1, fascia fibers (A), as

well as muscle bundles (B) are visible to the naked eye, highly oriented and molded by directional forces, depending on the tissues' functions. Note that transverse abdominal muscle is merely given as an example, though all the muscles have similarly oriented fibers.

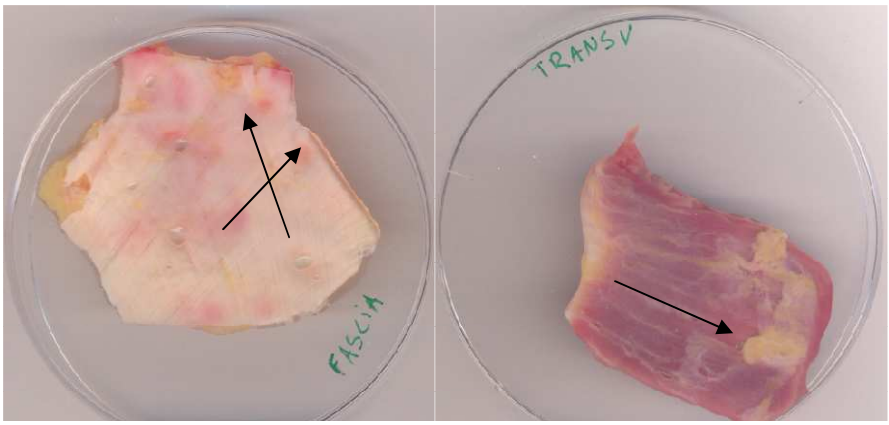

Figure 4.1 Fascia sample, highly oriented in two dominant directions (A); Transverse abdominal muscle, highly oriented in one dominant direction (B).

In order to prepare the test specimens, a scalpel was used to cut approximately rectangular uniaxial samples, according to the dominant fiber direction. Cutter tools – 5x5 mm central square region for hyperelastic materials and 7,5x7,5 mm central square section for biological samples – were used to cut cruciform biaxial vulcanized rubber, silicone and fascia samples, in order to allow a similar stress on both axes, because depending on the geometry of the test piece, the stress state can be highly inhomogeneous [41].

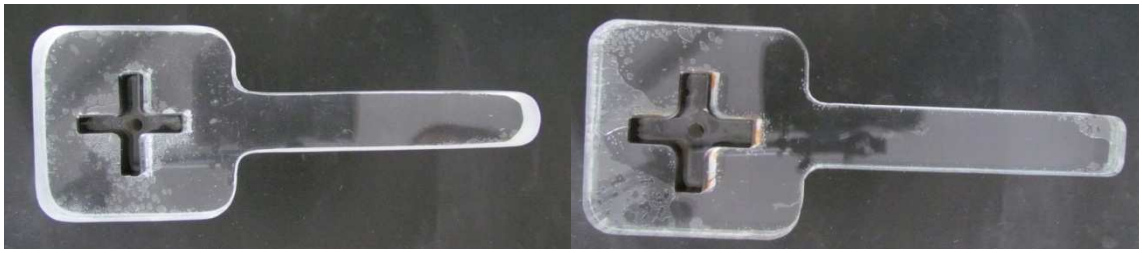

Figure 4.2 Cutter tools: on the left, a 5x5 central square region cutter; on the right a 7,5x7,5mm central square region cutter.

On biological samples, visible defects, such as tweezers indentation marks and fibrous tissue, can cause different mechanical behavior and for this reason were excluded, except in some of the muscle samples (*rectus abdominis* and external oblique from Cd07). These samples had damaged regions, presenting hematoma; as it

will be discussed later on, two types of specimen were excised from each of them and compared: non damaged muscle and damaged muscle.

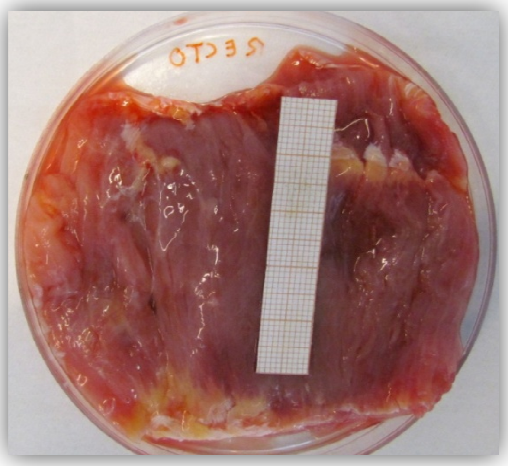

Figure 4.3 Rectus abdominis sample, from Cd07, with a hematoma region on the right.

Fascia samples are very thin, containing slim layers of superimposed fascia sheets. These layers have differently oriented fascia fibers and work as a unit, responding to the tissues' functions demands in the organism. When using both the cutter tool and the scalpel to prepare (biaxial and uniaxial) specimens, the sample was treated as a whole, meaning the thin layers were not intentionally dissociated. However, when a sample presented an unattached thin connective tissue layer, that did not present many visible fibers, and altered the desired final specimen shape, this layer was removed. When preparing biaxial samples, the cutter tool was placed on the fascia sample, taking notice in order to assure that the (more noticeable) fibers direction coincided to one of the cruciform shaped cutter's direction. The cutter was secured and pressure was applied, using a rubber hammer, so that the blade would carve the sample, in all directions. The residual connections, between the cut specimen and the remaining sample were severed using a scalpel.

As for muscle tissue, as it was previously described, it is composed by variable diameter muscle fibers, joined together forming bundles of fibers. These bundles are tightly grouped forming a united piece, as thick as the original muscle, from which it was isolated. *Rectus abdominis* and internal oblique muscles are especially thick; therefore, when preparing/ cutting samples, a special attention has to be given to be able to obtain a specimen as thin as desired, without damaging the fiber bundles. Though there are exceptions, in most of the cases, the original muscle sample was not excessively thick, and therefore it was possible to only cut the sample in the vertical plane, i.e. only cut the sides of the sample in order to obtain a rectangular shape. When the muscles were too thick (mainly samples from *rectus abdominis* and internal oblique), the samples were also cut in the horizontal plane, giving preference to the internal muscle zone, without damaging the muscle fiber bundles, meaning that the

more degraded zone, which was in contact with the exterior (saline solution) the longest was preferentially removed.

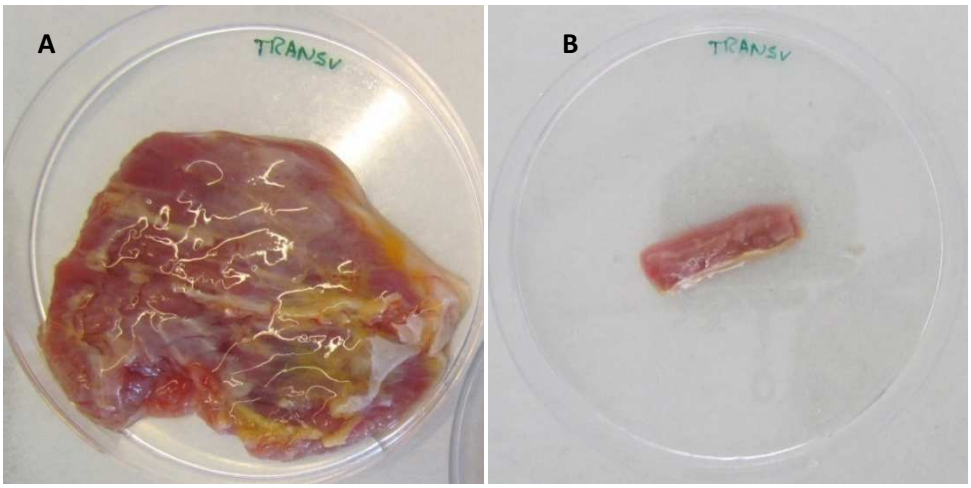

Figure 4.4 Transverse abdominal muscle prior and after sample preparation. A: original collected sample; B: final uniaxial specimen.

All specimens were assembled using a costume designed mounting frame to clamp the specimens at the four actuators' directions, in the undeformed configuration. The mounting frame, shown in figure 4.5, minimizes the specimen's damage prior to the tests and also permits that there is a fixed standard position, conferring reproducibility to the tests.

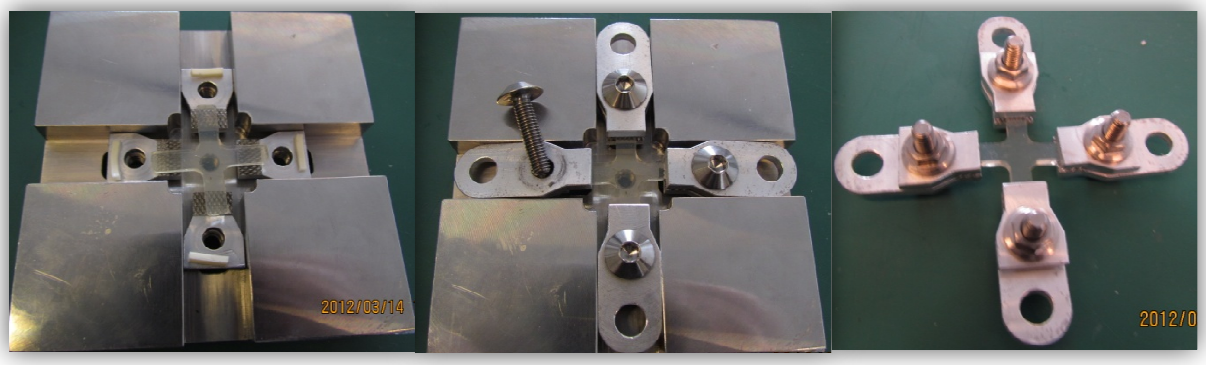

Figure 4.5 Assembly of a biaxial silicone specimen.

For uniaxial specimens, two grips were used, while for biaxial specimens, four were needed. Since tissues are soft and deformable, special attention was given, to prevent the tissue from becoming lopsided. Also, since soft tissues are slippery, Velcro hooks were pasted to the aluminum grips to better secure the specimens and distribute the stress concentrated in the grip-tissue contact region.

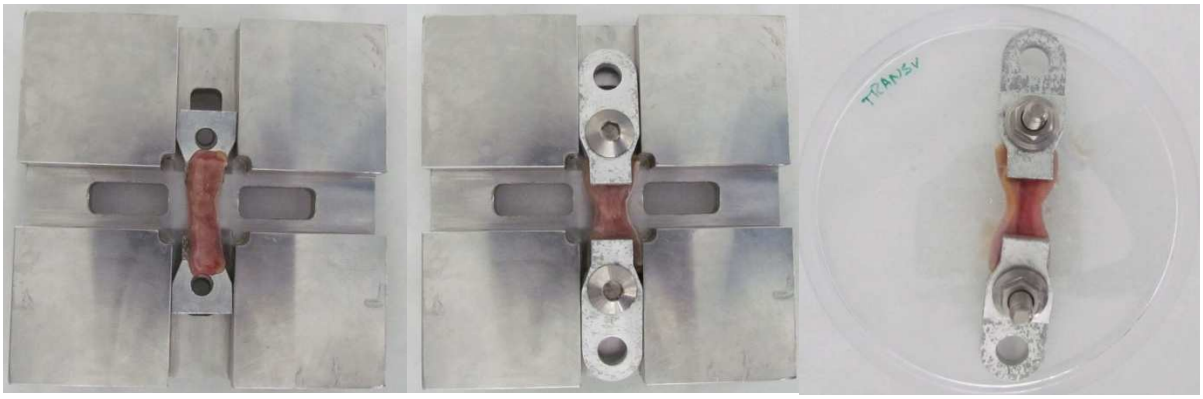

Figure 4.6 Assembly of a transverse abdominal uniaxial muscle specimen.

After assembly, the specimen is removed from the mounting frame, its thickness is measured, using a digital caliper (accuracy 0-100mm ±0.02 / 100-150mm ±0.03), and it is mounted in the tensile testing machine.

4.3 Tensile Testing Equipment

As stated, the tensile testing equipment used is a prototype developed at IDMEC's Biomechanics Laboratory. Figure 4.7 represents the experimental setup equipment's components.

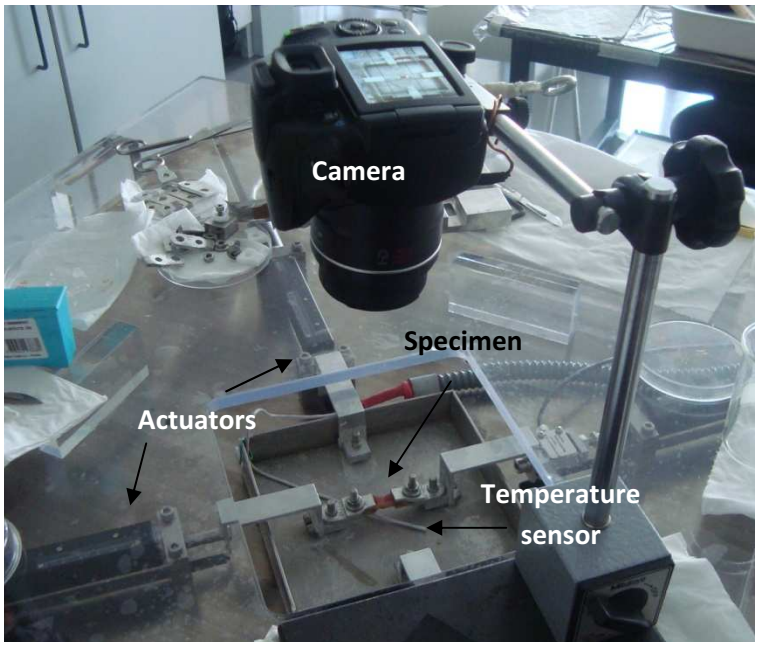

Figure 4.7 Tensile testing equipment, with mounted uniaxial muscle sample.

The biaxial tensile test system is constituted of four perpendicular aluminum arms that connect to four separately controlled displacement and force measurement

actuators. The aluminum grips holding the specimen are fitted to these aluminum arms, by adjusting the arms position to hook the grips. This is done inside the testing container, which is full with a 0,9% saline solution (B. Braun Medical [54]) kept at 37ºC, in some of the tests using hyperelastic materials and in all tests performed on biological tissues. The bath temperature is controlled by a thermostat (see the sensor shown in figure 4.7). Between the aluminum parts (arms and grips), there are teflon rings, placed to ensure that the interface between the pieces can slide over one another, without much friction (since Teflon, or Polytetrafluoroethulene, has one of the lowest coefficients of friction against any solid). However, in some tests performed on biaxial fascia specimens, the aluminum grips were not allowed to slide and freely adjust, because in the first tests it was verified that axial coupling had a strong influence on the results, i.e. when one of the sample's arms started to given in to the strain, the rotation in the loading plane led to an unpredictable/uncontrolled stress state.

This concludes the test setup, though it is worth noticing that the bath should be prepared approximately half an hour before testing, in order to have a stabilized temperature when the specimen is put inside the container. Before the test beginning, all specimens' initial dimensions were measured, using the digital caliper (accuracy 0-100mm ±0.02 / 100-150mm ±0.03), while the specimens were subjected to a 0,2N preload (in the case of silicone and biological samples) or 0,5N (in the case of vulcanized rubber).The preload guaranteed a pre-testing controlled initial geometry and loading conditions, contributing to the reproducibility of the experimental procedure.

From here on, the test is controlled by the software and video image is obtained by the camera positioned over the testing container, as displayed in figure 4.7. All uniaxial specimens were tested until failure, by applying a displacement rate of 5mm/min along the specimen in one direction. As for biaxial fascia specimens they were subjected to 5mm/min along both axis.

The used software/program is configured to present a simple interface, which allows the user to choose the force and displacement parameters adequate to each test.

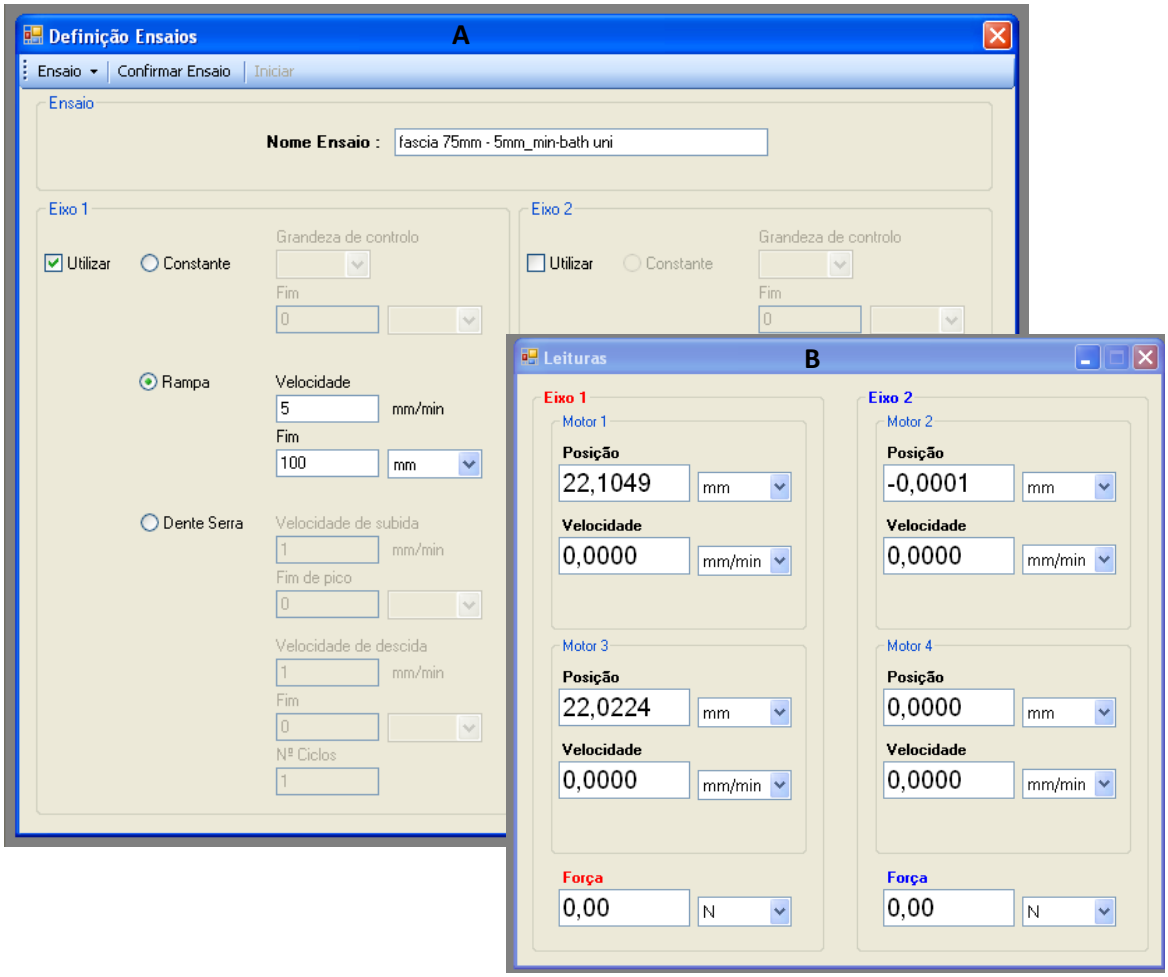

Figure 4.8 Testing parameters definition window (A); Axis readings (B).

As can be seen in Figure, (A) shows the testing parameters definition window, where the displacement rate can be selected for axis one, two, or both. During all tests, the load was applied on Ramp mode, using 5 mm/min displacement rate. After the parameter selection, the position of the four motors, their velocity and the applied force are displayed on the readings window (figure (B)).

4.4 Data processing

All tests were recorded and video image of some of the tests was captured, in order to have some quality control over the tests. If a specimen slips from the grips or if it is not aligned properly, the test is not valid, and thus, it was not considered.

Isotropic hyperelastic materials did not go through much data processing, as the data retrieved from the tests can be directly graphically represented, without further concerns.

As for tissues, since their structural properties are thought to vary depending on hormonal factors, age difference, donor's body mass, disease, etc [3, 38], some personal information was collected. However, there was not much information

available, concerning, for example, parity, diseases and medications, therefore, these factors were not considered on the results analysis.

To treat all data, and analyze the load and displacement obtained on each test, MATLAB® was used. MATLAB®is a high-level language and interactive environment which allows the execution of computationally intensive tasks, providing simple data analysis functions as well as fair and easy to edit data representations. In this case, this tool was used to obtain a clear data interpretation from which it is possible to get all the reliable information needed from the collected data. Stress-strecth curves were produced, in order to gain some insight into the influence of tissues characteristics on the mechanical properties, through comparisons between different samples. Existing MATLAB® scripts, developed by Pedro Martins, in the Biomechanics Laboratory [5], were used to process data.

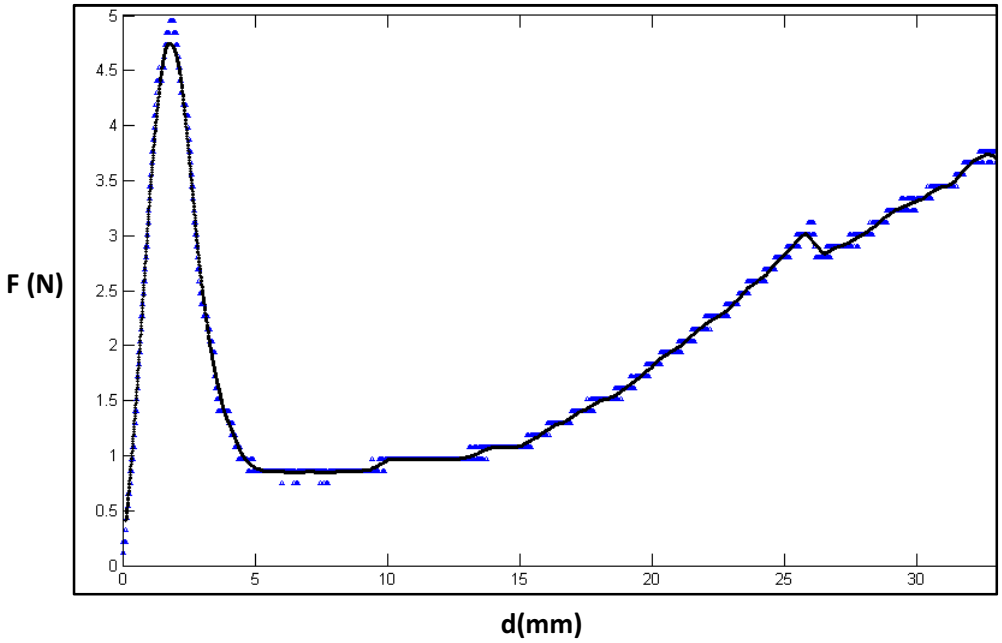

Figure 4.9 Force-displacement graphic representation of an example specimen, before processing.

Figure 4.9 represents the obtained force and displacement data, from which a curve is drawn, by convoluting the points acquired during the tests. The aperture number can be selected, in order to consider more or fewer points, considering a compromise between having a faithful representation of data and having a curve from which it is possible to obtain parameters that describe the mechanical behavior of the material. There is also information here that can be discarded, since the present work only focuses on the specimen until rupture.

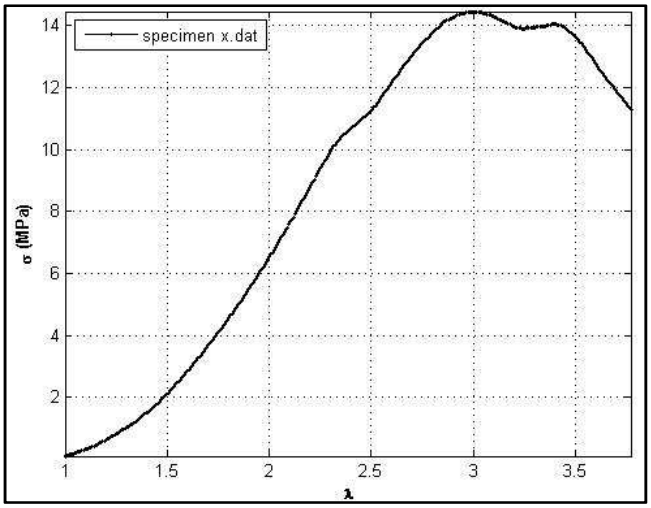

Figure 4.10 Stress-stretch graphic representation of an example specimen, after processing.

Figure 4.10 represents the final stress-stretch curve, from figure 4.9, obtained after adjusting the curve to the obtained data and selecting the final point of interest for the representation. From this graphic, Tensile Strength σ_{max} (MPa) and correspondent Ultimate Stretch λ_U, Strain Energy Density U_S (nJ/m^3), Tangent Modulus E_t (MPa) and Secant Modulus E_s(MPa), and Yield Strength σ_Y can be acquired.

After data visualization and interpretation, some numerical optimization of material parameters for hyperelastic materials were performed, with the purpose of studying physical hypothesis used to build a hyperelastic constitutive model able to characterize the mechanical behavior of abdominal fascia and muscle tissue.

Optimization algorithms take given numerical criteria and, depending on the experimental results produced, converge to an optimal and stable solution, i.e. they work by fitting a theoretical curve, based on more stable solutions for each experimental test and approximate to the experimental results curve representation. Furthermore, as more experimental tests take place, more information is gathered and as the optimization criteria improve, the optimization algorithm gets stronger.

Here, again, existing MATLAB® scripts, developed by Pedro Martins, in the Biomechanics Laboratory [5], were used.

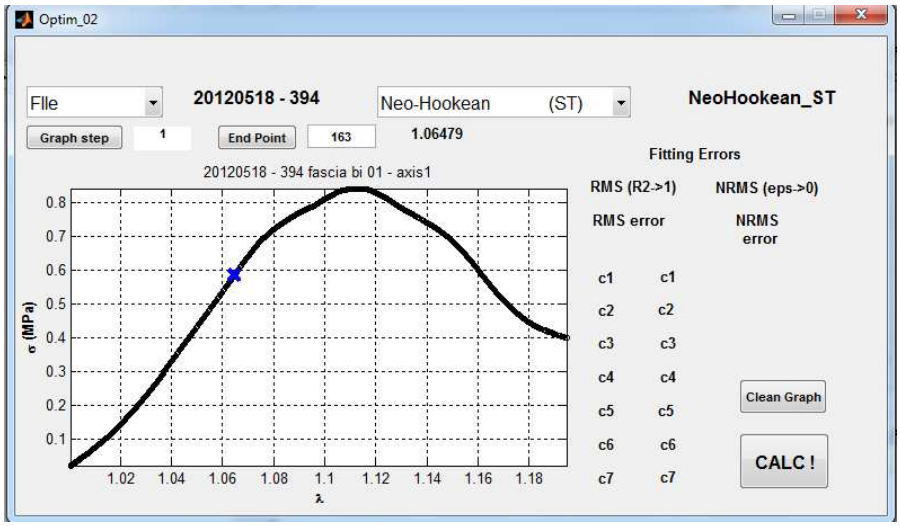

Figure 4.11 Numerical optimization software interface.

The scripts offer an interface that enables data input, data selection and model selection. Input data can come from experimental data files or Matblab's workspace variables, and the graphical end point of interest for a specific analysis can be determined. This interface also allows the input of optimization parameters that can be used to study a particular Strain Energy Function, depending on the chosen model. When all parameters are set, the optimization process can be started.

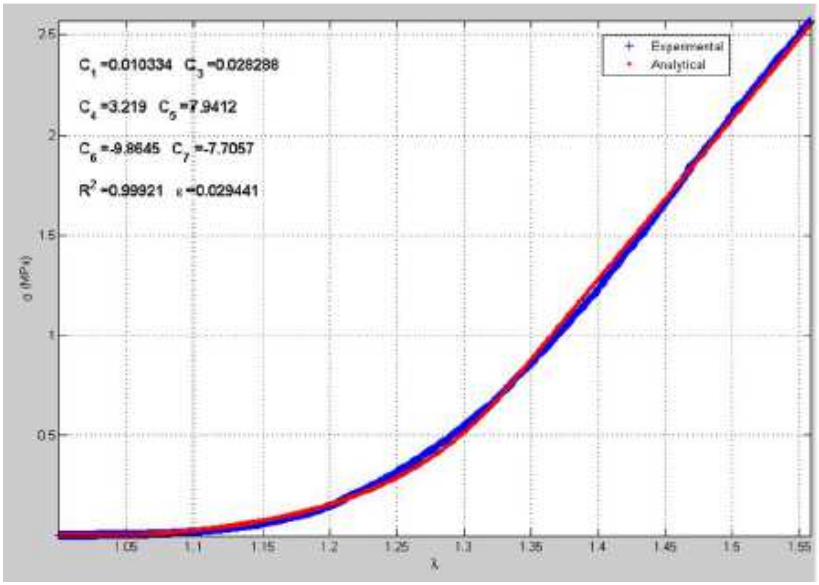

Figure 4.12 Fitting result for an example test, for the elastic behavior of the specimen.

Figure 4.12 A shows a graphic representation of a curve fitting, concerning the elastic behavior of an example specimen. Fitted parameters and error appear on the graphic display of results.

4.5 Final Remarks

This work is mostly focused on the experimental procedure, and does not extend on the use of numerical approximations, or model fitting. Nevertheless, some examples are attempted, to illustrate the possibility of a deeper mathematical correlation to the underlining physics, which explains the mechanical behavior of the studied biological tissues.

Chapter 5

5. Results and Discussion

The main goal of the present work was to study the mechanical behavior of isotropic hyperelastic materials – vulcanized rubber and silicone – and, most importantly, biological tissues – rectus abdominis, internal oblique, external oblique and transverse muscles and fascia tissue. From the data acquired by the tensile testing equipment – applied force and consequent deformation – it is possible to compare the behavior of all the different subjects and study the influence of several factors.

5.1 Primary Analysis

When preparing isotropic hyperelastic materials, the cutting direction is not important. The influence of the 37ºC saline bath was studied using these materials, therefore, two uniaxial and two biaxial specimens of vulcanized rubber and of silicone were cut, so that one could be tested inside the bath and the other without the bath. Summing up to a total of eight (8) specimens. It is important to mention that, when considering the biaxial specimens, their analysis was done, regarding a biaxial specimen as if it was actually composed of two separate uniaxial specimens, meaning that the two axes were analyzed separately, as if two independent uniaxial experiments. When interpreting these tests, this situation has to be accounted for.

All biological tissues' uniaxial tests were done having the tissue cut with fibers in the longitudinal direction. As to biaxial fascia tissue, the fibers were longitudinally displayed for axis 1, and oblique for axis 2, as none of the fascia samples had orthogonal fibers.

The total number of specimens analyzed is one hundred and nineteen (119): five (5) biaxial specimens (which were treated as ten (10) uniaxial ones); fifteen (15) uniaxial fascia specimens; twenty four (24) specimens of external oblique, twenty three (23) from the internal oblique, twenty eight (28) from *rectus abdominis* and twenty four (24) from the transverse muscle. The reason why there are not samples for every tissue type from all the cadavers is because in some individuals (particularly drowning victims) tissue's are strongly connected to one another, due to biochemical reactions *post-mortem*; as for fascia tissue, some of the collected samples had defects, and biaxial specimens were not as easily cut out, and sometimes there was not enough undamaged sample to cut; since it is hard to find out the actual time of death, sometimes biochemical reactions started before the death was certified, and the body started to decompose sooner than expected, resulting in putrefied samples, which cannot be mechanically tested.

All these samples were taken from a total of twelve (12) cadaver individuals, seven (7) male and five (5) female, referred to as Cd01 to Cd12. Individual age ranged from 17 to 73 years (mean=45, standard deviation=15.08). Data concerning weight and height were also collected and body mass index was calculated, according to the expression BMI=Weigth(Kg)/Height^2(m^2), and compared. Information regarding Menopausal state (Mnp) was gathered only for three individuals, and for this reason, this parameter will not be considered, when discussing all the information in order to put the results into context. All the relevant information gathered along the tissue collections is summarized in table II. Death certification date (DCT) and tissue collection date (TCD) not always coincide, because, due to legal issues, it is not always possible to do the autopsy on the same day of the obit certification. Still, it is worth mentioning that when a cadaver awaits autopsy, it is kept in a refrigerated environment, without freezing, for it could damage the tissues. All mechanical testing took place within the 24h after tissue collection, as previously discussed.

Table I: Information concerning the donor individuals.

Individual	Age	Sex	Height (m)	Weight (Kg)	BMI** (Kg/m^2)	Mnp**	DCD** (dd/mm/yyyy)	TCD** (dd/mm/yyyy)
Cd01	45	Male	1.83	80	23.89	-	17/05/2012	18/05/2012
Cd02	50	Male	1.6	77	30.08	-	17/05/2012	17/05/2012
Cd03	54	Male	1.66	64	23.23	-	17/05/2012	18/05/2012
Cd04	42	Female	1.7	66	22.84	N	25/05/2012	28/05/2012
Cd05	22	Female	1.67	85	30.45	N	26/05/2012	28/05/2012
Cd06	17	Male	1.78	71	22.41	-	30/05/2012	31/05/2012
Cd07	46	Male	1.71	76	26.00	-	04/06/2012	05/06/2012
Cd08	53	Female	1.57	53	21.50	-	10/06/2012	12/06/2012
Cd09	73	Female	1.52	70	30.30	Y	13/06/2012	13/06/2012
Cd10	57	Male	1.7	57	19.72	-	13/06/2012	14/06/2012
Cd11	36	Female	*	*	*	-	15/06/2012	18/06/2012
Cd12	45	Male	1.68	55	19.49	-	16/06/2012	19/06/2012

*data not available

**BMI refers to body mass index, Mnp to menopausal state; DCT to death certification date; TCD refers to tissue collection date.

Considering the following table, it is possible to characterize individuals from whom the samples were collected, regarding their body mass index.

Table II - Standard weight status categories associated with Body Mass Index (BMI) ranges for adults [55].

BMI	Weight Status
Below 18.5	Underweight
18.5 - 24.9	Normal
25.0 - 29.9	Overweight
30.0 and Above	Obese

According to Table I and II, individuals Cd01, Cd03, Cd04, Cd06, Cd08, Cd10 and Cd12 have normal weight, while individual Cd07 is overweighted and Cd02, Cd05 and Cd09 can be considered borderline obese. It is, however, important to consider that this is a relative measurement, and that, since men usually have more muscle mass as opposed to fat, when compared to women, men frequently have a slightly greater BMI than women. Data concerning height and weight were not obtainable for Cd11, thus this person is not considered when studying the possible BMI effects on tissues' mechanical properties.

5.2 Assessment of the Mechanical Properties

In order to analyze all samples, their initial measurements were considered, and the mean values were obtained. Isotropic hyperelastic materials are very uniform, and though their shape slightly varied, depending on the cut, their thickness was maintained at 2mm for vulcanized rubber and 0.5mm for silicone samples. As for length and width, both vulcanized rubber and silicone were cut to have similar dimensions, having a length of approximately 15mm (mean=15.86mm; StDev=2.31)and width of approximately 5mm (mean=4.93mm; StDev=0.21) for all samples.

Muscle thickness (mean mean=2.79mm; stardard deviation StDev=0,85) is much greater than fascia's (mean=0.95mm; StDev=0.37). As for length and width, both muscle and fascia were cut to have similar dimensions. Muscle tissue has a mean length of 14.30mm, StDev=4.14 and mean width of 6.66mm, StDev=1.81, while fascia tissue has a mean length of 12.11mm, StDev=2.91 and mean width of 6.39mm, StDev=1.41.

Though sample's dimensions do not have a major impact on the final results, the specimen's geometry is important, when considering the necking effect, which is not very significant on biaxial specimens but can have some consequence on uniaxial ones. Given the size limitations of collected samples, it is advised that a proportion of at least approximately 1:3 for width:length ratio should be considered. When using biological

tissues, due to logistic limitations, this proportion was not possible to obtain for every specimen; this effect was not considered on calculations, but can induce some errors.

5.2.1 Classical Approach

As it was explained on Chapter 3, figure 3.4, several parameters can be obtained from the stress-stretch curve, representing the mechanical behavior of the material under study. Here, data were obtained for Tensile Strengthσ_{max} (MPa) and correspondent Ultimate Stretchλ_U, Strain Energy Density U_S (nJ/m^3), Tangent Modulus E_t (MPa) and Secant ModulusE_s(MPa), and Yield Strengthσ_Y. Figure 5.1 shows some of the parameters being retrieved from the graphic representation of an uniaxial fascia sample, from Cadaver03. All specimens exhibited a non linear mechanical response, and this graphic representation is here given as an example.

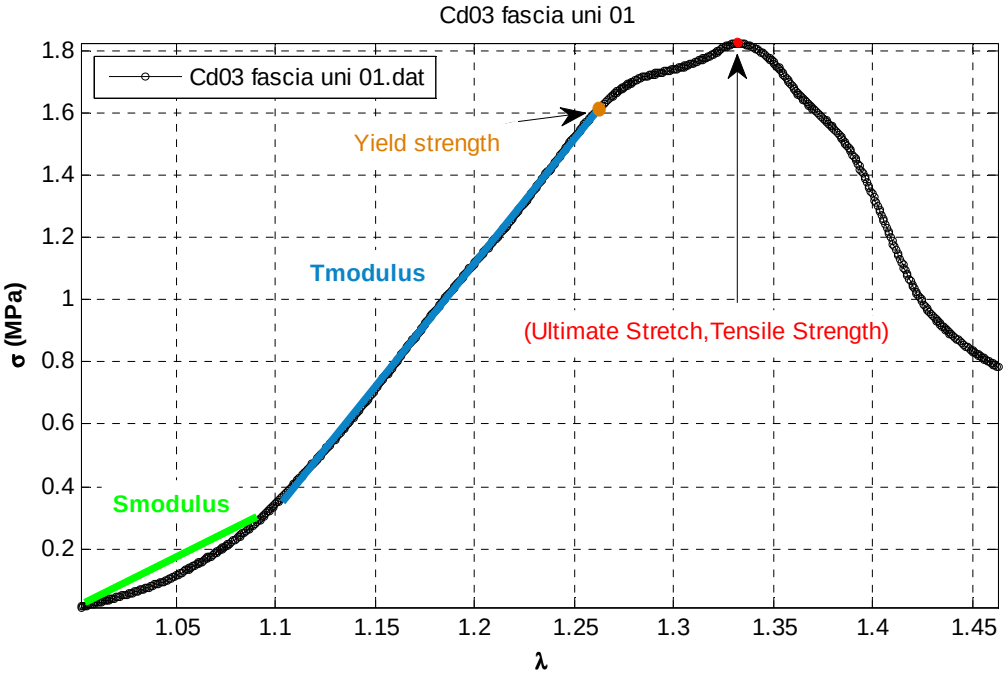

Figure 5.1 Graphic representation the stress-stretch curve of an uniaxial fascia sample from Cd03, and some parameters that were obtained from it. This specimen was subjected to a displacement rate of 5mm/min.

The data presented in this chapter was collected, according to the procedures discussed in Chapter 4. The mechanical tests performed are considered destructive tests, meaning that the specimens tested are irreversibly damaged. The mechanical testing process was applied for isotropic hyperelastic materials, and afterwards on biological tissues, as described.

5.2.1.1 Isotropic Hyperelastic Materials

Table III: Obtained parameters from the stress-stretch curves of all the isotropic hyperelastic materials' uniaxial (uni) and biaxial (bi) samples.

Specimen	condition	σ_{max} (MPa)	λ_U	U_S (nJ/m^3)	E_t (MPa)	σ_Y (MPa)	E_s(MPa)
bi silicone1	dry	15.51	3.78	18.55	6.89	9.89	3.24
bi silicone2	dry	13.84	3.46	14.73	6.67	9.39	3.46
bi silicone1	bath	8.99	2.93	7.48	6.08	6.04	2.39
bi silicone2	bath	8.33	2.69	5.75	6.43	6.64	2.30
uni silicone	dry	13.43	3.87	15.98	5.47	8.95	2.39
uni silicone	bath	6.29	3.50	6.26	3.23	3.96	1.13
bi vrubber1	dry	4.29	1.67	1.84	6.25	3.44	14.77
bi vrubber2	dry	4.37	1.57	1.50	8.24	2.63	14.12
bi vrubber1	bath	4.14	1.82	2.22	4.39	3.20	10.83
bi vrubber2	bath	4.10	1.61	1.43	6.62	2.91	6.18
univrubber	dry	3.24	1.35	0.64	10.49	2.04	16.18
univrubber	bath	2.46	1.53	0.62	4.59	1.57	5.07

By comparing both specimens, it is possible to see that silicone sustains higher stresses (mean=11.06 MPa, StDev=3.68), when compared to Vulcanized rubber (mean=3.77 MPa, StDev=0.76), though the bathed silicone was not tested until rupture. Silicone gives in, when stress is applied, and deforms much more (mean=3.37, StDev=0.47) than does vulcanized rubber (mean=1.59, StDev=0.16); this is due to its flexible molecular arrangement [51]. Graphic representations in Figure 5.2, show that for dry materials (vulcanized rubber or silicone), the initial curve slope is more accentuated than for the dry samples (higher tangent modulus), which points to their stiffer behavior. Yield strength is also much higher for silicone than vulcanized rubber, and when comparing dry and bathed samples, it is observed that bathed samples start to give in sooner before the breaking point, again pointing towards a softer behavior.

The stress-stretch curves in Figure 5.2 show the mechanical response, i.e. Cauchy stress (σ) vs stretch (λ), of both vulcanized rubber and silicone, under uniaxial loading, while dry and subjected to a 37ºC saline bath. All specimens exhibit a non linear mechanical response, as can be seen in the presented plots.

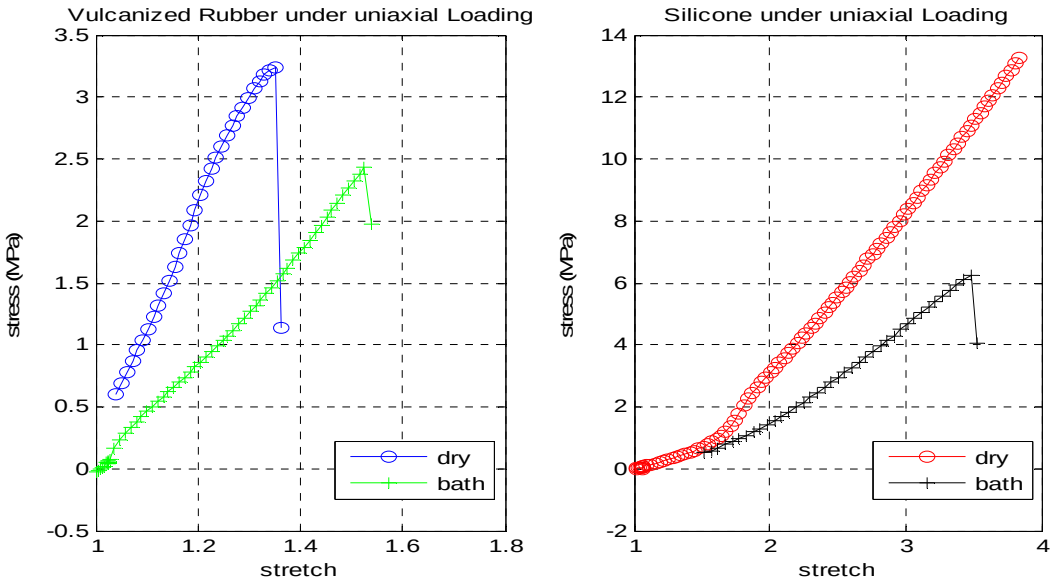

Figure 5.2 Graphic representation of vulcanized rubber (on the left) and silicone (on the right), under uniaxial loading, both dry and inside a 37ºC saline bath.

It is possible to observe that the 37ºC saline bath has a significant effect on the vulcanized rubber behavior: when dry, vulcanized rubber is less deformable, and a greater stress is necessary, in order to stretch the sample; when the sample is in the 37ºC saline bath, it becomes softer, more compliant, being able to sustain a larger deformation, though it does not support high stresses.

As to the silicone sample, while dry silicone can sustain larger stresses than the bathed silicone, in this case bathed silicone's deformation is not as large. These differences, however are not very significant, because only one specimen was considered for each case, thus to reach definitive conclusions, more specimens testing is needed. Here it is noticeable that dry silicone sustains larger deformations, since the specimen was tested until the maximum stretch the equipment allows and did not break, which permits the observation that silicone is a soft and flexible polymer.

The stress-stretch curves in Figure 5.3 shows the mechanical response, i.e. Cauchy stress (σ) vs stretch (λ), of vulcanized rubber, under biaxial loading, while dry and subjected to a 37ºC saline bath. Both perpendicular directions of each specimen are represented separately. Again, all specimens exhibit a non linear mechanical response, as can be seen in the presented plots.

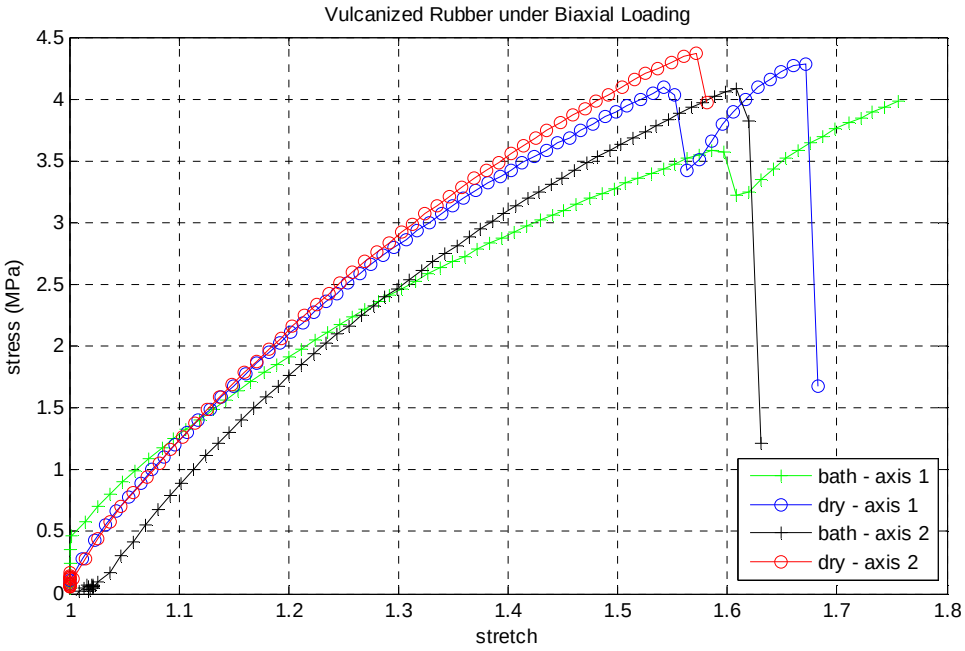

Figure 5.3 Graphic representation of vulcanized rubber, under biaxial loading, both dry and inside a 37ºC saline bath. For each specimen, both perpendicular directions are represented.

Under biaxial loading, vulcanized rubber has a similar behavior than does when under uniaxial loading: it sustains a similar stretch and the range of stresses is also not very different. It is possible to infer that, once again, when the specimen is dry, it sustains higher stresses, breaking at approximately the same stretch that the bathed samples. There is some deviation, when comparing both directions of one sample; this is probably due to the sample's stiffness and possibly to axial coupling, meaning that the force applied in one axis influences the other's response.

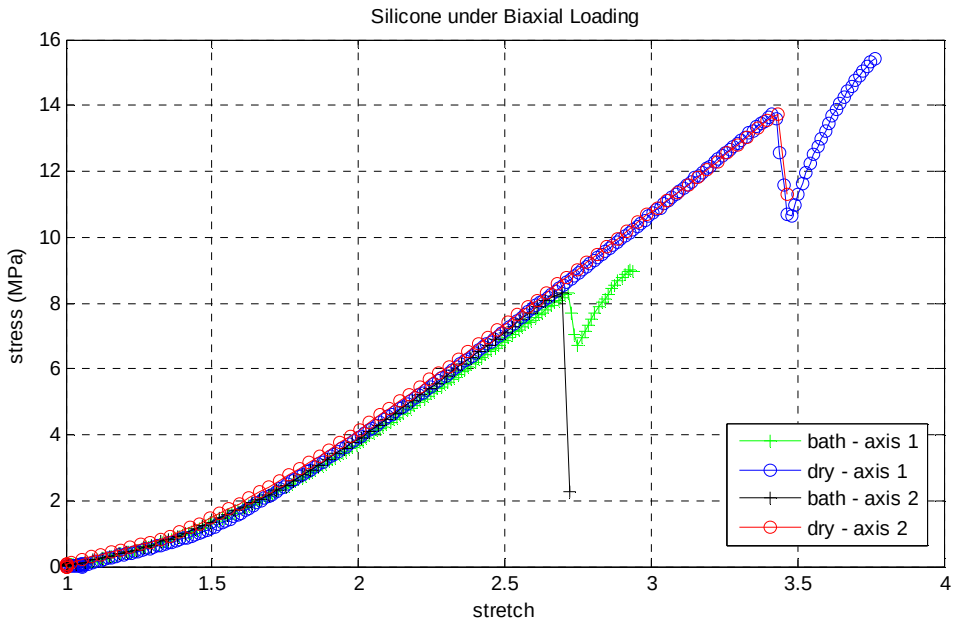

Figure 5.4 Graphic representation of silicone, under biaxial loading, both dry and inside a 37ºC saline bath. For each specimen, both perpendicular directions are represented.

Under biaxial loading, it is firstly visible that for the same sample, the silicone stretched on both directions behaves similarly, i.e. there is no axial coupling, meaning that the changes happening in one axis do not influence the other. It is possible to observe that the bathed silicone sustains a smaller deformation, when compared to the dry specimen and even when compared to the uniaxial bathed specimen. As to the dry silicone, the deformation is similar to the uniaxial sample, but under biaxial loading, the supported stress is higher.

For biaxially tested specimens, it is visible (on Figures 5.3 and 5.4) that the tangent modulus for bathed materials (both vulcanized rubber and silicone) is less accentuated, when compared to dry specimens. Again, this indicates that bathed materials become softer at a 37ºC humid environment.

By comparing uniaxially tested materials to the biaxial experiments, it is not possible to reach a confident conclusion as to the changes in the materials' stiffness, since the curves' profiles are similar; none the less, biaxially tested silicone seems to have a higher tangent modulus, when compared to uniaxial silicone.

Though further testing would be needed to characterize vulcanized rubber and silicone materials, this was not the main objective of the present work, thus a greater focus was given to biological tissues samples.

5.2.1.2 Anisotropic Hyperelastic Materials

Contrary to isotropic hyperelastic materials, mentioned in the last section, biological materials can be considered anisotropic hyperelastic materials, since their mechanical properties can be different for distinct directions.

Tabel IV: Mean values and standard deviation (StDev) for all the parameters obtained from the stress-stretch curves of all the samples.

Specimen		σ_{max} (MPa)	λ_U	U_S (nJ/m^3)	E_t (MPa)	σ_Y (MPa)	E_s(MPa)
Uniaxial Fascia	**mean**	**2.86**	**1.56**	**0.95**	**9.06**	**2.27**	**3.54**
	StDev	2.39	0.28	1.70	6.78	1.75	2.72
All muscles	**mean**	**0.47**	**1.92**	**0.21**	**0.79**	**0.40**	**0.31**
	StDev	0.39	0.40	0.23	0.57	0.35	0.16
External oblique	**mean**	**0.57**	**1.98**	**0.25**	**1.00**	**0.48**	**0.33**
	StDev	0.32	0.34	0.19	0.67	0.28	0.16
Internal oblique	**mean**	**0.39**	**1.94**	**0.17**	**0.65**	**0.34**	**0.26**
	StDev	0.19	0.37	0.10	0.29	0.18	0.13
Rectus abdominal	**mean**	**0.23**	**1.60**	**0.07**	**0.52**	**0.20**	**0.33**
	StDev	0.14	0.18	0.05	0.26	0.14	0.16
Transverse	**mean**	**0.73**	**2.19**	**0.38**	**1.03**	**0.63**	**0.31**
	StDev	0.58	0.44	0.33	0.74	0.54	0.19

From the data displayed on table IV, it is possible to establish several parallels, for example, between uniaxial fascia and muscle tissue: it is possible to observe that uniaxial fascia is less deformable than muscle, presenting a mean ultimate stretch value of 1.56 (StDev=0.28), as compared to all the muscles (either the muscles mean value (1.92, StDev=0.40), or the muscles, separately). The correspondent tensile strength (σ_{max}) is much greater for uniaxial fascia tissue (mean=2.86MPa, StDev=2.39) than for muscles (again, either their mean value (mean=0.47MPa, StDev=0.39), or separately). This means that though muscles don't support as much stress as fascia, they have a more compliant behavior, deforming more when lower stresses are applied.

As for yield strength, fascias' values are higher than muscles', but only because fascia sustains higher stresses; in fact, it is observable that fascia tissue starts to give in sooner before the breaking point, which points towards a more adjustable behavior of fascia. i. e. when subjected to high stresses, fascia starts to give in, and some fibers rupture, but it continues to support higher stresses than do muscles, which after yield point, break more rapidly.

As for muscles, the secant modulus is similar for all and for this reason, comparisons are not very significant. The tangent modulus for fascia tissue is greater than for muscle, again pointing towards a stiffer behavior of fascia; secant module is greater for fascia than for muscles, but these values are only comparable between same type of samples, because fascia's graphic representations are in another order of magnitude, when compared to muscles.

When it comes to comparing uniaxial and biaxial fascia tissue, these parametersare only correspondent between uniaxial and biaxial tissue from the same person, because several factors can influence the tissue's characteristics. Furthermore, there are only five biaxial specimens, as compared to fifteen uniaxial ones. For these reasons, the following table contains all the parameters results for (uniaxial and biaxial) fascia tissue from the same individual (one of the biaxial fascia samples was not considered, due to the lack of uniaxial specimen from the same subject, to compare it with). Beyond that, when comparing uniaxial and biaxial fascia specimens, it is more adequate to compare uniaxial samples with the biaxial axis that supported most of the tensile effort, i.e. axis 1. This is due to the fact that considering biaxial specimens, while one axis (axis 1) was tested according to the fibers direction, the other (axis 2) was not, because, as detailed in chapter 4, fascias' fibers are not orthogonal, and therefore, there is a difference between the two axis, related to the different stress state of the two: while fibers from axis one are being stretched and allowed to elongate, until rupture, fibers from axis two are being pulled obliquely, and much of the efforts are being supported by the fascia's extracellular matrix, instead of the fibers themselves.

Table V: Mechanical properties for uniaxial and biaxial fascia specimens for each subject. Notice that for the biaxial specimens, the values used were obtained from the graphic representation of only axis 1 of the specimen. For Cd08 and Cd10 two uniaxial specimens were available.

subject	specimen	σ_{max} (MPa)	λ_U	U_S (nJ/m^3)	E_t (MPa)	σ_Y (MPa)	E_s(MPa)
Cd07	uniaxial	2.80	1.43	0.52	8.80	2.54	3.76
	biaxial	2.63	2.93	2.92	1.38	2.26	1.77
Cd08	uniaxial1	1.32	1.64	0.28	5.22	1.17	1.07
	uniaxial2	3.73	1.68	0.86	11.11	3.26	2.30
	biaxial	2.44	1.69	0.62	7.23	2.16	1.42
Cd10	uniaxial1	3.50	1.72	1.46	5.38	2.92	4.51
	uniaxial2	2.55	1.42	0.46	9.66	2.18	3.35
	biaxial	2.90	2.13	1.55	4.89	2.03	1.21
Cd11	uniaxial	2.71	1.82	0.84	4.87	2.42	1.56
	biaxial	8.47	2.52	4.57	10.17	7.09	1.96

From table V interpretation, it is possible to infer that biaxial specimens stretch more than do uniaxial ones; this is valid for every case. However, when comparing tensile strength, there seems to be no tendency towards a definite comparison: most cases seem to have similar behavior, independent of the sample being uniaxial or biaxial and only for Cd11 fascia tissue sustains a much larger stress while being tested biaxially. Yield strength and secant modulus analysis point to a similar conclusion. As to the tangent modulus, the information on table V suggests that changing from uniaxial to biaxial, produces changes in the material behavior. However, there is not a tendency for the material's stiffness to increase or decrease. It was expected that stiffness would increase when going from uniaxial to biaxial systems (mazza 2011), but there are no sufficient data here to sustain this hypothesis.

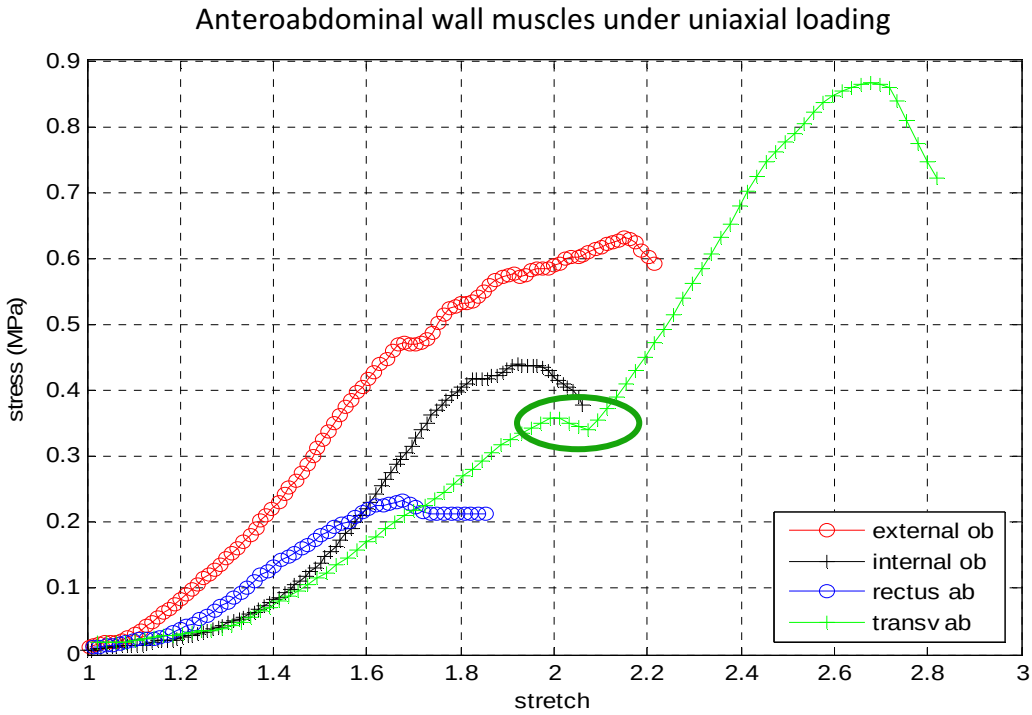

Figure 5.5 Graphic representation of the anteroabdominal wall muscles under uniaxial loading. One specimen of each tested muscle, from different cadavers, is represented. Green circle points out an adjustment period of the transverse abdominal muscle specimen.

Figure 5.5 shows a representation of the four studied muscles, under uniaxial loading conditions. This graphic representation, though only contains one specimen of each of the muscle types, closely resembles the mean values obtained for all the muscles(Table IV), therefore, its interpretation goes for all the experiments presented, except for the comments otherwise.

It is very noticeable that transverse abdominal muscle sustains larger stresses than do the others, *rectus abdominis* being the one that sustains lower stresses. This also goes for deformation: transverse abdominal muscle sustains larger deformations, while *rectus abdominis* stretches less. External oblique muscle, when comparing to the internal oblique, seems to sustain larger stresses, and have higher deformation too, though here the values become close. By observing the graphic representation it is more noticeable here that the tangent modulus for the external oblique muscle is the highest, though for the transverse muscle it is also high (mean=1.03, StDev=0.74, as can be seen in table IV), just not for the specimen here presented, which shows a soft curve slope. This means that both external oblique and transverse muscles are stiffer than the internal oblique muscle (though there is an accentuated curve slope on this graphic reresentation) and *rectus abdominis* muscles. Concerning yield strength, usually *rectus abdominis* starts to give in right before breaking point, followed by internal oblique, external oblique and finally transverse abdominal, which seems to be softer. In this graphic representation it is possible to see an adjustment phase (green circle on figure 5.5) for the transverse abdominal muscle, after yield strength point, where probably, when some of the fibers broke, others (which were not yet stretched

to their limit, which causes the curve to have a slight slope) took their place, supporting the stress, and resisted from thereon, until breaking point.

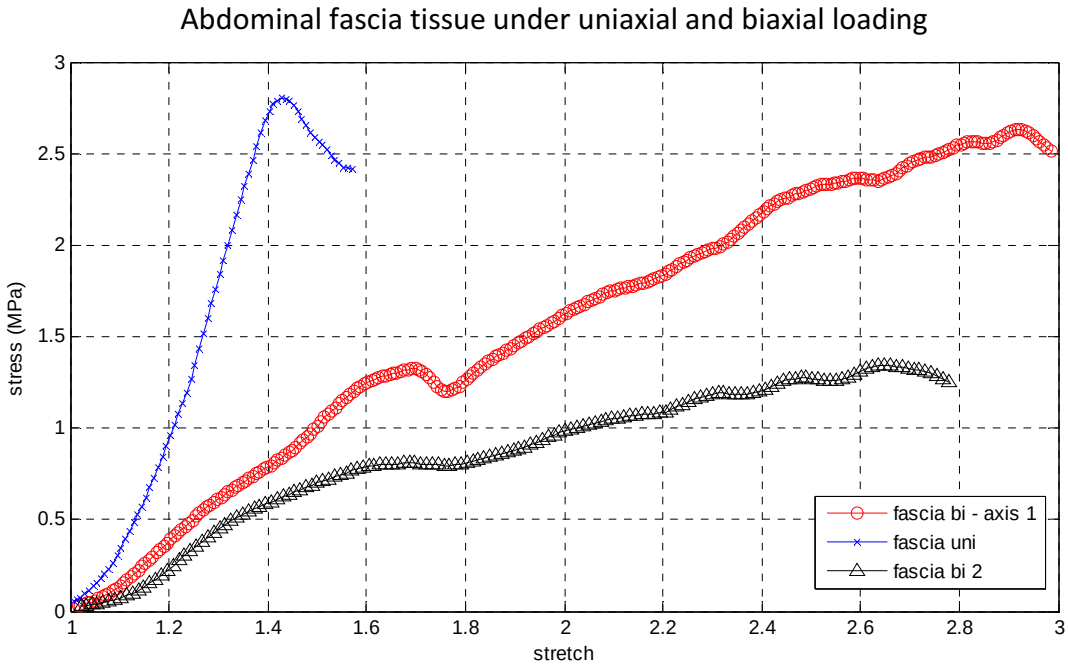

Figure 5.6 Graphic representation of the fascia tissue, under uniaxial (blue) and biaxial (red and black) loading. One specimen of uniaxially tested fascia and both axis of one biaxially tested from the same cadaver (Cd07) are represented.

A first overview of the results would evidence some degree of axial coupling present, when testing the biaxial specimen, i.e., the curve profile of the two axis does not overlap, meaning that one axis response could affect the other's. Yet, again it is important to consider that axis one was tested according to the fibers direction and not axis two and therefore, this difference between the two axis curves' profiles is probably not due to axial coupling, but related to the different effort state of the two-different mechanical properties. Consequently, axis two breaks at a lower tensile strength point than does axis one, and also its ultimate stretch is also lower (table V) as is its tangent modulus value (the curve slope for axis two is not as accentuated). For the same reason, the yield strength point is lower for axis two, when compared to one.

When it comes to the comparison between uniaxial and biaxial specimens, it is noticeable that biaxial specimen has a slightly lower tensile strength, when comparing the uniaxial sample with the biaxial sample containing the aligned fibers (axis 1). This comparison, as seen before, is not statistically significant because there were not enough samples available for testing, thus remains to be confirmed.

Individual Characteristics' Influence on Tissues' Mechanical Properties

All people are different by nature and constantly change their fascias' and muscles' internal structure, depending on what they eat, on the exercise they do or do not do, etc. For example, a muscle's mechanical behavior can vary from one person to

the other, based not just on the experimental variables, but also depending on the person from whom the sample was collected.

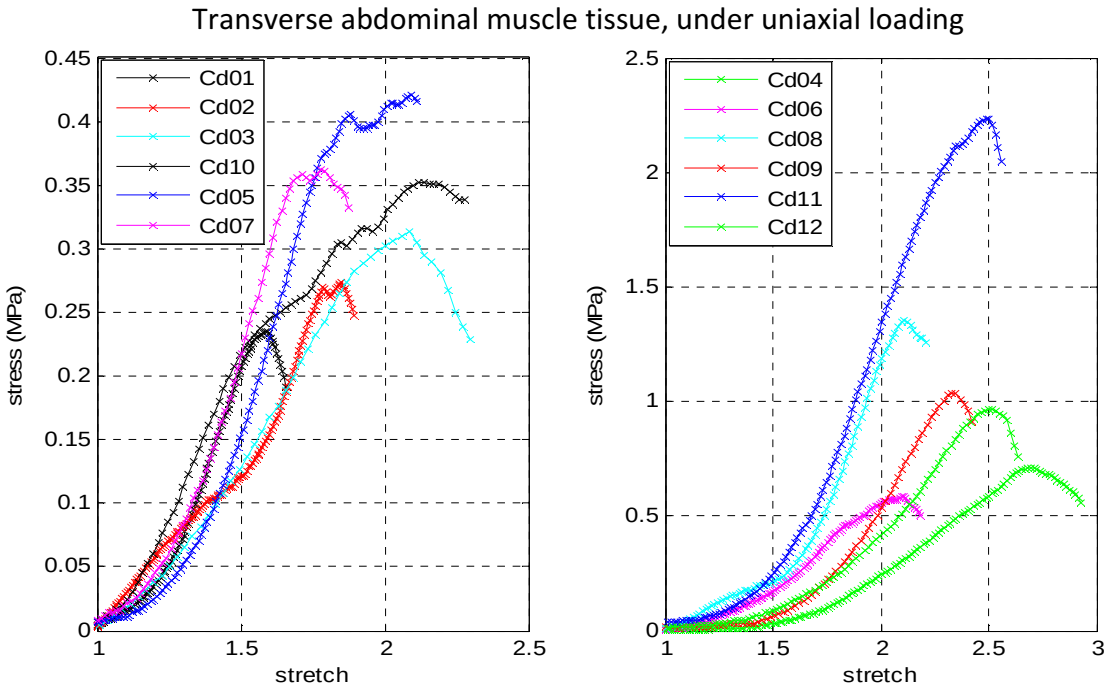

Figure 5.7 Graphic representation of the transverse abdominal muscle from all twelve cadavers. The only reason for two different graphics is to display the curves with less confusion.

Figure 5.7 shows the same muscle type for all twelve cadavers, independently of age, sex, physical activity, eating habits, etc. It is easily observed that all specimens have very different mechanical behavior, demonstrating that all comparisons discussed previously are fairly limited.

Since biological tissues' mechanical properties are so dependent on a person's age, sex, body mass index, etc, [3, 38]. Some comparisons are here presented, in an attempt to reach conclusions about the influence of a few variables, namely age, sex, body mass index and presence of hematoma in a tissue.

-Person's Age and Sex

As people get older, it is expected that their tissues change, becoming less elastic, for instance [3]; this effect could be more noticeable, if the influence of hormones is considered.

In this section, tissues from six cadavers are considered, three female and three male which are compared side by side. Each group contains a specimen from a younger, an adult and an older donor. This allows the comparison of age, within the sex, as well as the parallel between sexes. The same six cadavers (Cd09, Cd05, Cd08, Cd10, Cd06 and Cd12) were compared in all graphic representations and, for this reason, biaxial fascia tissue, uniaxial fascia tissue and *rectus abdominis* muscle

sometimes are not represented, due to the lack of specimens available. The two groups are divided as:

Female: Cd09 (73 years old), Cd05 (22 years old), Cd08 (53 years old)

Male: Cd10 (57 years old), Cd06 (17 years old) and Cd12 (45 years old)

Tissues from these individuals may not be representative of the population, which has to be taken into account. Also, it is important to mention that the choice of the donor that would attempt to represent the results had to do with the differences of age between all specimens and available samples to compare.

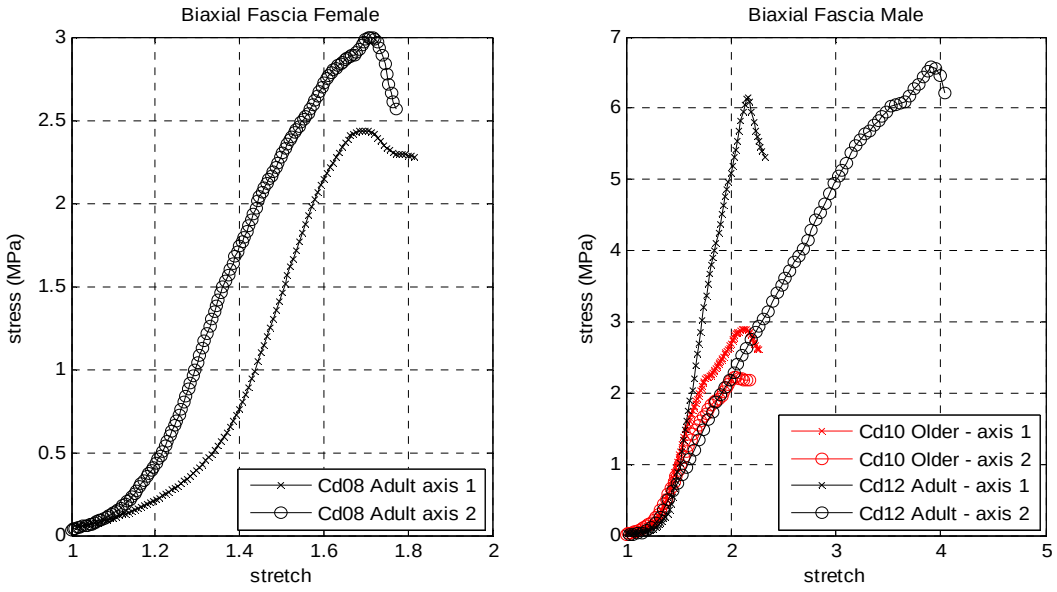

Figure 5.8 Graphic representation of biaxial fascia specimens for both female (on the left) and male (on the right) subjects individuals with different ages. There was none available sample for younger or older females, neither for younger male subjects.

By observing Figure 5.8, two comparisons can be done: on the one hand, female and male adult specimens have similar curve profiles, though male's specimen sustains much larger stress and stretch than does female's. On both male and female specimens, axis two supports higher stresses, which is also not very common for biaxially tested specimens. On the other hand, on male's graphic representation, it is possible to infer that the older donor's specimen sustains much smaller stress and stretch, showing a behavior very similar to the female adult specimen, in terms of stress and stretch. Though there is a significant difference of characteristics between men and women, pointing towards a stiffer behavior of males, as well as for adult male specimen, when compared to the older one, these results cannot be conclusive, due to the lack of specimens presented for biaxial fascia.

Uniaxial fascia tissue is represented for both male and female in Figure 5.9.

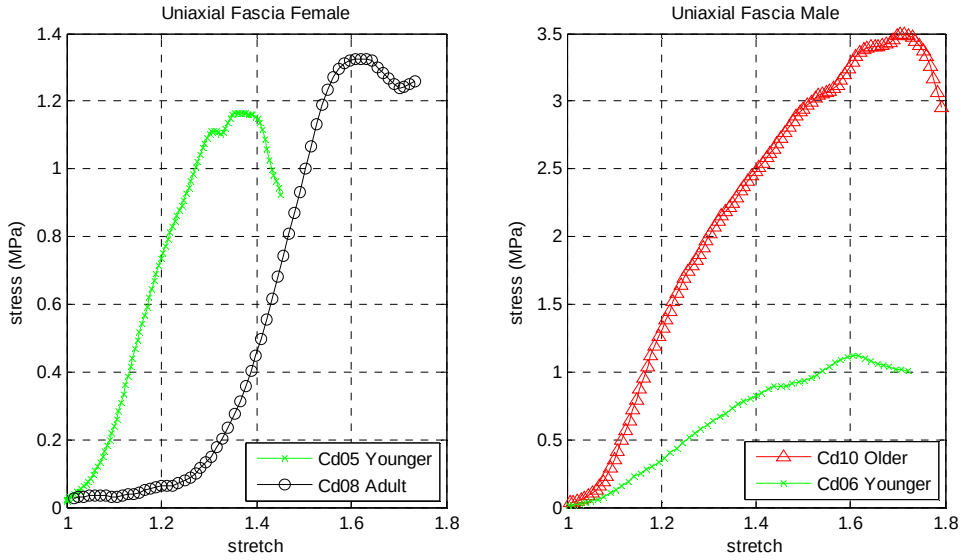

Figure 5.9 Graphic representation of uniaxial fascia specimens for both female (on the left) and male (on the right) subjects individuals with different ages.

These graphic representations seem to point to a similar behavior for the younger donors (male and female), displaying a similar tensile strength and somewhat close ultimate stretch value, which is higher for the male specimen, meaning that the male sample here has a softer behavior than does female. As for the female adult sample, when compared to the younger woman, presents a stiffer behavior, a higher tensile strength and ultimate stretch, which points to a softer behavior of the younger woman's fascia. The same happens on the male graphic representation: the older donor seems to have a stiffer fascia tissue, having a more accentuated curve slope (E_t) and higher tensile strength and ultimate stretch values.

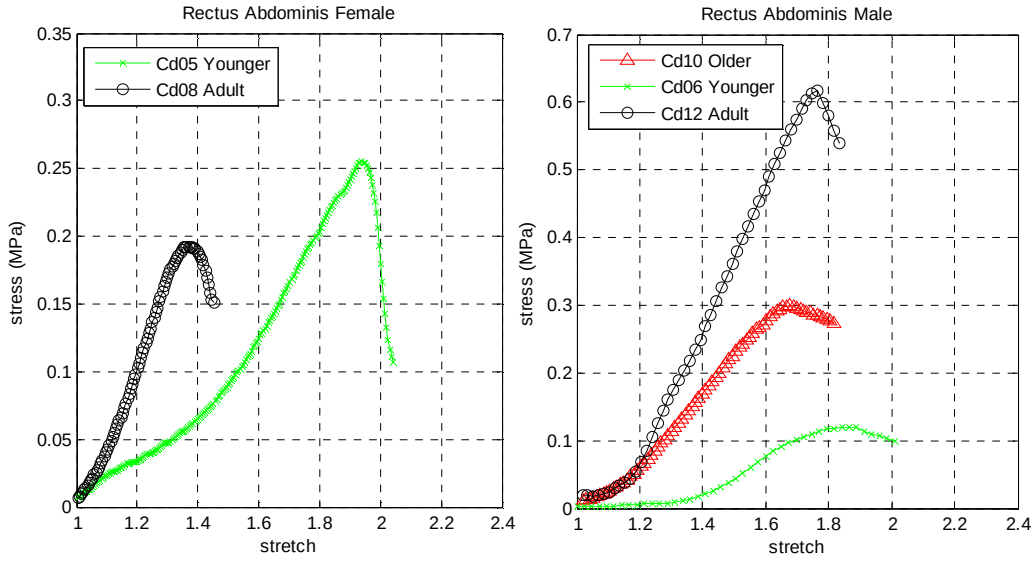

Figure 5.10 Graphic representation of rectus abdominis specimens for both female (on the left) and male (on the right) subjects individuals with different ages.

Graphic representations of *rectus abdominis* muscle(figure 5.10) show that there seems to be a significantly different behavior depending on the age of the sample: male samples, though having similar ultimate stretch values, seem to diverge when concerning tensile strength; the younger specimen shows a softer behavior, while the adult sample has the stiffest performance. As for female samples, younger specimen seems to stretch much more than does the adult sample, and also sustains larger stresses before breaking. By comparing male and female representations, young female specimen has a higher tensile strength, and similar ultimate stretch, while male adult specimen has higher ultimate stretch and tensile strength. Younger male specimen seems to have a lower yield point, but still, further from the point of rupture, which suggests that the specimen adjusted and started to give in to the stress, continually and not abruptly.

Specimens from external oblique, internal oblique and transverse muscles were available for all the cadavers considered, meaning that there are samples for each sex and for the three age categories that were initially defined. This provides a more complete comparison for these muscles, considering all variables.

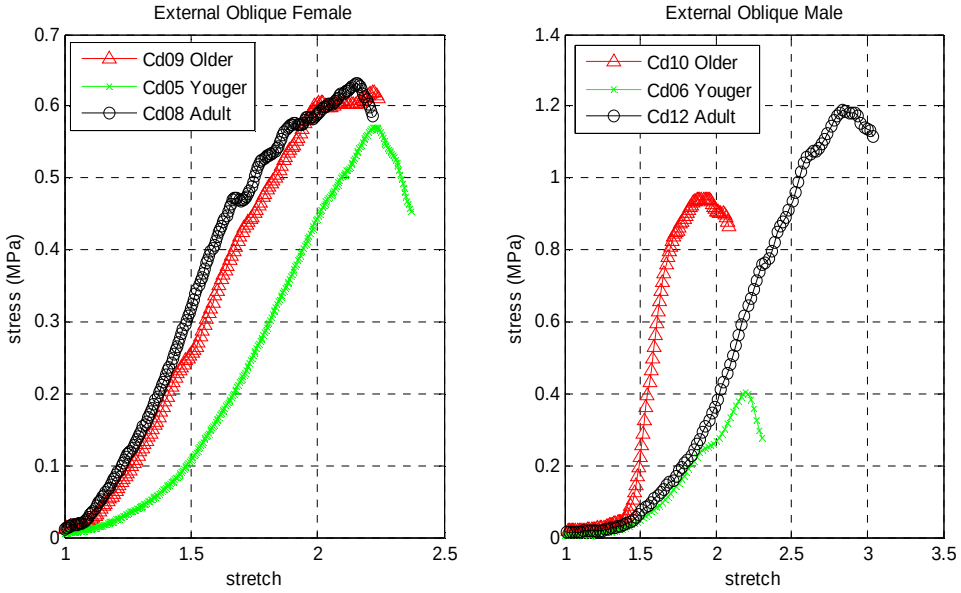

Figure 5.11 Graphic representation of external oblique specimens for both female (on the left) and male (on the right) subjects individuals with different ages.

Graphic representation of women's external oblique suggests that the younger specimen is more compliant, having a larger ultimate stretch value, though sustaining lower stress; As for adult and older specimens, they seem to have a similar curve profile. Male younger specimen stretch is similar to the younger female specimen's, but both adult and older specimens have much higher tensile strength. Here, adult male specimen seems to be softer than the older specimen, which displays an accentuated curve slope (E_t) and a lower ultimate stretch. Yield strength for the female

younger specimen seems to be higher than for adult and older specimens, also indicating a softer behavior of the younger specimen.

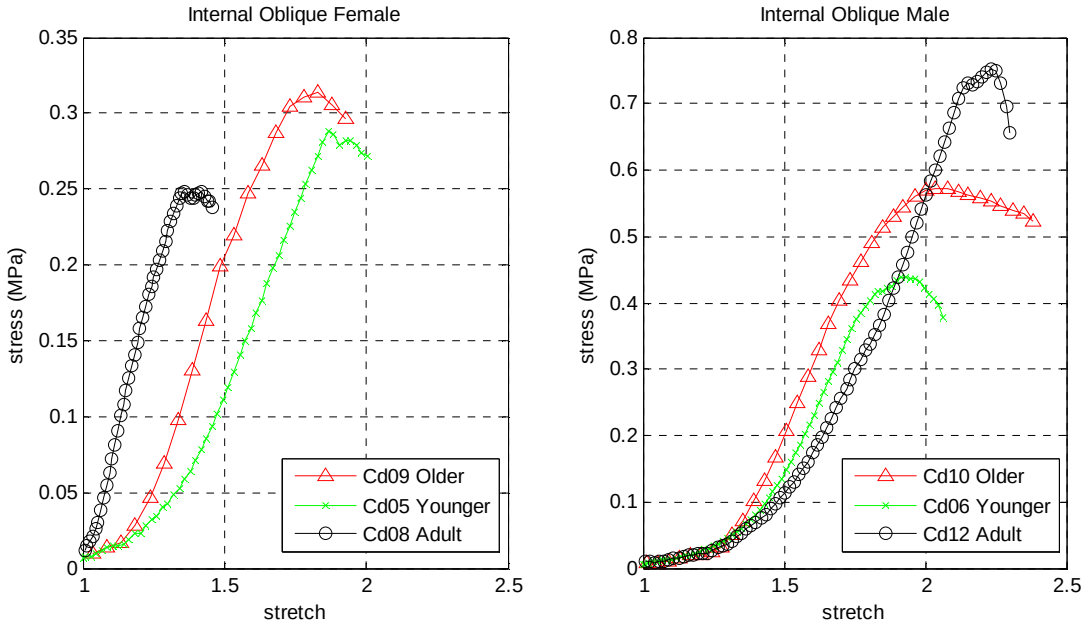

Figure 5.12 Graphic representation of internal oblique specimens for both female (on the left) and male (on the right) subjects individuals with different ages.

Internal oblique curve profiles for female donors present lower tensile strength values than do male's specimens. As for stretch, men have higher ultimate stretch values for adult the specimen and for the older one too. Younger subject has a similar ultimate stretch value, comparing women to men. Female adult specimen here stretch less than the older and the younger specimen, as opposed to males, whose younger specimen has the lowest ultimate stretch and adult specimen the highest one.

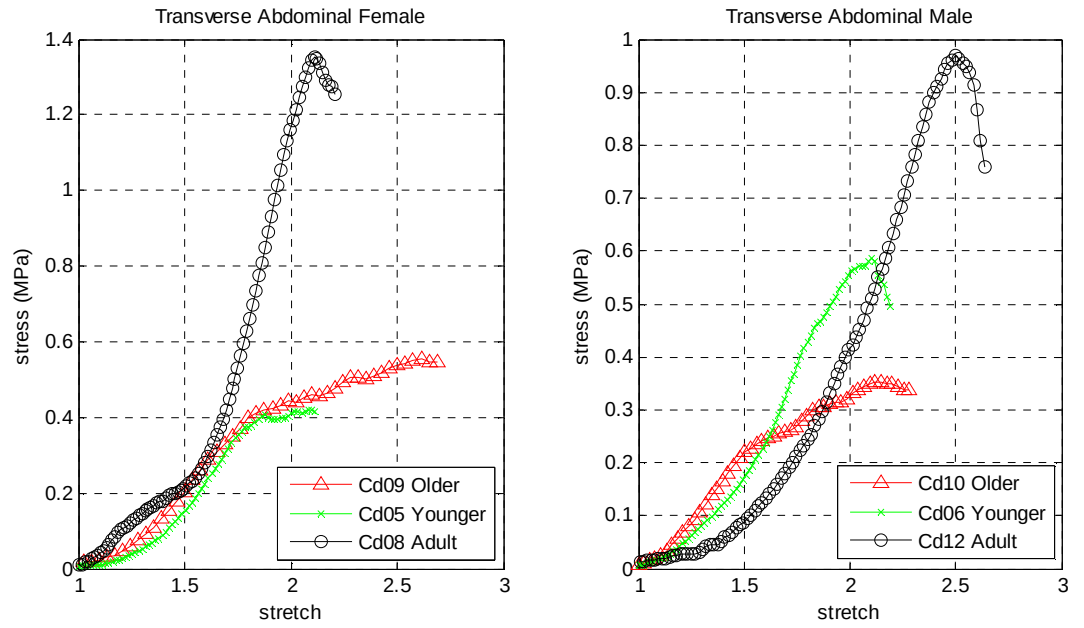

Figure 5.13 Graphic representation of transverse specimens for both female (on the left) and male (on the right) subjects individuals with different ages.

Adult samples of both female and male transverse muscle donors present a much higher tensile strength value, when compared to the older and younger samples of the same sex. The female younger specimen has a similar behavior compared to the older specimen. As for the male transverse muscles, the older specimen seems to have a softer behavior, breaking at low stress, but having a similar ultimate stretch as the younger sample. Yield strength for both younger and older specimens, whether it is male or female, has a lower value than does the adult specimen, pointing towards a softer behavior of the younger and older specimens.

Female specimens tend to have lower tensile strength than do male ones. Stretch values are similar for men and women, though there is a tendency to be higher for male samples. In general, male samples seem to be able to sustain larger stresses and behave more compliantly than do female specimens.

As for age differences, adult specimens, whether male of female seem to have the highest tensile strength values, while younger specimens are softer and older ones seem to behave more similarly to adult samples than younger ones. This may be, in the male case, because the older samples come from a not very old man. Much more testing should be done, in order to have statistically significant results for all these comparisons. Only then it is possible to admit that age and/or sex truly influence the mechanical properties of fascia and muscle tissue.

-Body Mass Index

Our constituting tissues' mechanical properties are very much dependent on what we eat and on our metabolism, in general. If a person is overweighted or obese, this means that more fat is accumulated inside the deeper layers of skin. Abdominal muscle and fascia tissue have a great supportive capability, being able to adjust their behavior in order to, for example, prevent hernias from occurring, as was described in chapter one.

This section is dedicated towards establishing a relationship between the body mass index of an individual and the mechanical behavior of this individual muscles and fascia. With this purpose, several comparisons between all tissue types are considered, for three individuals: Cd02, Cd07 and Cd10. These subjects were chosen because of their body mass index, which allows them to be categorized as having normal weight (Cd07), being overweighted(Cd10) and obese (Cd02).

Rectus Abdominis Muscle and Uniaxial Fascia Tissue

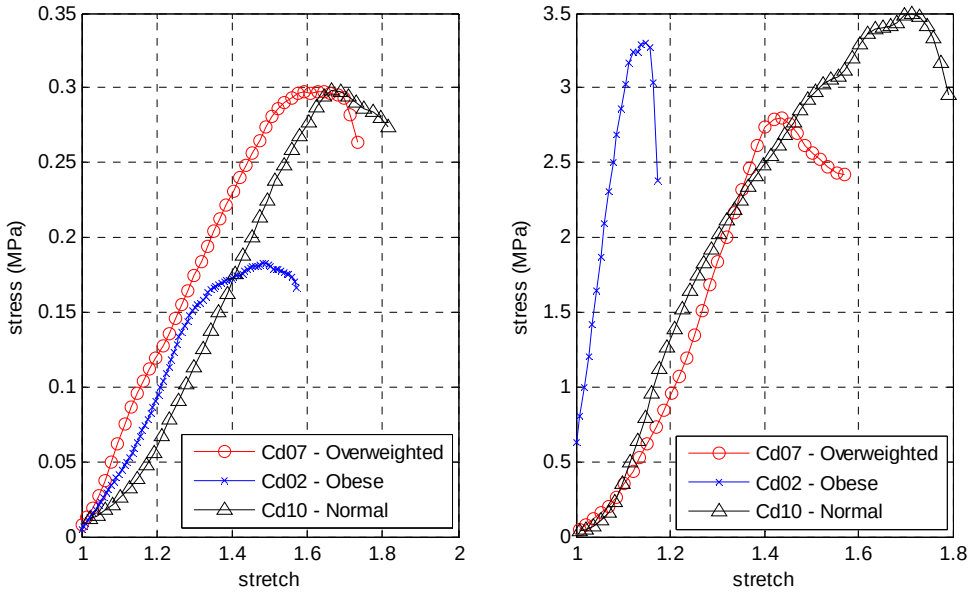

Figure 5.14 Graphic representation of rectus abdominis muscle (on the left) and uniaxial fascia (on the right) for three individuals with different body mass index.

Figure 5.14 represents the mechanical behavior of the *rectus abdominis* muscle and fascia; these tissues, mainly fascia, are thought to carry most of the pressure the anterior abdominal wall, as described in chapter one and two. Here it is noticeable that the obese *rectus abdominis* sustains much lower stress, has a lower ultimate stretch value and yield point. This suggests that the obese *rectus abdominis* muscle specimen is more compliant than the other samples. As for fascia tissue, there is also a noticeable difference from the obese specimen to the others: obese sample has a much lower ultimate stretch and a more accentuated curve slope (E_t), which point to a stiffer behavior of the obese fascia specimen, when compared to overweighted and normal samples.

There was no biaxial fascia sample for the obese individual (Cd02), therefore, the comparisons concerning this material are more limited. Nonetheless it is possible to observe some differences between normal weighted and overweighted donors' specimens.

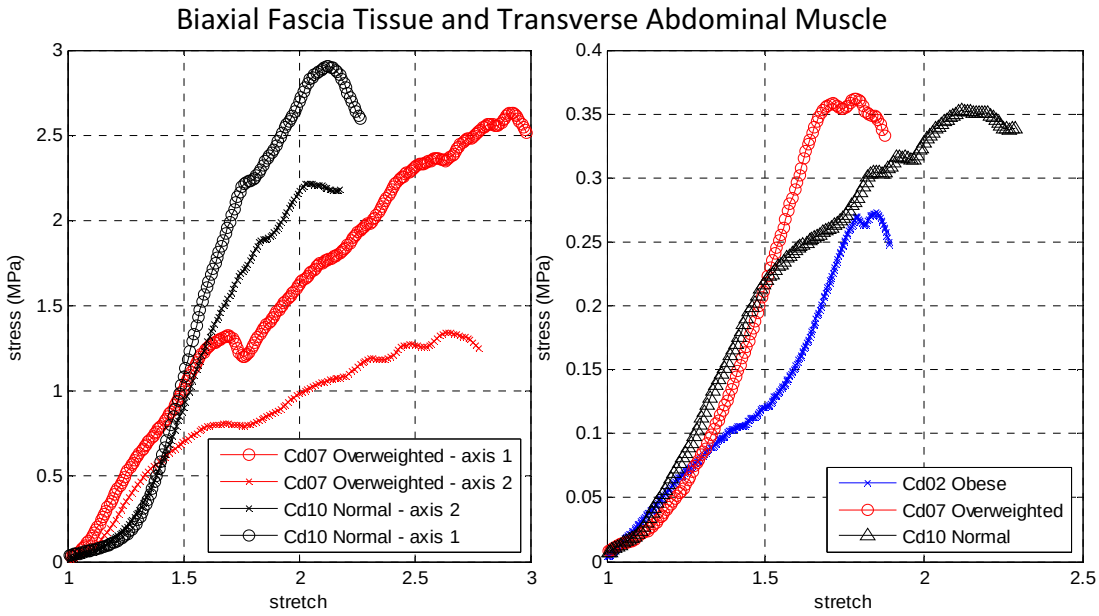

Figure 5.15 Graphic representation of biaxial fascia from two individuals with different body mass index (on the left) and of transverse abdominal from three individuals with different body mass index (on the right).

Note: There were no biaxial fascia samples from the obese individual.

From figure 5.15, it is possible to infer that overweighted fascia specimen has a lower yield strength and seems generally more compliant than normal specimen (lower tensile strength and higher ultimate stretch value). As for transverse abdominal muscle samples, it is possible to observe that obese specimen has the lowest yield strength, followed by normal specimen. overweigthed specimen has the higher tensile strength and lower ultimate stretch, being the stiffest material presented here.

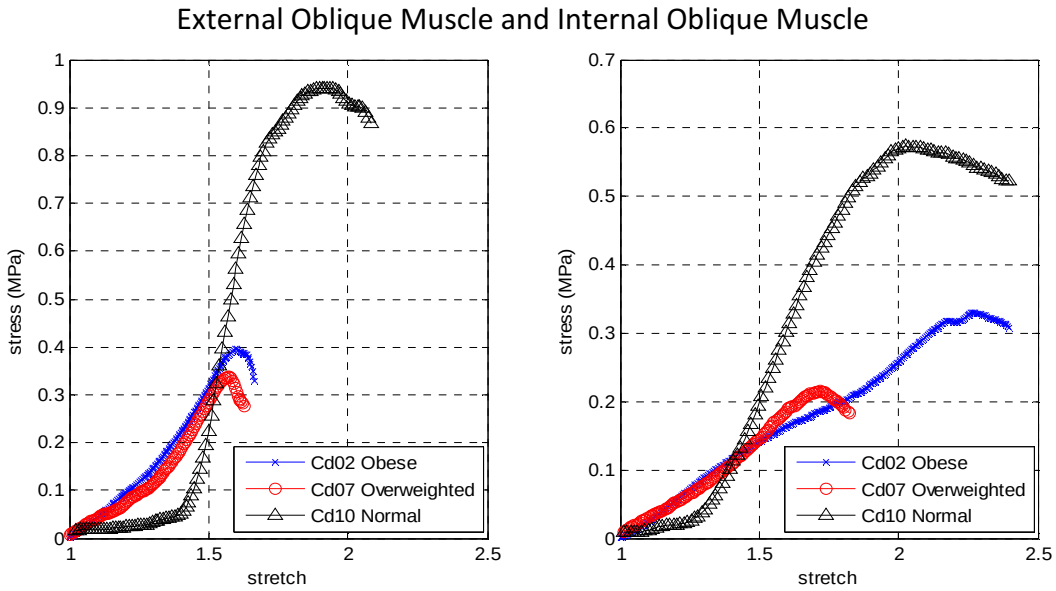

Figure 5.16 Graphic representation of the external oblique muscle (on the left) and internal oblique muscle (on the right) for three individuals with different body mass index.

Figure 5.16 suggests that normal external oblique muscle, as well as the normal internal oblique supports much larger stresses than do obese and overweighted specimens of the two muscles. Stretch values are also higher for normal external oblique, and for internal oblique, when compared to the overweighted sample, though not when compared to the obese specimen. For both external and internal oblique muscles, overweighted samples and obese samples seem to have a softer behavior, deforming more as the stress is applied, though rupture before than normal specimens.

For all compared tissues, it seems to be a tendency for the sample from the obese donor behave differently than the other specimens. This is, however a premature conclusion, since much more samples would be needed to have a statistically significant comparison of the influence of an individual's body mass index on his tissue's mechanical properties.

-Hematoma

Cd07 had a hematoma on the abdominal region and, as a result, the samples of *rectus abdominis* and external oblique muscles collected during autopsy had regions showing hematoma and other without. Here are the results for the comparison between mentioned tissues.

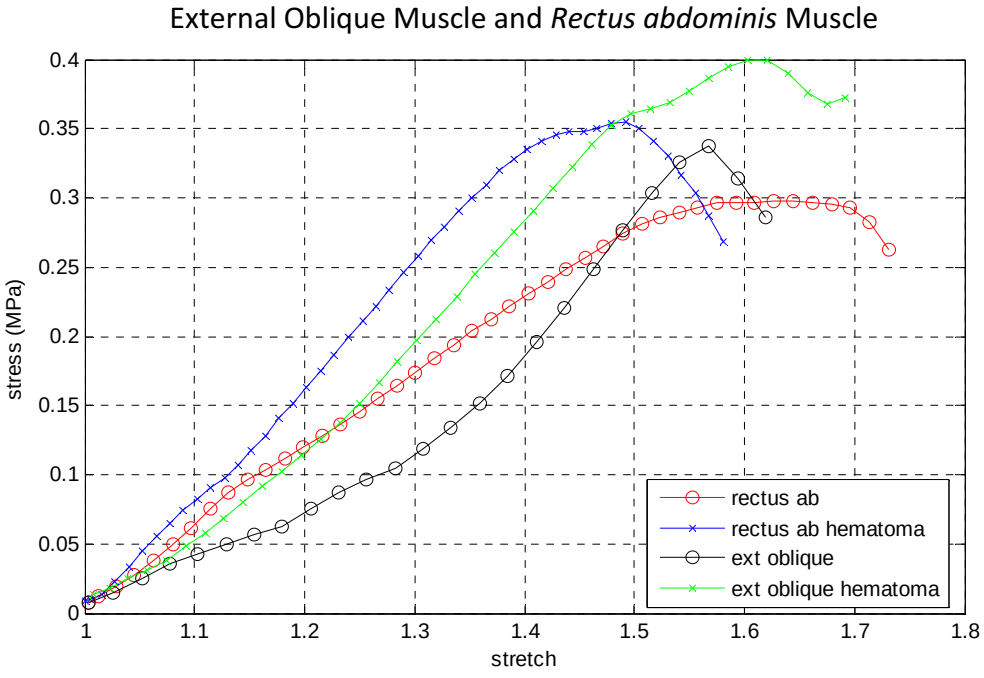

Figure 5.17 Graphic representation of the mechanical behavior of rectus abdominis and external oblique muscles under uniaxial loading, with and without hematoma.

Figure 5.17 demonstrates that there are slight differences between the muscles containing hematoma and without it: both muscles present a stiffer behavior when with hematoma, having an accentuated curve slope (tangent modulus) and higher

tensile strength, when compared to the same muscles without hematoma. As to ultimate stretch, it is higher for the external oblique without hematoma, as compared to the same muscle containing hematoma. For *rectus abdominis* such comparison inverts. Still, there seems to be a different behavior resulting from this condition, which was the only different factor between tests of the same muscle. However, there is only one sample for each set of conditions, and therefore these results cannot be considered statistically significant without further testing.

5.2.2 Hyperelastic Behavior

As it was described in chapter 4, though this work focuses mostly on the experimental procedure and on the classical approach to determine the mechanical properties of the materials, some model fitting was attempted, to illustrate the possibility of correlating hyperelastic models to the material's behavior. The curves presented are examples of the curve fittings performed to study the nonlinear mechanical behavior of biological materials

Also, a table summarizing all the used fitting parameters and errors, for all samples, is presented.

Table VI: Summary of all fitting parameters and errors from all the numerical approximations. Uniaxial (uni) and biaxial (bi) were used.

specimen	C_1	C_2	C_3	R^2	ε
Vulcanizedrubber uni	0.70008	-	-	0.9972	0.052795
Silicone uni dry	0.53511	-0.21382	-	0.99556	0.061634
Silicone uni bath	0.14921	0.016915	-0.00079577	0.99963	0.018135
Fascia uni	0.63652	-	-	0.95392	0.14473
Rectus abdominis	0.095068	-	-	0.99545	0.0377
Fasciabi	1.13910	0.99212	-	0.99836	0.026806
Internal oblique	0.029967	0.012648	-	0.96601	0.089729
Fasciabi	0.17742	1.0548	-2.5164	0.99955	0.01399
Transverse	0.031537	0.02242	0.019052	0.994	0.054177

As described in chapter 3, when using the Neo Hookean model, only one parameter is set to adjust the curve fitting; for Money Rivlin there are two paramenets to be set, and for Yeoh approach, three parameters are set. All the fittings seem to have low error values, which can be confirmed through the visual analysis of the graphic representations that follow. Ideally, when fitted curves and experimental ones overlap, these parameters would be comparable, and conclusions could be inferred from these results, but since few samples are used, and the model fitting was not the

core objective of this work, the presented table, as well as the graphic representations should be perceived as examples of what can be achieved by future work, and to illustrate the possibility of a deeper mathematical correlation to the underlining physics, which explains the mechanical behavior of the studied isotropic hyperelastic materials and biological tissues.

5.2.2.1 Isotropic Hyperelastic Materials

This section presents a few graphic representations of the experimental curves of isotropic hyperelastic materials, and superimposed fitting curves. One example is given for each applied model (Neo Hookean, Money Rivlin and Yeoh), and different samples are used for each curve.

Firstly, figure 5.18 presents a graphic representation of a curve fitting result for a uniaxial vulcanized rubber dry specimen. There seems to be a close fitting, since the curves overlap. When using Neo Hookean model, only one parameter is adjusted, thus the presented analytical red line is linear.

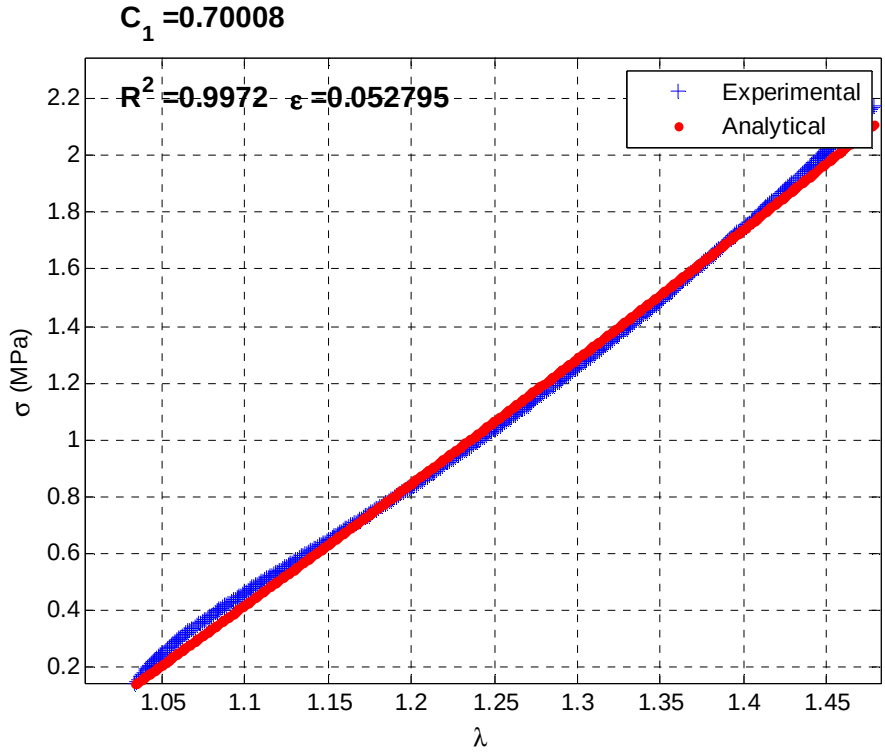

Figure 5.18 Fitting result for an example test of vulcanized rubber uniaxial dry specimen, using the Neo Hookean model. Fitted parameters and error appear on the graphic display of results.

Figure 5.19 presents a graphic representation of a curve fitting result for a uniaxial silicone dry specimen. Again, there seems to be a close fitting, with some differences on the beginning of the curves.

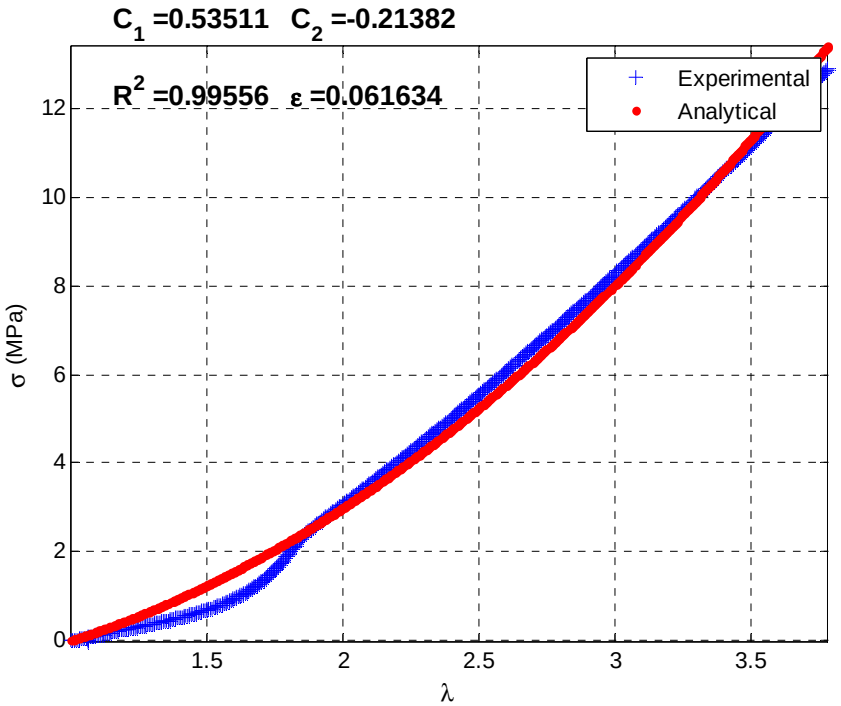

Figure 5.19 Fitting result for an example test of silicone uniaxial dry specimen, using the Money Rivlin model. Fitted parameters and error appear on the graphic display of results.

Figure 5.20 presents a graphic representation of a curve fitting result for a uniaxial silicone bathed specimen. This fitting seems to completely overlap the experimental curve. When using the Yeoh model, three parameters can be determined, thus the curve profile fits closely to the experimental data.

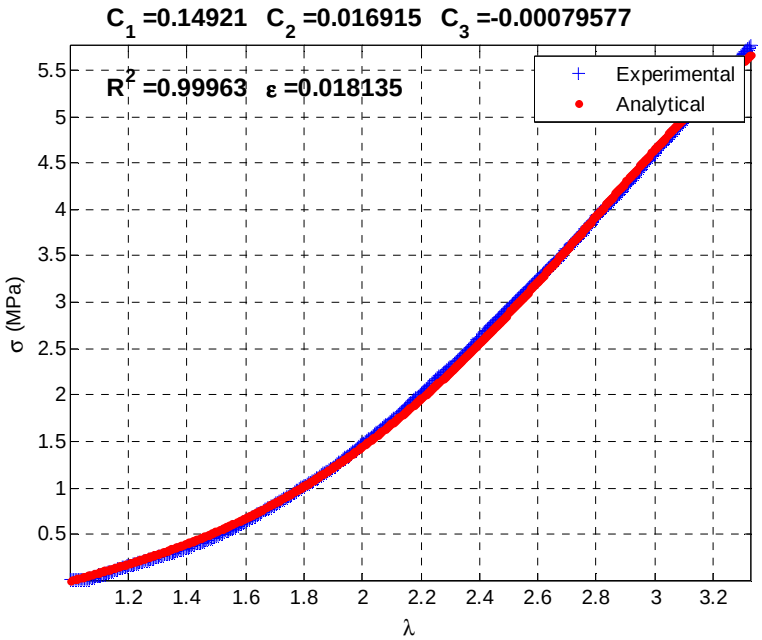

Figure 5.20 Fitting result for an example test of silicone uniaxial bathed specimen, using the Yeoh model. Fitted parameters and error appear on the graphic display of results.

5.2.2.2 Anisotropic Hyperelastic Materials

Figure 5.21 presents the graphic representation of a curve fitting result for a uniaxial fascia specimen. Since the experimental curve profile is not linear, the Neo Hookean curve fitting is not very adequate.

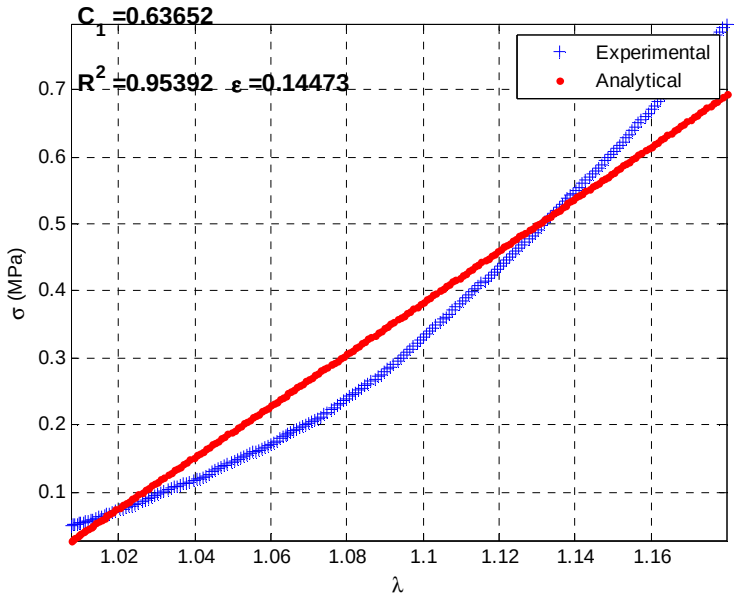

Figure 5.21 Fitting result for an example test of fascia uniaxial specimen, using the Neo Hookean model. Fitted parameters and error appear on the graphic display of results.

Contrary to Figure 5.21, in figure 5.22 there seems to be a superimposition of the two curves: the *rectus abdominis* specimen used seems to present a linear behavior, within the chosen intervals, therefore, the NeoHookean model seems more adequate.

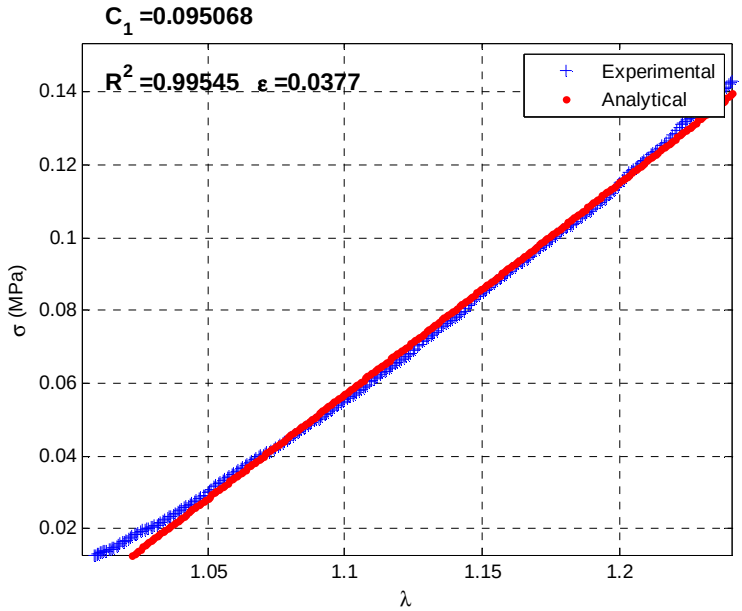

Figure 5.22 Fitting result for an example test of rectus abdominis uniaxial specimen, using the Neo Hookean model. Fitted parameters and error appear on the graphic display of results.

Figure 5.23 presents a graphic representation of a curve fitting result for one axis of a biaxial fascia specimen. Again, there seems to be a close fitting, using the Money Rivlin model.

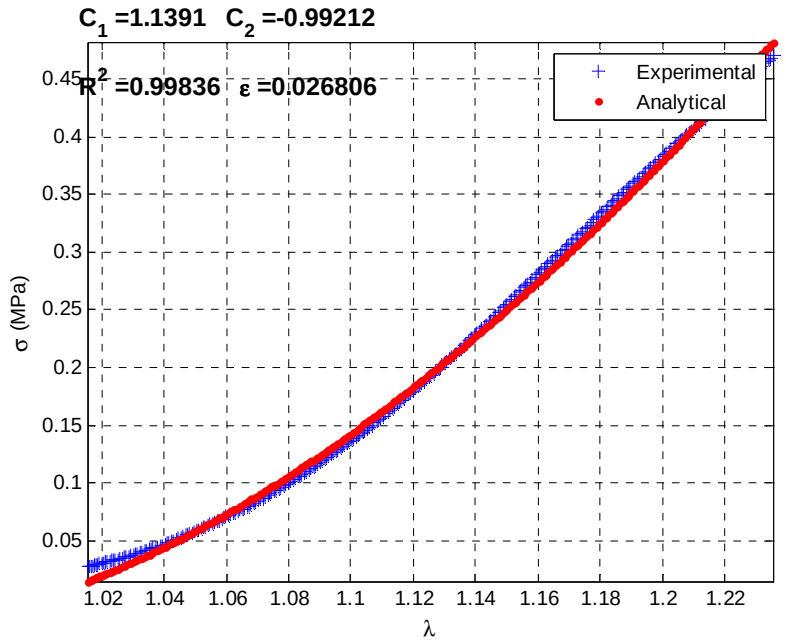

Figure 5.23 Fitting result for an example test of fascia biaxial specimen, using the Money Rivlin model. Fitted parameters and error appear on the graphic display of results.

Figure 5.24 presents a graphic representation of a poor curve fitting result of an internal oblique muscle, using the Money Rivlin model.

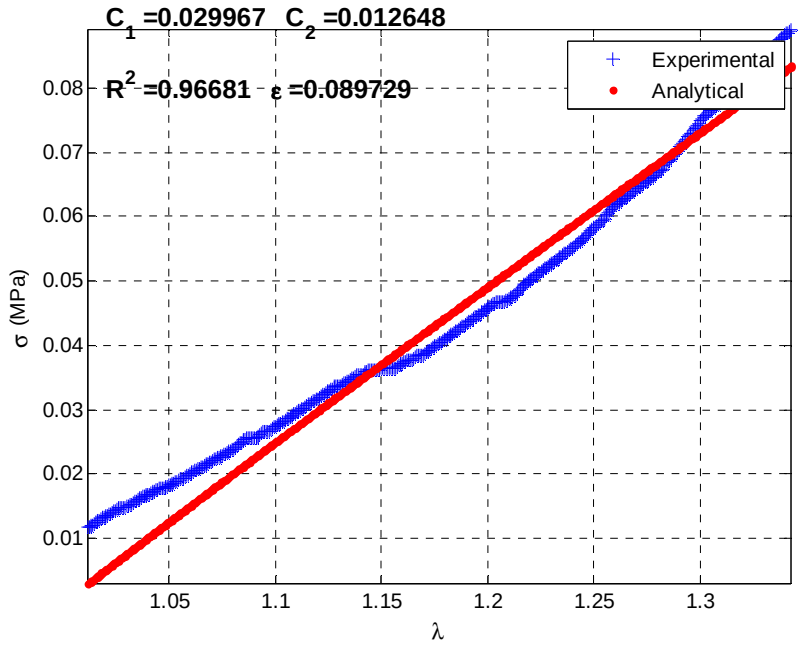

Figure 5.24 Fitting result for an example test of internal oblique uniaxial specimen, using the Money Rivlin model. Fitted parameters and error appear on the graphic display of results.

As for Figure 5.25, it presents a graphic representation of a satisfactory approximation of a biaxial fascia (axis 1) specimen, using the Yeoh model.

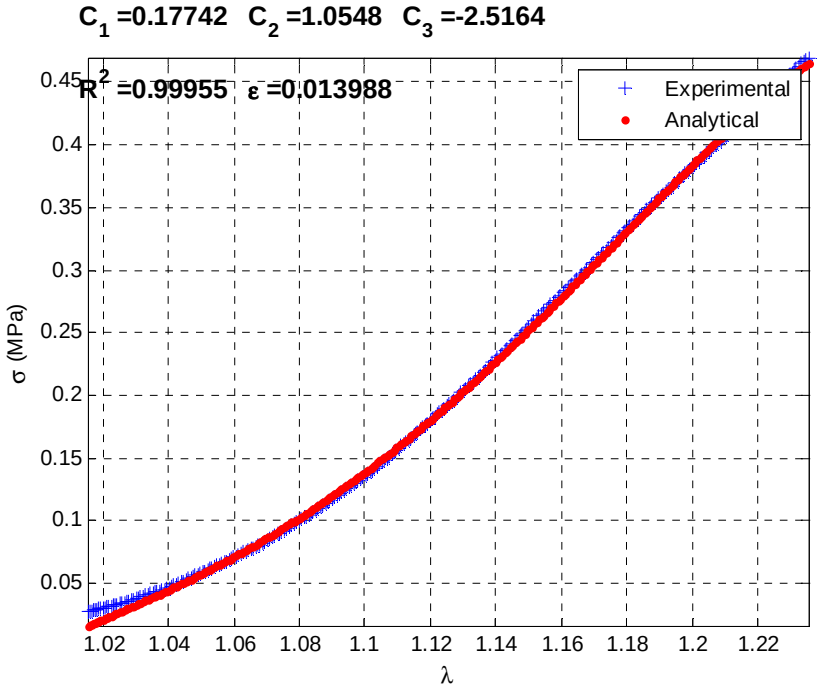

Figure 5.25 Fitting result for an example test of fascia biaxial specimen, using the Yeoh model. Fitted parameters and error appear on the graphic display of results.

Finally, figure 5.26 presents the result fitting for a transverse abdominal sample, usinh the Yeoh model. Here there seems to be an approximation, only when reaching the elastic region of the graphic, as expected.

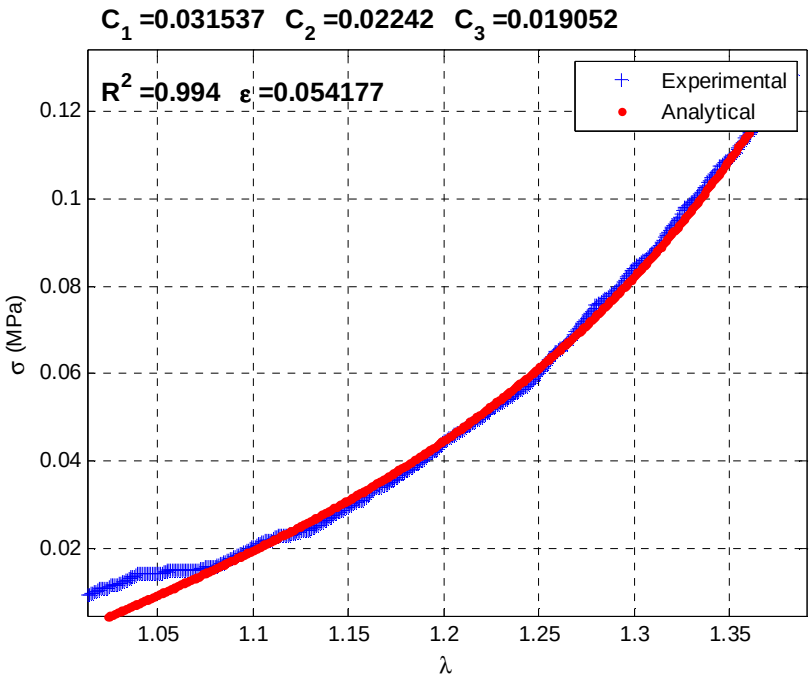

Figure 5.26 Fitting result for an example test of transverse abdominal uniaxial specimen, using the Yeoh model. Fitted parameters and error appear on the graphic display of results.

Hyperelastic constitutive models are more adequate to model the mechanical behavior of materials that evidence large deformations for small applied forces. To respect the behavior of a given material, the constitutive relation must incorporate as much as possible the available knowledge on the physical characteristics of the material. In the future, it is intended to study the abdominal wall muscles (*rectus abdominis*, internal oblique, external oblique and transverse andominal), with custom material models, as developed by [6] for fascia, and several other previous works [5, 12, 13, 16-18, 56].

5.2.3 Final Remarks

Results verify that different materials behave distinctively, in fact, all materials used (vulcanized rubber, silicone, muscle tissue and fascia) have mechanical unique behaviors. Some of the conclusions inferred from the results are here summarized:

1. Experimental conditions also play a significant role during experimental testing: the 37ºC saline bath influence on isotropic hyperelastic materials was confirmed, having an effect especially noticeable on silicone samples.
2. Though muscle tissue does not support as much stress as fascia tissue does, evidence suggested that muscles have a more compliant behavior, deforming more than fascia, when subjected to lower stresses.
3. Uniaxial and biaxial fascia comparison cannot be considered statistically significant, because of the limited number of available samples.
4. It was also observed that transverse abdominal muscle sustains larger stresses than do the other muscles, being that *rectus abdominis* seems to be the muscle which sustains lower stresses.
5. Individual's characteristics influence the mechanical behavior of biological tissues.
6. Male subjects generally presented stiffer fascia and muscle tissue.
7. Differences when comparing individuals of different ages were found, but these differences cannot be considered significant because there were not enough samples for the results to be conclusive. Nevertheless, evidence suggests that specimens from adult subjects present a stiffer behavior, while younger and older specimens are generally more compliant.
8. As for body mass index results, it is suggested that obesity has an effect on mechanical behavior of tissues, though there are few samples (only one for each body mass index category) and for this reason, the chosen people may not be representative of that specific category.
9. Hematoma produces alterations of the mechanical behavior of tissues. Results suggest there is an increase of stiffness, when hematoma is present. This conclusion is

again limited by the number of samples and the fact that these samples may not be representative of a larger population.

10. Hyperelastic constitutive models seem adequate to model mechanical behavior of biological materials, which evidence large deformations under small applied stresses.

Chapter 6

6. Conclusion

Through biomechanics it is possible to achieve some degree of understanding of the biophysical phenomena that take place at the molecular, cellular, tissue, organ and organism levels. For this reason biomechanics is as important and rewarding as it is challenging. Tissues' structures and behavior are very complex, dependent of many variables and greatly misunderstood, demanding sophisticated theoretical ideas, as well as clever and robust computational methods of analysis. Due to the morbidity and mortality rates, resulting from disease and injury, diagnostic and treatment improvements are essential, and since many rely on biomechanical comprehension, there is a profound need to invest in this area of knowledge [49].

The basis for the research this work proposed relies on previous tensile tests carried out using biological tissues, by [6], which fall under the scope of the work done on the mechanical behavior of female pelvic cavity [5, 12-15, 18]. Biaxial tests were the next step, since they can provide useful additional information for the abdominal fascia tissue characterization, by reproducing physiological deformation and loading conditions of the tissue more accurately. Human abdominal muscle and fascia tissue biomechanical testing is ground breaking research that shows much promise. The present work as the previous research was only possible, due to the collaborative effort from engineers and medical professionals.

Mechanical testing of human tissues is always a challenge, due to the ethical concerns, paperwork and also due to the health risks that can be related to human tissues handling.

Post mortem effects must be considered in every test; *rigor mortis* greatly influences mechanical properties, as do the conservation conditions of samples. Some samples were not easily collected during autopsy, because of the effects of *post-mortem* reactions, thus it is crucial to consider these situations, when extrapolating results for living tissue's mechanical properties.

The data collected suggests that, as described, each different layer of abdominal tissue contributes to the biomechanical behavior of the abdominal wall [20]. Though the different muscle types seem to have similar mechanical properties, the differences between fascia and muscle were significant.

In order to compare the existing donor individuals specimens, samples from different age groups, sex and body mass index were compared, as well as samples containing a hematoma region. Several differences were encountered, for instance, an

obese person's muscle and fascia seem to behave differently than do specimens provided by a normal weighted person. A distinct behavior occurs also when comparing older, younger and adult specimens. Moreover, hematoma seems to have an influence of tissues stiffness. As for sex's influence, it was clear that males provided more resistant specimens, in most cases. The discussion of each case and set of variables is detailed in chapter 5. Nevertheless, these results cannot be considered determinant, since the sample's pool was very limited.

Hernia formation is often linked to obesity as well as to defects of the fascia tissue [26]; the present work does not compare mechanical properties of defective fascia tissue, but a preliminary study on samples with different body mass index was attempted, reaching to the conclusion that obesity does have an effect on the mechanical behavior of both fascia and muscle. However, the existing pool of subjects is very small and on that limited sample's number, few were borderline obese; not one case of severe obesity was encountered. Also, none of the donors had hernias on the abdominal region and there was no information about hernia related medical/family history.

Biological tissue testing implies that some adaptations of the experimental procedure are necessary, for instance, in order to avoid excessive accumulation of stress near the clamp, Velcro hooks were glued to the aluminum grip. This produced very satisfactory results, avoiding specimen rupture close to the grips.

Biaxial specimens presented families of fibers disposed in oblique directions to each other, and for this reason, when cutting the samples, it was possible to obtain a specimen where one axis had the fibers longitudinally oriented, but the other axis presented oblique fibers. This induces errors, because on analysis of the two axis, two different stress conditions are being studied. In order to reduce axial coupling effects, rigid position grips were used when testing biaxial specimens; still, extra attention has to be payed when dealing with biaxial specimens with obliquely disposed fibers.

Previous studies suggested that material's stiffness would increase from uniaxial to biaxial stress states [41]. Results from the presented experiments did not back up this suggestion. This can be a result of a small and diverse pool of samples, though. In order to confirm, more tests should be done, especially on biaxial specimens.

The main purpose of the laboratorial work here presented was to obtain experimental data concerning the mechanical properties of abdominal fascia and muscle, which could be analyzed so that the behavior of these materials would be understood. Results for mechanical tests done on isotropic hyperelastic materials are also presented, though their main objective was simply to provide a standard testing procedure and assure reproducibility of the biomechanical tests. There were also efforts towards the study of hyperelastic models that might be used with finite

element processes under various loading conditions, having a potential impact in fields such as medicine, bioengineering (finite element simulations of the abdominal wall)and biomaterials (improved mesh properties of hernia repair implants). Constitutive modeling and the characterization of the mechanical properties of the abdominal fascia tissue are fundamental to achieve an accurate modeling and simulation of the abdominal structures, in particular when using the finite element method.

Chapter 7

7. Future Directions

Ideally, the tests would take place right after tissue collection, in order to avoid problems concerning tissue storage and transportation. Though this is not an easily changeable procedure, some additional effort could be done to assure the tests occur right after autopsy, and also, if there are several cadavers available for collection, those that have not been refrigerated before autopsy could be preferable to mechanically test.

In order to monitor the *post mortem* effects, a simple pH measuring procedure can be implemented as routine in every test; it is important to consider that when testing several specimens on a short interval between them, the same saline solution is kept in the testing container. This causes the bath to become more acid as the tests take place, and consequently, there should be an effort to study if those (minor) differences can have a (major) effect on tests. It is also important to think about the 37ºC saline bath as a bacterial culture media, which can both have mechanical implications for the samples, and health repercussions for the researchers.

When conducting this sort of research, which depends on the existence of subjects from whom the samples are collected, there is not much room for choosing the ideal sampling range. The age group, sex, body mass index, etc, which are thought to largely influence test results, highly limit the number of available specimens for tests. For this reason, the best solution would be to test samples from all available cadavers and collect enough mechanical assays for the results comparisons between groups to be statistically significant.

Testing conditions can be improved, to closer resemble living physiological conditions: for instance, as discussed, pH values could be monitored during tests. Furthermore, tests under several temperature states, and test done inside and outside the saline bath should be done, in order to map out the experimental variables and their mechanical effects.

Since experimental factors can have significant effects on the measured mechanical properties of a tissue but the effects can vary from tissue type to tissue type, it is in our best interest not to extrapolate the results of one tissue model to another, without considering the variations dependent on the tissues constituents [38, 45]. Again, in order to reach definitive conclusions about the experimental conditions, further testing is needed.

Accompanying the mechanical testing, histological and immunohistochemical must be done, to provide microscopic evidence of the biomechanical components structure before and after being subjected to mechanical efforts. This way, it should be possible to understand the phenomena occurring inside the tissue, as it deforms and compare influencing factors to the specimen's microstructure and its constituents.

Some experimental procedures entail errors that can be avoided, such as the use of contact methods to measure the specimens' dimensions. This procedure could be substituted by noncontact methods of analysis, such as optical methods. Also, cutting methods could be improved to avoid the subjectivity associated with sample preparation; for example, if cutter tools were used, on both uniaxial and biaxial specimens, the initial specimen shape would be more homogeneous.

Graphic representation analysis of the biomechanical tests is somewhat subjective: curve slopes and yield strength point are chosen, depending on graphic observation. This means that interpretation of the results is largely dependent on a person's good sense and knowledge of the matter. Before interpretation, the process of obtaining data from the graphic representations could be perfected, through a more sophisticated integrated software system, which analyzed the curve and took the parameters from it.

A material's reaction to a certain demand depends on that material's intrinsic characteristics, and the main goal of constitutive theories is to develop mathematical models which describe their real behavior, in order to, in the future, be able to predict the mechanical behavior of similar materials [42]. Here, the study is only focused on stress and strain components within a nonlinear regime, and variables such as temperature are not considered, but could be, on more complex future work, after the basis for such studies are solid.

After reaching conclusive results as to the mechanical properties of fascia and muscle tissue, as well as their role on supporting pressure from other anatomical structures, only then it is possible to carry out the development of synthetic meshes appropriate to substitute or reinforce these living tissues. It will also be possible to, based on biomechanical testing such as described in this work, develop finite element simulations of tissues, organs and even entire systems, providing a helpful tool for health professionals to use in the study of physiology and pathophysiology, as well as in the clinical practice and even for *in-silico* surgery simulations.

Biological tissues' mechanical properties can also vary, depending on age, sex, body mass index, etc, of the individual [3, 38], which provide a large spectrum of variables to be studied, on a sufficiently large subjects' number so that results can be considered statistically significant.

Clearly, much more testing needs to be done in order to standardize testing protocols and obtain a larger number of specimens, representative of each target group, such that meaningful data can be collected and be directly compared between experiments. Then, it will be possible to acknowledge patterns of mechanical behavior for individuals of several target groups and be able to predict the biomechanical consequences of living behaviors and intrinsic characteristics of a person or population.

References

1. Seeley, R.R., T.D. Stephens, and P. Tate, *Anatomy & Physiology*2003: McGraw-Hill.
2. *The muscles of the anterior abdominal wall*. Available from: http://clinical-line.blogspot.pt/2010/09/muscles-of-anterior-abdominal-wall.html.
3. Junqueira, L.C. and J. Carneiro, *Basic Histology, 11th ed*2007: McGraw-Hill.
4. Fung, Y., *Biomechanics: mechanical properties of living tissues*1993: Springer.
5. Martins, P., *Experimental and numerical studies of soft biological tissues*, in *Departamento de Engenharia Mecânica*2010, Faculdade de Engenharia da Universidade do Porto.
6. Martins, P., et al., *Mechanical characterization and constitutive modelling of the damage process in rectus sheath.* JOURNAL OF THE MECHANICAL BEHAVIOR OF BIOMEDICAL MATERIALS, 2012. **8**(0): p. 111-122.
7. Bate-Smith, E. and J. Bendall, *Changes in muscle after death.* British medical bulletin, 1956. **12**(3): p. 230-235.
8. Kobayashi, M., et al., *Reconsideration of the sequence of rigor mortis through postmortem changes in adenosine nucleotides and lactic acid in different rat muscles.* Forensic science international, 1996. **82**(3): p. 243-253.
9. Trindade, V.L.A., et al., *Experimental study of the influence of senescence in the biomechanical properties of the temporal tendon and deep temporal fascia based on uniaxial tension tests.* Journal of Biomechanics, 2012. **45**(1): p. 199-201.
10. Afonso, J., et al., *Mechanical properties of polypropylene mesh used in pelvic floor repair.* International Urogynecology Journal, 2008. **19**(3): p. 375-380.
11. Afonso, J.S., et al., *Structural and thermal properties of polypropylene mesh used in treatment of stress urinary incontinence.* Acta of Bioengineering and Biomechanics, 2009. **11**(3): p. 27-33.
12. Peña, E., et al., *Experimental study and constitutive modeling of the viscoelastic mechanical properties of the human prolapsed vaginal tissue.* Biomechanics and modeling in mechanobiology, 2010. **9**(1): p. 35-44.
13. Peña, E., et al., *Mechanical characterization of the softening behavior of human vaginal tissue.* J. Mech. Behav. Biomed. Mater., 2010. **4**: p. 275-283.
14. Martins, J.A.C., et al., *Finite element studies of the deformation of the pelvic floor.* Journal of Biomechanics, 2006. **39**(Supplement 1): p. S347-S347.
15. Martins, P., et al., *Prediction of nonlinear elastic behaviour of vaginal tissue: experimental results and model formulation.* Computer Methods in Biomechanics and Biomedical Engineering, 2010. **13**(3): p. 327-337.
16. Martins, P.A.L.S., et al., *Vaginal tissue properties versus increased intra-abdominal pressure: a biomechanical study.* Gynecologic and Obstetric Investigation, 2011. **71**(3): p. 145-150.
17. Martins, P.A.L.S., et al., *The Influence of Pelvic Organ Prolapse on the Biomechanical Properties of Vaginal Tissue.* International Journal of Urology, 2011. **bf Submitted for publication**.

18. Calvo, B., et al., *On modelling damage process in vaginal tissue.* Journal of Biomechanics, 2009. **42**(5): p. 642-651.
19. Kirilova, M., et al., *Experimental study of the mechanical properties of human abdominal fascia.* Medical Engineering & Physics, 2011. **33**(1): p. 1-6.
20. Kureshi, A., et al., *Matrix mechanical properties of transversalis fascia in inguinal herniation as a model for tissue expansion.* J Biomech, 2008. **41**(16): p. 3462-3468.
21. Axer, H., D.G. Keyserlingk, and A. Prescher, *Collagen Fibers in Linea Alba and Rectus Sheaths:: II. Variability and Biomechanical Aspects.* Journal of Surgical Research, 2001. **96**(2): p. 239-245.
22. B. Hernández, E.P., G. Pascual, M. Rodríguez, B. Calvo, M. Doblaré, J.M. Bellón, *Mechanical and histological characterization of the abdominal muscle - a previous step to modelling hernia surgery.* JOURNAL OF THE MECHANICAL BEHAVIOR OF BIOMEDICAL MATERIALS, 2010(4): p. 392-404.
23. Silveira, R.Â.B., et al., *Mapping traction strength of the anterior rectus sheath in cadaver.* Acta Cirurgica Brasileira, 2010. **25**(4): p. 347-349.
24. Rath, A., J. Zhang, and J. Chevrel, *The sheath of the rectus abdominis muscle: an anatomical and biomechanical study.* Hernia, 1997. **1**(3): p. 139-142.
25. Ozdogan, M., et al., *Changes in collagen and elastic fiber contents of the skin, rectus sheath, transversalis fascia and peritoneum in primary inguinal hernia patients.* Bratisl Lek Listy, 2006. **107**(6-7): p. 235-238.
26. Moore, K.L., A.F. Dalley, and A.M.R. Agur, *Clinically oriented anatomy*. Vol. 5. 1999: Lippincott Williams & Wilkins Philadelphia, PA.
27. [cited 2012 January]; Available from: http://healthtopics.hcf.com.au/HerniasHydrocoeles.aspx.
28. Hollinsky, C. and S. Sandberg, *Measurement of the tensile strength of the ventral abdominal wall in comparison with scar tissue.* Clinical Biomechanics, 2007. **22**(1): p. 88-92.
29. Hernández, B., et al., *Mechanical and histological characterization of the abdominal muscle. A previous step to modelling hernia surgery.* JOURNAL OF THE MECHANICAL BEHAVIOR OF BIOMEDICAL MATERIALS, 2011. **4**: p. 392–404.
30. Ramos-Vara, J., *Technical aspects of immunohistochemistry.* Veterinary Pathology Online, 2005. **42**(4): p. 405.
31. Humphrey, J.D., *Cardiovascular Solid Mechanics*2002: Springer-Verlag.
32. de Sousa Martins, P.A.L., *Experimental and Numerical Studies of Soft Biological Tissues*, 2010, Faculdade de Engenharia da Universidade do Porto.
33. Schleip, R., W. Klingler, and F. Lehmann-Horn, *Active fascial contractility: Fascia may be able to contract in a smooth muscle-like manner and thereby influence musculoskeletal dynamics.* Medical hypotheses, 2005. **65**(2): p. 273-277.
34. Moore, K.H., *Urogynecology: Evidence-Based Clinical Practice*2006: Springer.
35. Drake, R.L., W. Vogl, and A.W.M. Mitchell, *Gray's anatomy for students.* 2005.
36. Fung, Y.C., *Biomechanics: Mechanical properties of living tissues, 2nd ed*1993: Springer-Verlag.
37. Harris, J.L., P.B. Wells, and J.D. Humphrey, *Altered mechanical behavior of epicardium due to isothermal heating under biaxial isotonic loads.* Journal of Biomechanical Engineering, 2003. **125**(3): p. 381-388.

38. Bass, E.C., et al., *Biaxial testing of human annulus fibrosus and its implications for a constitutive formulation.* Annals of Biomedical Engineering, 2004. **32**(9): p. 1231-1242.
39. Billiar, K.L., A.M. Throm, and M.T. Frey, *Biaxial failure properties of planar living tissue equivalents.* Journal of Biomedical Materials Research - Part A, 2005. **73**(2): p. 182-191.
40. David, G., et al., *Regional multiaxial mechanical properties of the porcine anterior lens capsule.* Journal of biomechanical engineering, 2007. **129**(1): p. 97-104.
41. Schmidt, A., et al., *Multiaxial Mechanical Characterization of Interpenetrating Polymer Network Reinforced Acrylic Elastomer.* Experimental Mechanics, 2011. **51**(8): p. 1421-1433.
42. Holzapfel, G.A., *Nonlinear Solid Mechanics: A Continuum Approach for Engineering*2000: John Wiley & Sons.
43. MATERIAL SAMPLE FOR TESTING BIAXIAL STRESS CONDITIONS [cited January 2012]; Available from: http://www.faqs.org/patents/imgfull/20110138925_03.
44. Abramowitch, S.D., et al., *Tissue mechanics, animal models, and pelvic organ prolapse: a review.* Eur J Obstet Gynecol Reprod Biol, 2009. **144 Suppl 1**: p. S146-S158.
45. Billiar, K.L. and M.S. Sacks, *A method to quantify the fiber kinematics of planar tissues under biaxial stretch.* Journal of Biomechanics, 1997. **30**(7): p. 753-756.
46. Chevalier, L., et al., *Digital image correlation used to analyze the multiaxial behavior of rubber-like materials.* European Journal of Mechanics, A/Solids, 2001. **20**(2): p. 169-187.
47. Driessen, N.J.B., C.V.C. Bouten, and F.P.T. Baaijens, *A Structural Constitutive Model For Collagenous Cardiovascular Tissues Incorporating the Angular Fiber Distribution.* Journal of Biomechanical Engineering, 2005. **127**(3): p. 494-503.
48. Criscione, J.C., M.S. Sacks, and W.C. Hunter, *Experimentally tractable, pseudo-elastic constitutive law for biomembranes: I. Theory.* Journal of Biomechanical Engineering, 2003. **125**(1): p. 94-99.
49. Humphrey, J.D., *Continuum biomechanics of soft biological tissues.* Proceedings: Mathematical, Physical and Engineering Sciences (Series A), 2003. **459**(2029): p. 3-46.
50. Jun, J.H., et al., *Effect of thermal damage and biaxial loading on the optical properties of a collagenous tissue.* Journal of Biomechanical Engineering, 2003. **125**(4): p. 540-548.
51. Erman, B. and J.E. Mark, *Structures and Properties of Rubberlike Networks*1997: Oxford University Press.
52. Ogden, R.W., *Non-Linear Elastic Deformations*1984: Dover Publications inc.
53. Lai, W.M., D. Rubin, and E. Krempl, *Introduction to Continuum Mechanics*1996: Butterworth Heinemann.
54. Infarmed. [cited 2012; Available from: http://www.infarmed.pt/prontuario/mostra.php?origem=ono&flag_palavra_exacta=1&id=1518&palavra=Soro+Fisiol%F3gico+B.Braun&flag=1.
55. Prevention, C.f.D.C.a. [cited 2012; Available from: http://www.cdc.gov/healthyweight/assessing/bmi/adult_bmi/index.html.

56. Martins, P., R. Natal Jorge, and A. Ferreira, *A Comparative Study of Several Material Models for Prediction of Hyperelastic Properties: Application to Silicone-Rubber and Soft Tissues.* Strain, 2006. **42**(3): p. 135-147.